3-28-2005

Analysis Of The Impact Of The Location Of A Window Type Air-Conditioner On Thermal Comfort In An Office Room

Hamza Begdouri
University of South Florida

Analysis Of The Impact Of The Location Of A Window Type Air-Conditioner On Thermal Comfort In An Office Room

by

Hamza Begdouri

A thesis submitted in partial fulfillment
of the requirements for the degree of
Master of Science in Mechanical Engineering
Department of Mechanical Engineering
College of Engineering
University of South Florida

Major Professor: Muhammad Rahman, Ph.D.
Autar Kaw, Ph.D.
Frank Pyrtle, III, Ph.D.

Date of Approval:
March 28, 2005

Keywords: heat, convection, flow, relative humidity, contaminant removal

Dedication

To my father for his patience and support

A mon père pour sa patience et son support

لأبي لصبره وتأييده

Acknowledgments

I would like to thank Dr. Muhammad Rahman for giving me the opportunity to do my masters under his guidance. Also I would like to thank Dr. Luis Rosario for his wonderful assistance, Dr. Autar Kaw and Dr. Frank Pyrtle for their uplifting sprits and their sharpness, Micheal Jurczyk MSME and Son Ho MSME for their help and commitment to excellence.

All the staff at the mechanical engineering department at the University of South Florida, Sue Britten, Sherly Tervort, and wes Frusher.

Mr. Richard Lafond, Director of Engineering at Leslie Controls for his help and leniency.

Table of Contents

List of Tables

List of Figures

Analysis of the Impact of the Location of a Window Type Air-Conditioner

on Thermal Comfort in an Office Room

Hamza Begdouri

ABSTRACT

This study considers airflow simulations to evaluate the impact of different window air-conditioner locations on the thermal comfort in an office room (OR). This thesis compares the air distribution for an office room by using computational fluid dynamics (CFD) modeling to previously studied rooms. The air distribution was modeled on a typical office room window air conditioning unit, air supply from a high pressure on the top and the low pressure exhaust on the bottom considering the existing manufacturing ratios for surface areas. The discharge angle for the supply grill of the AC unit was varied from 20 to 40 degrees. The position of the air conditioner was also varied and studied at 60%, 75% and 90% of the total height of the room. In addition, the location of the occupant within the office room was varied, two locations were studied, one where the occupant is far from the unit and the other to closer to the AC unit at the middle of the room. Predictions of the air movement, room temperature, room relative humidity, comfort level, and distribution of contaminants within the office room are shown. Analysis of these simulations is discussed. Energy estimations are also performed and evaluated. The positions of the air-conditioner unit, the inlet angle and the occupant position in the office room have shown to have an important impact on supply controlling

air quality and thermal comfort. Results are in good agreements with the experimental data.

The primary function of a HVAC (heating refrigerating and air conditioning) system is the generation and maintenance of comfort for occupants in a conditioned space [1]. This work also provides a detailed analysis of three-dimensional mixed convective flow induced by a window air conditioning system. Using a three dimensional CFD simulation, several characteristics of human comfort are analyzed. The results of this study show a strong relation between the position of the wall-mounted air conditioning unit and the thermal comfort of the occupant. The results are in good agreement with the experimental data and the two dimensional simulation.

Chapter 1 - Introduction

1.1 Overview of Two Dimensional Simulation of Window Type Air-Conditioning in an Office Room

The air conditioning system has a great impact on the quality of life in this century indicating the great significance of this field in the world. Air-conditioning systems usually provide year-round control of several air conditions, namely, temperature, humidity, cleanliness, and air motion. Window air units are easy to install and can be plugged into any office circuit that is not shared with any other major equipment. Larger room air conditioners need their own dedicated circuit.

The air-conditioning market in the world has grown considerably in the last few years. It continues its phenomenal growth in line with the many residential and commercial projects taking place particularly in developing countries. As competition intensifies in the global residential air conditioning market, prices will tend to fall. This trend should open markets to new end-users who could not previously afford air conditioning because it was considered to be a luxury item. By increasing end-user exposure to air conditioning in shops, offices and cars, there is a transition among consumers to an air-conditioned lifestyle. This means that the market for self-contained, window or wall-type air conditioning machines is growing rapidly because its price and simplicity of installation.

One of the most common air conditioning problems in office spaces is improper operation. All office's windows and outside doors must be closed when an air conditioner unit is operating. Other common problems with existing window air conditioners result from faulty installation, poor service procedures, and inadequate maintenance. Improper installation of your air conditioner can result in bad airflow distribution. Many times, the air conditioner location does not match that stated by the manufacturer's specifications. If proper refrigerant charging is not performed during installation, the performance and efficiency of the unit is impaired. Service technicians often fail to find refrigerant charging problems or even worsen existing problems by adding refrigerant to a system that is already full. Air conditioner manufacturers generally make rugged, high quality products. If an air conditioner is installed correctly, or if major installation problems are found and fixed, it will perform efficiently for years with only minor routine maintenance. However, many window air conditioners are not installed correctly due to lack of general guidelines. As an unfortunate result, modern energy-efficient air conditioners can perform almost as poorly as older inefficient models [2].

In several countries, the use wall mounted air conditioners is great because of low cost, maneuverability and frequently due to seasonal sever weather conditions. However, many applications are arbitrarily judged due to lack of information and guidelines about these units. Few occupants of rooms either offices or bedrooms equipped with wall-mounted air conditioners are ever satisfied with comfort levels. Occupant would routinely change positions or the setting on the units.

Similar to FEA (Finite Element Analysis), CFD use is a very reliable technique in studying and analyzing fluid patterns. Most importantly CFD is helpful in solving for

specific fluid properties by simultaneously computing multiple fluid equations. The simulation procedure is depends on needs for each application, it allows changes of boundary conditions accordingly. CFD is used in every domain where it is important to predict fluid behavior e.g. medical study of bodily fluids, transmission lines carrying steam or fuel etc.

The continued progress of CFD in recent times have disclosed the potential of economical yet effective way for improving HVAC system in the design phase, with less experiment required . One advantage of CFD simulations is that it allows specific of a room that has relevant airflow. CFD models have been used to study indoor air quality (IAQ) situations, pollutant distribution, and performance of air conditioning systems (Chow and Fung [3], Emmerich [4], Gadgil and [5]). Hirnikel [6] investigated contaminant removal of three distribution systems for bars and restaurants by using CFD simulations. They showed that directional airflow systems could reduce people's exposure to contaminants.

Experimental work has been done on studying wall-mounted air conditioning units; most described experiments are based on physical measurements of different variables. Some of these studies were associated CFD models have been applied to study HVAC system for window unit applications [7] [8].

CFD has previously gave remarkable results for similar studies of thermal comfort and contaminant removal [9], where similar characteristics of the human comfort inside an office room where numerically computed thus clarified multiple predictions made in setting the boundary conditions. Several models of CFD simulations are being utilized in building and moving vehicles for HVAC studies, statistical, dynamic, and

transient models [10]. Listed and coupled with their optimum applications they can give outstanding predictions depending on the use.

List of these models and the newest improvements that have been achieved in the last eight years are listed in the ASHRAE (American society of heating refrigerating and air-conditioning engineers) literature review of advance thermal comfort presented by Yanzheng [11]. This list shows recent advances in thermal comfort modeling bases on heat balance, direct statistical and neutral network approaches.

They show that the heat exchange component of the model provides the input for the thermoregulation model, the heart of the comfort level model.

The present study analyses fluid flow in an office room presented in a two dimensional model. Using CFD simulations, numerical simulations were made to investigate the velocity, temperature, thermal comfort and air quality in the office room. Proper assumptions are made and several observations are noted. The corresponding results are studied and explained in the following sections

1.2 Overview of Three Dimensional Simulation of Window Type Air-Conditioning in an Office Room

Comfort in rooms cooled by window-type air conditioner has always been an issue, most commonly thought to be a malfunction of the unit itself. Several studies including the present one have proved that comfort levels are influenced mainly by more physical parameters including installed position, supply air speed, angle of flow, inlet flow temperature, as well as indoor air distribution. Change in size of the cooled space is not always compensated by change of air flow speed or inlet temperature in order to

obtain optimum comfort, because of relative humidity changes and typical air distribution.

Installed position of the window-type air-conditioning unit, if all other boundary conditions are constant, is the most important parameter to create optimum comfort levels.

Many studies have been made in the past using CFD Computational Fluid Dynamics to study HVAC systems in office rooms. CFD has proven to be most effective and cost efficient for HVAC systems especially in the design phase. One advantage of CFD simulations is that it allows specific conditions of a room that has relevant airflow.

However, there is no standard turbulent model or numerical scheme for all indoor room simulations, which indicates that the first priority and one of the most important steps of CFD simulation, is to choosing the appropriate turbulent model to suit a specific application.

Wall mounted air-conditioners are usually installed in the middle of the office room, from high above the standing height to the bottom of the room if the windows are low enough. This arbitrary height position and the distance from the occupant to the unit are usually the cause of human discomfort provoking a change of the setting of the unit. Settings of wall-mounted unit can be changed, both for airflow speed or inlet angle can change and improve thermal comfort in offices, however, it is not necessarily the answer. The present study analyses fluid flow in an office room presented in one three dimensional model. Velocity, air quality, temperature, and thermal comfort were investigated using CFD simulations and numerical computations. Proper assumptions are

made and several observations are noted. The corresponding results are studied and explained in the following sections.

Indoor thermal comfort conditions are primarily computed using velocity, relative humidity and temperature. These conditions are determined by solving coupled equations for the conservation of mass, momentum and energy for the carrier fluid including species then by solving the same equations for the each specie (water vapor, and contaminant gas). It is primarily assumed that for air conditioning applications in a closed space that the conditions are steady state, and the focus is directed to certain regions of interest e.g. the immediate working space around the person.

The objective of this section is to predict the impact of the location of a wall-mounted air conditioner on the thermal comfort and compare it to a previous tow dimensional model as well as other similar CFD simulations.

1.3 Thesis Outline

This thesis presents and compares the CFD simulations of two identical office rooms cooled with a window type air conditioning unit. Chapter 2 outlines the simulation approach for each problem. The two dimensional problem is described in Chapter 3, where inlet angle, location of the unit with respect to height, and the occupant location position have been varied. The thermal comfort has been studied and compared to each variation. In Chapter 4, an identical problem was studied in three dimensional simulation, where horizontal and vertical sections have been studied. Heat transfer and thermal comfort indices were analyzed and compared for each section. FIDAP, a Fluent.Inc CFD

software package, was used for all simulations. The output was analyzed using FIDAP post processing package and Microsoft excel. Additional experimental data was taken from literature.

1.4 Nomenclature

C	Mean contaminant concentration, kg of contaminant/kg of air mixture
c_p	Specific heat of air, J/(kg.K)
D	Mass diffusivity of species in air, m^2/s
f_{cl}	Ratio of clothed surface area to nude surface area
g	Gravity acceleration, m/s^2
h	Heat transfer coefficient, $W/(m^2.K)$
I	Thermal resistance, m^2K/W
k	Thermal conductivity of air, W/(m.K)
m	Concentration of species, kg of species/kg of air mixture
M	Metabolic heat generation flux, W/m^2 of naked body area
p	Pressure; partial pressure (with subscript), Pa
T	Temperature; mean temperature (with subscript), °C
u	velocity, m/s
v	Mean air speed relative to the body, m/s
W	External work, W/m^2 of naked body area
Y	Thermal sensation index
Ei	Energy consumption Ratio
ΔT_{Actual}	Average temperature difference to outside temperature
ΔT_{Design}	Simulation temperature difference to outside temperature

Greek Symbols

β	Thermal expansion coefficient, 1/K
ϕ	Relative humidity
μ	Viscosity of air, kg/(m.s)
ρ	Density of air, kg/m^3

Subscripts

S_1	Water vapor
S_2	Contaminant
a	Air
BZ	Breathing zone
cl	Clothing
E	Exhaust
ref	Reference
S	Supply

Chapter 2 - Simulation Approaches

2.1 Introduction

It is necessary to have the velocity, temperature and the relative humidity in order to determine the indoor thermal conditions in a room. These conditions are determined by solving coupled equations for the conservation of mass, momentum and energy for the carrier fluid including species then for the each specie. It is primarily assumed that for air conditioning applications in a closed space that the conditions are steady state, and the focus is directed to certain regions of interest e.g. the immediate working space around the person.

Variations of the unit position are studied, changing of the inlet flow angle are also explored. Also the effect of the person's location within the office room is presented. Energy estimations are also performed.

The fluid properties were taken at reference temperature of T_{ref} =22 ^{0}C = 295 K and their values are as follows:

μ= 1.8273 E-5 kg/(m.s)

c_p= 1.0043 E3 J/(kg.K)

k= 2.5776 E-2 W/(m.K)

ρ= 1.1967 kg/m^3

β=3.3932E-3 K^{-1}

D1= 0.2513E-5 m^2/s

D2= 0.2308E-5 m^2/s

2.2 Governing Equations

For an incompressible flow of air as a carrier for multiple components such as water vapor, contaminant gas, and of course dry air, and considering only the density of the buoyancy term to be varying keeping all properties of the fluid to constants, the equation of conservation of mass applied to a whole carrier fluid is :

$$\nabla \cdot \mathbf{u} = 0 \tag{2.1}$$

Assuming no chemical reactions nor source and that the mass diffusivities of all species are constant, thermal diffusion (Soret effect) is negligible, the mass conservation equation of water vapor and contaminant gas as carried species is

$$\mathbf{u} \cdot \nabla m_1 = \mathrm{D}_1 \nabla^2 m_1 \tag{2.2}$$

And,

$$\mathbf{u} \cdot \nabla m_2 = \mathrm{D}_2 \nabla^2 m_2 \tag{2.3}$$

In most HVAC application, the concentrations of the species are minimal which makes the buoyancy dependency on them negligible. Thus the equation of conservation of linear momentum looks as follows,

$$\rho \mathbf{u} \cdot \nabla \mathbf{u} = -\nabla p + \mu \nabla^2 \mathbf{u} + \rho \mathbf{g} \beta \left(T - T_{ref} \right) \tag{2.4}$$

With no heat generation nor inter-diffusion, also having constant thermal conductivity throughout the process, the equation of energy conservation is

$$\rho c_p \mathbf{u} \cdot \nabla T = k \nabla^2 T \tag{2.5}$$

The parameters of boundary conditions of our problem were implemented in the solving method for equation from Eq.2.1 through Eq.2.5 as follows,

To satisfy continuity and momentum Eq.2.1 and Eq.2.4 respectively, a constant velocity was given to the inlet fluid keeping all other parts (walls and light) at zero velocity including person. For Eq.2.2 and Eq.2.3 which are the contaminant and the water vapor equations, a constant flux of both was associated with the person, constant flux of water vapor for the inlet keeping the flux of the contaminant at zero, and zero flux of both species for all other elements of the room. A constant temperature was given to the inlet, walls and person, also a constant heat flux was associated with light fixture in order satisfy Eq.2.5.

By computing these equations for a two-dimensional flow problem, temperature, pressure, velocity on the x-axis, velocity on the y-axis, species 1, and specie 2 are solved for.

Relative humidity is obtained using, temperature, pressure, and water vapor concentration and following the procedure described by ASHRAE [12] as follows:

$$\phi = \frac{p_w}{p_{ws}} \tag{2.6}$$

Where,

$$p_w = \frac{(101325 + p)m_1}{0.62198 + 0.37802m_1} \tag{2.7}$$

And,

$$p_{ws} = 1000\exp\left[-\frac{5.800\times10^3}{T+273.15} - 5.516 - 4.864\times10^{-2}(T+273.15) + \right.$$
$$+ 4.176\times10^{-5}(T+273.15)^2 - 1.445\times10^{-8}(T+273.15)^3 + \tag{2.8}$$
$$\left. + 6.546\ln(T+273.15)\right]$$

2.3 Thermal Comfort Assessment

For thermal comfort assessment, Fanger model [13] is mostly used by ASHRAE [12]. Because it is based on steady state energy balance this model was specifically designed for office room applications even though its use has taken a broader domain.

PMV, Predicted Mean Vote is a parameter that determines thermal comfort based on the metabolic rate, kind of clothing, velocity, temperature, and humidity in the occupied space. Fanger determines the PMV to be,

$$\begin{aligned}\text{PMV} = {} & \{0.303\exp[-0.036(M-W)]+0.028\}\{(M-W) \\ & -3.05\times10^{-3}[5733-6.99(M-W)-p_w]-0.42[(M-W)-58.15] \\ & -1.7\times10^{-5}M(5867-p_w)-0.0014M(34-T_a) \\ & -3.96\times10^{-8}f_{cl}\left[(T_{cl}+273)^4-(T_a+273)^4\right]-f_{cl}h_c(T_{cl}-T_a)\}\end{aligned} \tag{2.9}$$

where

$$\begin{aligned}T_{cl} = {} & 35.7-0.028(M-W) \\ & -I_{cl}\{3.96\times10^{-8}f_{cl}\left[(T_{cl}+273)^4-(T_a+273)^4\right]+f_{cl}h_c(T_{cl}-T_a)\}\end{aligned} \tag{2.10}$$

$$h_c = 2.38(T_{cl}-T_a)^{0.25} \text{ or } h_c = 12.1\text{v}^{0.5}, \text{ whichever is greater} \tag{2.11}$$

$$f_{cl} = \begin{cases}1.00+1.29I_{cl} \text{ for } I_{cl} \le 0.078 \text{ m}^2\text{K/W} \\ 1.05+0.645I_{cl} \text{ for } I_{cl} > 0.078 \text{ m}^2\text{K/W}\end{cases} \tag{2.12}$$

PMV is directly related to the Predicted Percentage Dissatisfied PPD index, it is an estimating on human reaction to such temperatures and humidity ratios in the room. This relation is stated as follows.

$$\text{PPD} = 100\text{-}95^{-n} \tag{2.13}$$

Where,

$$n = 0.03353\ \text{PMV}^4 + 0.2179\text{PMV}^2 \tag{2.14}$$

Thermal sensation (*Y)* is another parameter shown usually as an index that reflects the effect of surrounding (humidity, length of exposure) and personal (sex, size) variables on the thermal response and comfort level, Rohles and Nevins [14] predict the thermal sensation for average sexes combined with a standard 3 hour exposure time to be

$$Y = 0.243T_a + 0.000278p_w - 6.802 \qquad (2.15)$$

ASHRAE, which also set a similar scale for the PMV has set a scale for the thermal sensation to vary between -3 and 3: -3 being the coldest and 3 being the hottest as follows:

3= hot

2= warm

1= slightly warm

0= neutral

-1= slightly cool

-2= cool

-3= cold

Another variable studied in the evaluation of comfort levels in a closed working space is the Contaminant Removal Effectiveness (CRE). It is determined by evaluating the average concentration in the breathing zone; the breathing zone is defined as: the region within an occupied space between planes is between 3 and 72 in. (75 and 1800 mm) above floor and more than 2 ft (600 mm) from the walls or fixed air-conditioning equipment [15] concentration at the inlet and at the outlet. And it is given by

$$\text{CRE} = \frac{C_E - C_S}{C_{BZ} - C_S} \tag{2.16}$$

Where C_{BZ} is the mean (average) concentration is the room, C_S is the mean concentration in the supply, and C_E the mean concentration at the exhaust (outlet). Assuming that there is no contaminant in the supply air Eq.16 becomes,

$$\text{CRE} = \frac{C_E}{C_{BZ}} \tag{2.17}$$

2.4 Energy Consumption

Percentage Energy consumption is an important feature to be estimated in our work given by,

$$\%\ Energy\quad Consumptio\quad n = [\frac{\Delta T_{Actual} - \Delta T_{Design}}{\Delta T_{Design}}] \times 100 \tag{2.18}$$

This estimation is based on a 20 ^{0}F temperature difference between the design conditions and the actual temperature difference from our simulations under the same outside conditions.

Chapter 3 - Two Dimensional Simulation of Window Air-Conditioner in an Office Room

3.1 Introduction

The objective of this chapter is to predict the impact of the location of a wall-mounted air conditioner on the thermal comfort by varying discharge angles of the inlet, unit location, and occupant position. This part of the work also compares results to previous CFD work and experimental data from previous work [7, 8].

As Table 3-1 presents the complete set of conditions used in the simulations. Three different sets of simulations were performed, simulation 1 to 3 the inlet angle was changed from 20 to 40 degrees, while the height location of the unit and the position of the occupant were kept constant.

Simulations 2, 4, and 5 considered the changes in the location of the AC unit keeping constant the inlet angle and the position of the occupant. Simulations 2 and 6 represent the changing the position of the occupant while keeping all other parameters constants

All these sets of simulations will allow the analysis of three factors influencing the thermal comfort in the office space: Location of the unit, inlet angle, and position of the occupant.

Table 3-1 Simulation matrix

Simulation Number	Inlet Angle	% Unit Height from Total Height	Position of Occupant
1	20	75%	L1
2	30	75%	L1
3	40	75%	L1
4	30	60%	L1
5	30	90%	L1
6	30	75%	Lx

3.2 CFD Model

The office room was modeled as 2D rectangular region as shown in Figure 3-1**,** with an air conditioning unit at a given height of one of its sides (wall) of the room, a person configured as an upright smaller rectangle placed at a distance from the unit, and a light fixture located at about half the width of the room and placed on the upper horizontal side (ceiling).

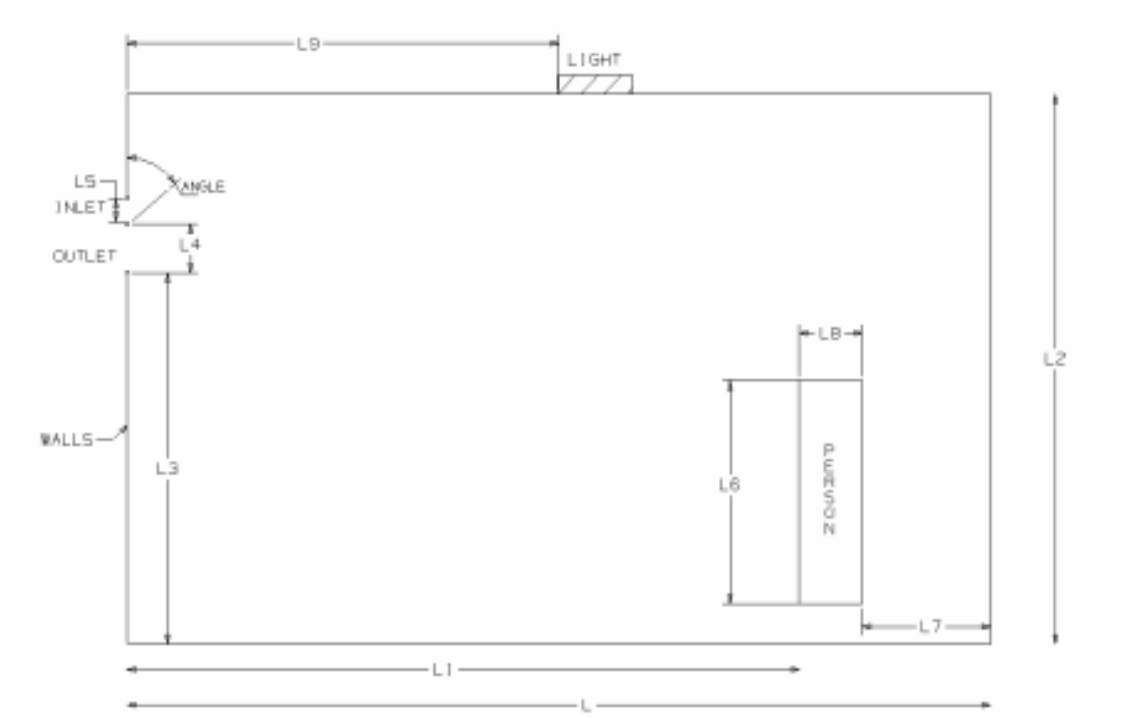

Figure 3-1 Sketch of the 2D model of office room

The numerical values of dimensions L1 to L9 used for the computations in this paper are presented in Table 3-2.

Table 3-2 Dimensions parameters of Fig.3-1, meter(s)

Name	Length	Name	Length
L	4.8	L5	0.2
L1	3.2	L6	1.1
L2	2.7	L7	1.2
L3	1.7	L8	0.2
L4	0.3	L9	2.4

The boundary conditions were chosen in order to complete the computational simulations. As Table 3-3 Shows, these conditions are based on a typical office room cooled by a window AC unit.

Table 3-3 Boundary conditions

Entity	Temperature and Heat Flux	Velocity m/s	Water Vapor Concentration	Contaminant Concentration
Inlet	T=19 ^{0}C	3.50	c1 = 0.01	c2= 0
Walls	T=24 ^{0}C	0	0	
Person	T = 34 ^{0}C	0	Flux=5E-6 kg/(m.s^2)	Flux=1E-8 kg/(m.s^2)
Light	Flux= 50 W/m^2	0	0	0
Outlet	T=0 C Flux=0	0	0	0

The CFD simulations estimated variables such as pressure, velocity, temperature, and contaminant concentration for each cell throughout the entire office in accordance with mass, energy, and concentration equations. For each simulation, velocity and temperature were calculated first by solving the coupled equations, and then species concentrations (water vapor, and contaminant gas) were studied with known a velocity field.

With velocity, temperature, pressure and the species concentration known and using the method outlined by ASHRAE [15], the relative humidity is computed by inputting the temperature and the water vapor concentration executing and for every cell of the studied space.

Thermal sensation was calculated by using the person's immediate surrounding temperature and pressure from the output CFD files and inputting in it into Eq.2.15.

All cases simulated used the boundary conditions presented in Table 3-3. The predicted mean vote (PMV) was calculated using equations Eq.2.9 to Eq.2.12 and the predicted percentage classified (PPD) index was evaluated using equations Eq.2.14 and Eq.2.15. Energy estimation was calculated using Eq.2.18 for each unit location being evaluated. In addition, contaminant removal effectiveness was calculated using Eq.2.13

3.3 Results and Discussion

Figure 3-2 represents the velocity distribution in an office room being cooled by a window air conditioning unit; the figure shows the velocity profile for the base case (simulation 2 in Table 3-1). The velocity vector and magnitude (speed) are illustrated for every section of the studied room. The fluid enters the room from the inlet on the left at angle of 30 at a speed of 3.5 m/s, it is heading for the ceiling when it gets pushed to a steeper angle as incoming air encounters the air coming back from the previous circulations, the fluid then hits the ceiling and flows a parallel path until it reaches the light. Airflow then curves at sharp angle towards the floor, turns towards the left side of the room, flows parallel to the wall then exist through the outlet. Also there are few splits of flow throughout the office room, the most important one is around and away from the person where airflow turns to the opposite wall after hitting the ground and mixes with the incoming air at the light fixture.

Figure 3-3 shows the temperature profile for the basic case, on the side of the unit the temperature remains relatively unchanged and low. Once air gets closer to the person

and the light, temperature rises quickly. Air is considerably warmer at the light and around the person. Also, notice that the temperature is warmer on the other side of the person where the split of airflow around the person as Fig. 3-2 shows.

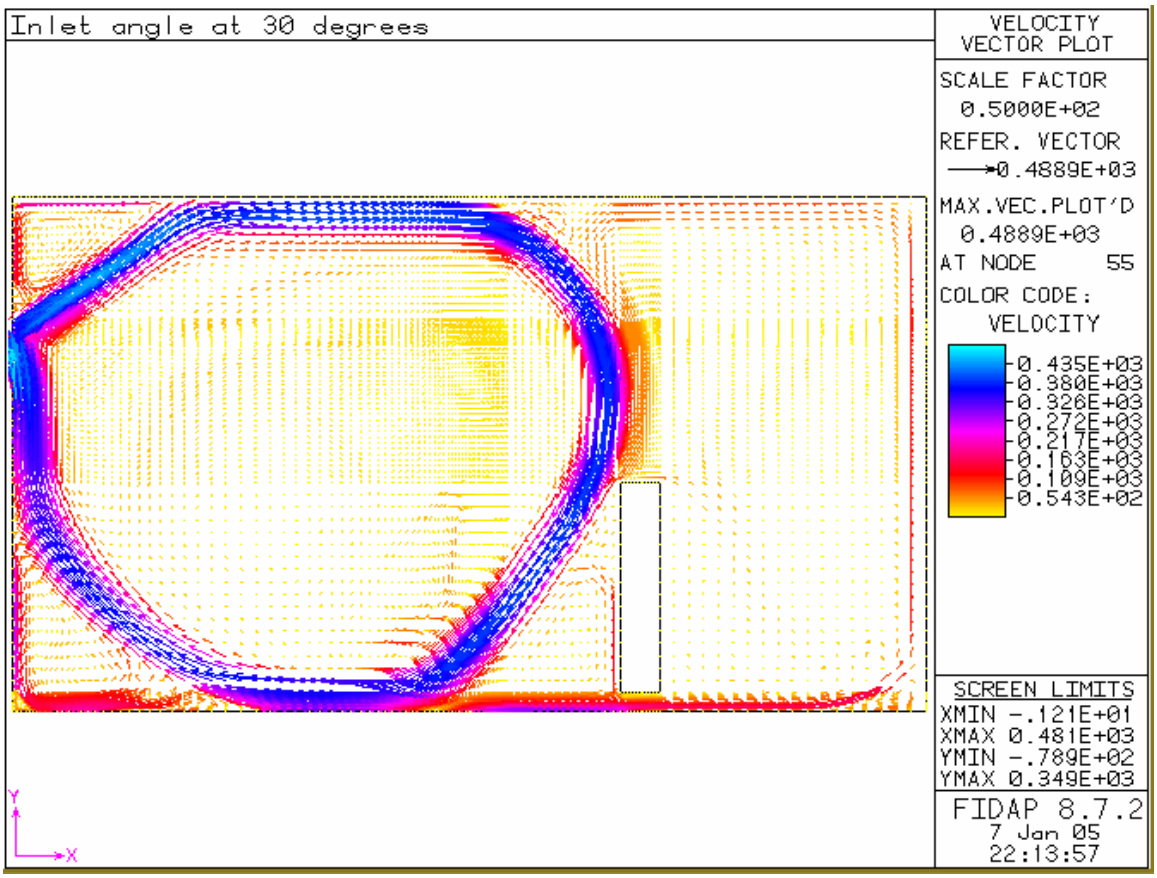

Figure 3-2 Velocity field, base case, values of speed are in (cm/s)

The temperature profile is similar to the analysis of [8] where the vertical cross-section of the plan adjacent to the unit (Fig. 3-2, case b [8]) shows the same pattern inside the room.

Water vapor in the room comes from two sources, the inlet flow and the person's transpiration; Fig.3-4 shows the water vapor concentration, which is used with temperature in order to predict relative humidity at every section of the room. Notice that

the concentration increases once the flow reaches the occupant; the air-vapor mixture collects the vapor from the person and transports on the flow path. The driest section is around the light where the temperature is at its highest and the moistest sections are around the person where transpiration is constant and on the far corner of the room where there is not much linear flow, only a stagnant circular motion of air.

Figure 3-5 indicates contaminant distribution, assuming as in the boundary conditions that the contaminant comes from the person only, is noticeable that contaminant concentration is at its highest around the person. The flow then transports contaminant with different concentrations at different locations.

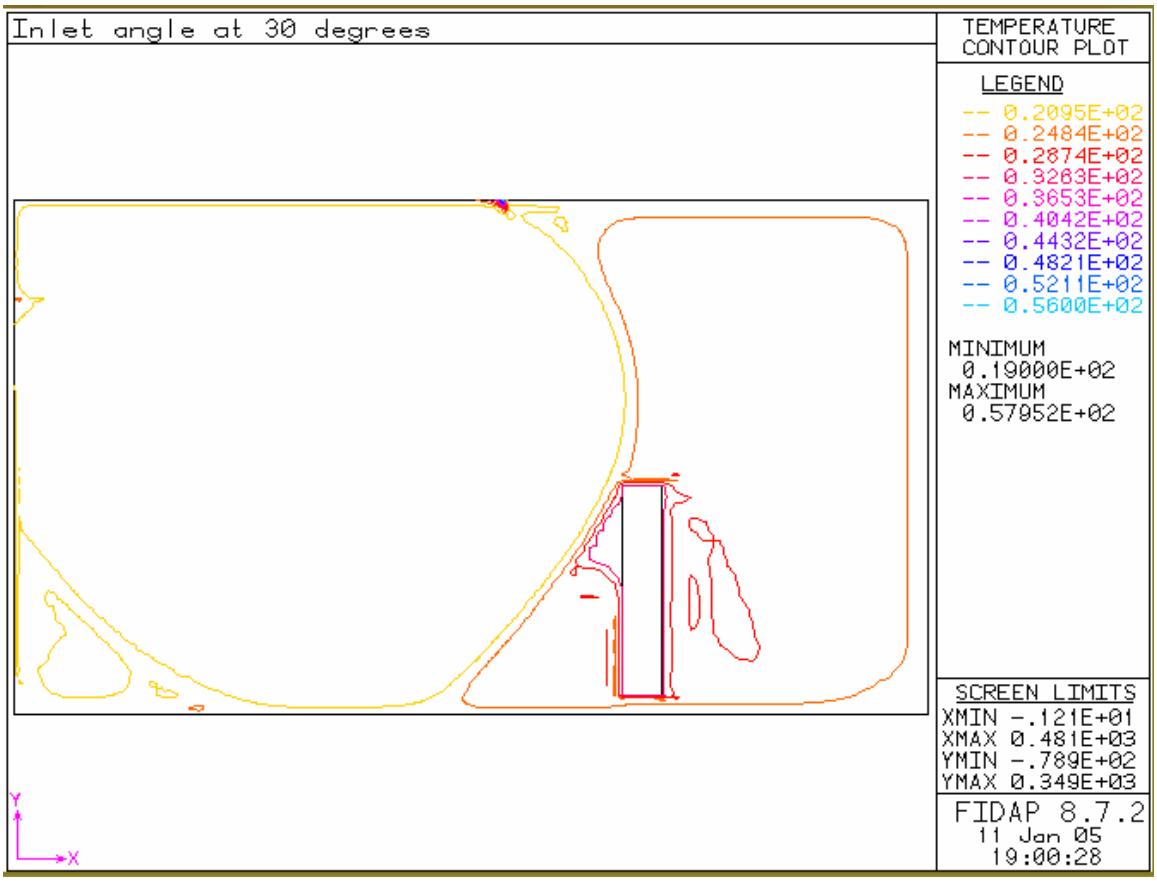

Figure 3-3 Temperature profile, base case

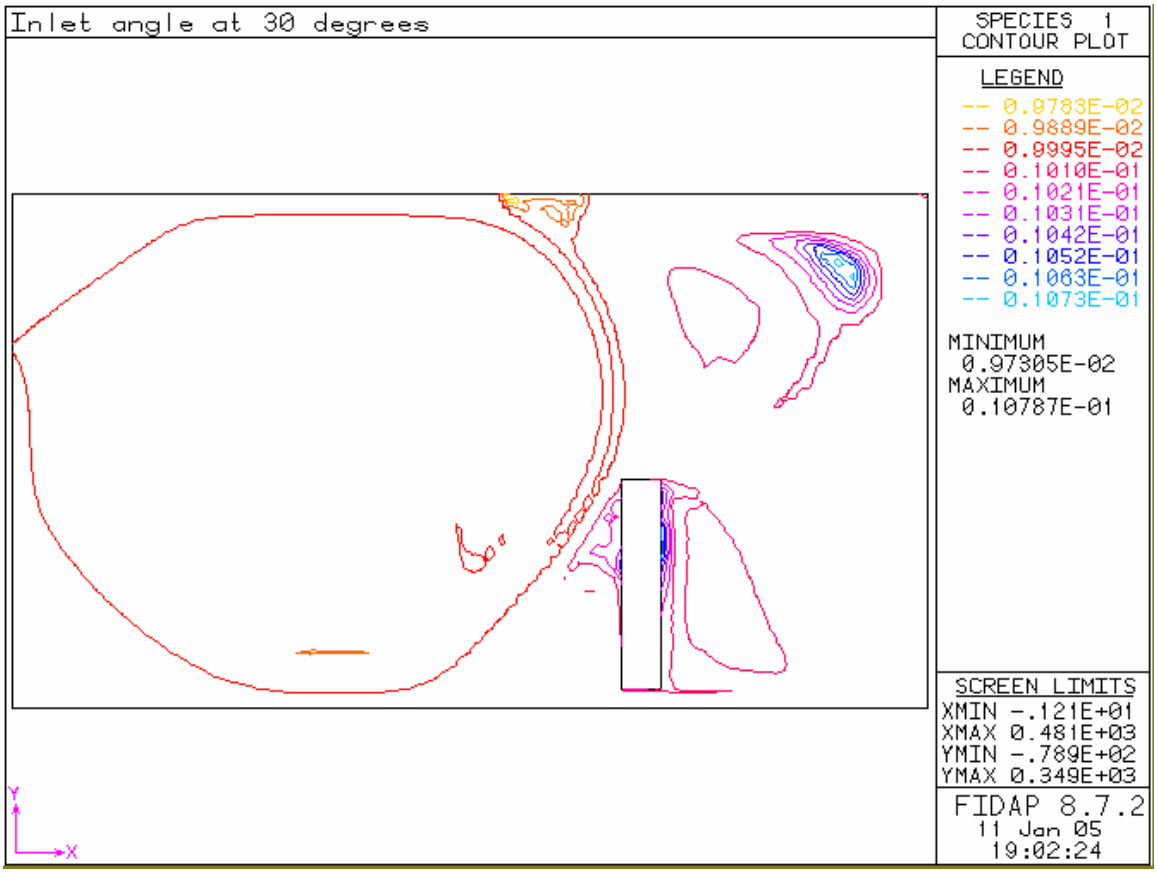

Figure 3-4 Water vapor distribution, base case

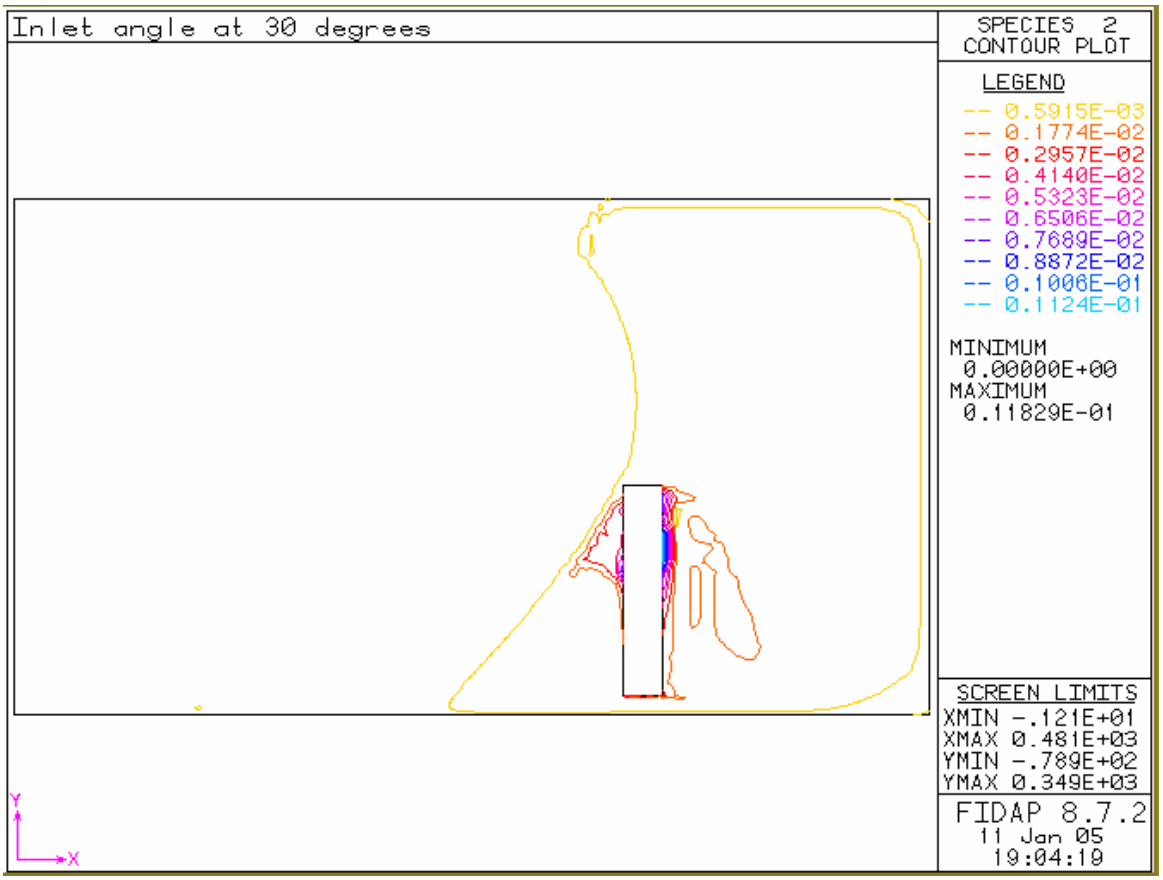

Figure 3-5 Contaminant concentration, base case

When inlet angle is changed to 20 degrees (case1, Table3-1) as Fig.3-6 shows, as predicted the air direction is similar to the base case with the exception that the flow travels along the ceiling for a shorter distance, it is however clear that flow follows almost the same pattern as the previous case and flow split under the occupant is not as significant. This behavior explains the temperature profile shown in Fig.3-7 where warm temperature behind the person is taking a wider region and more cold temperatures are distributed along the walls.

Water vapor is mainly present between the person and the unit where temperatures are cooler, Fig.3-8. This behavior should result in high relative humidity as it is the case. Figure 3-9 displays the contaminant concentration distribution in the office room. Since the occupant is the only source of contaminant, it is normal that the highest concentrations are in the person's immediate surroundings. However, the amount of contaminant transported is lower than the base case.

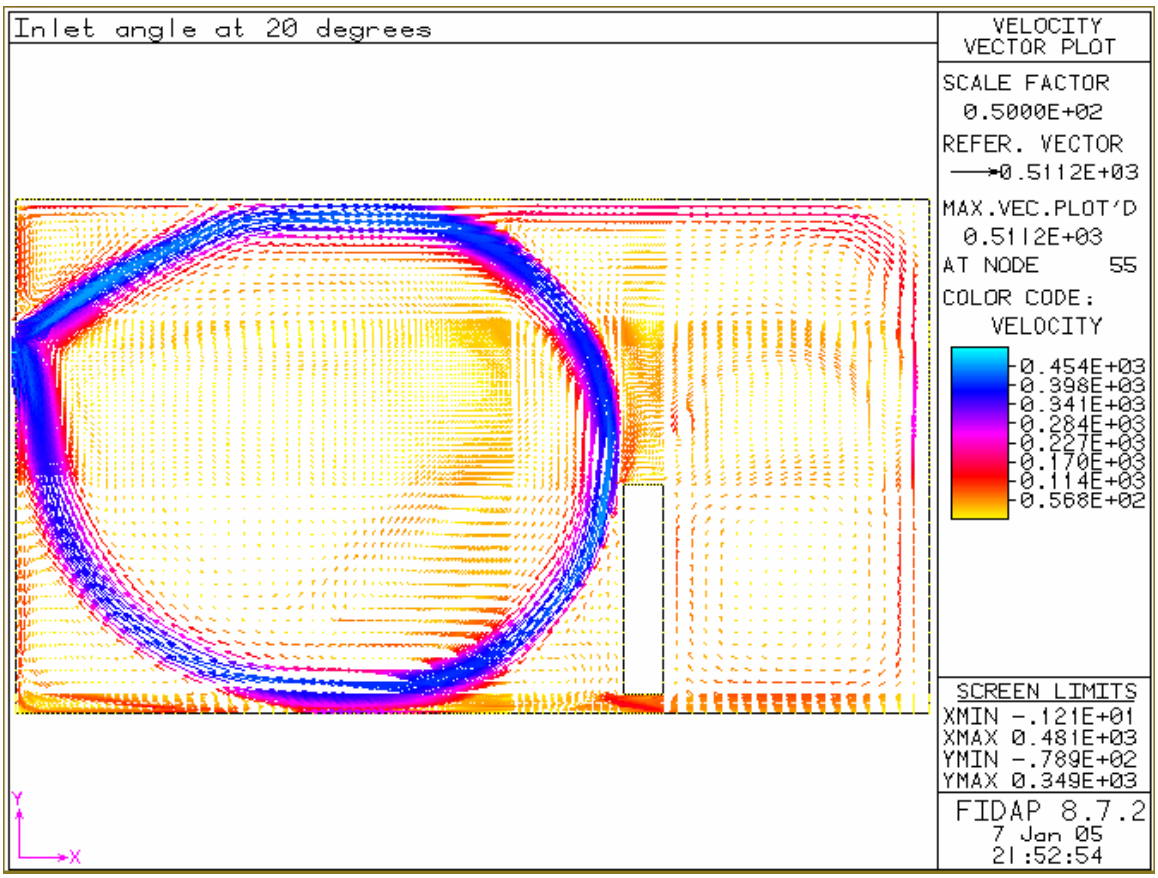

Figure 3-6 Velocity field, 20^{o} inlet angle, values of speed are in (cm/s)

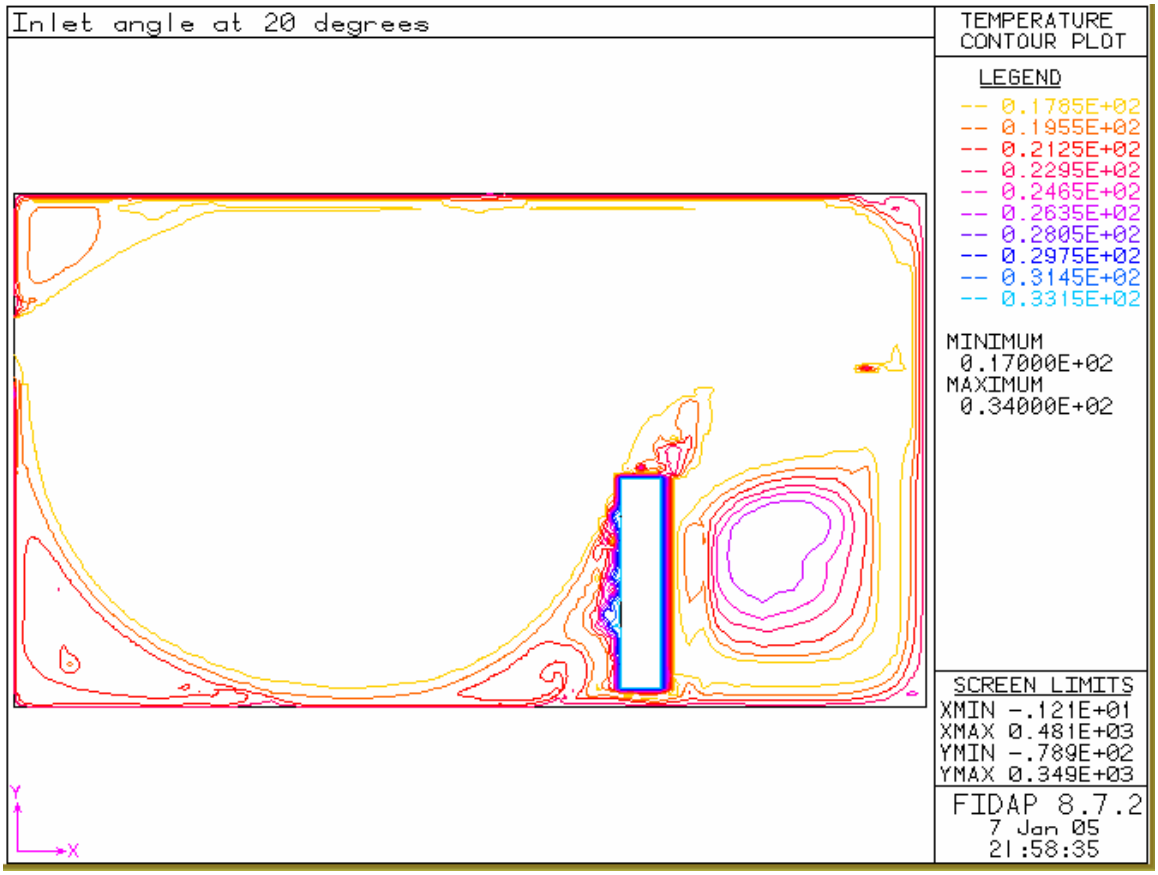

Figure 3-7 Temperature profile, inlet angle at 20^{o}

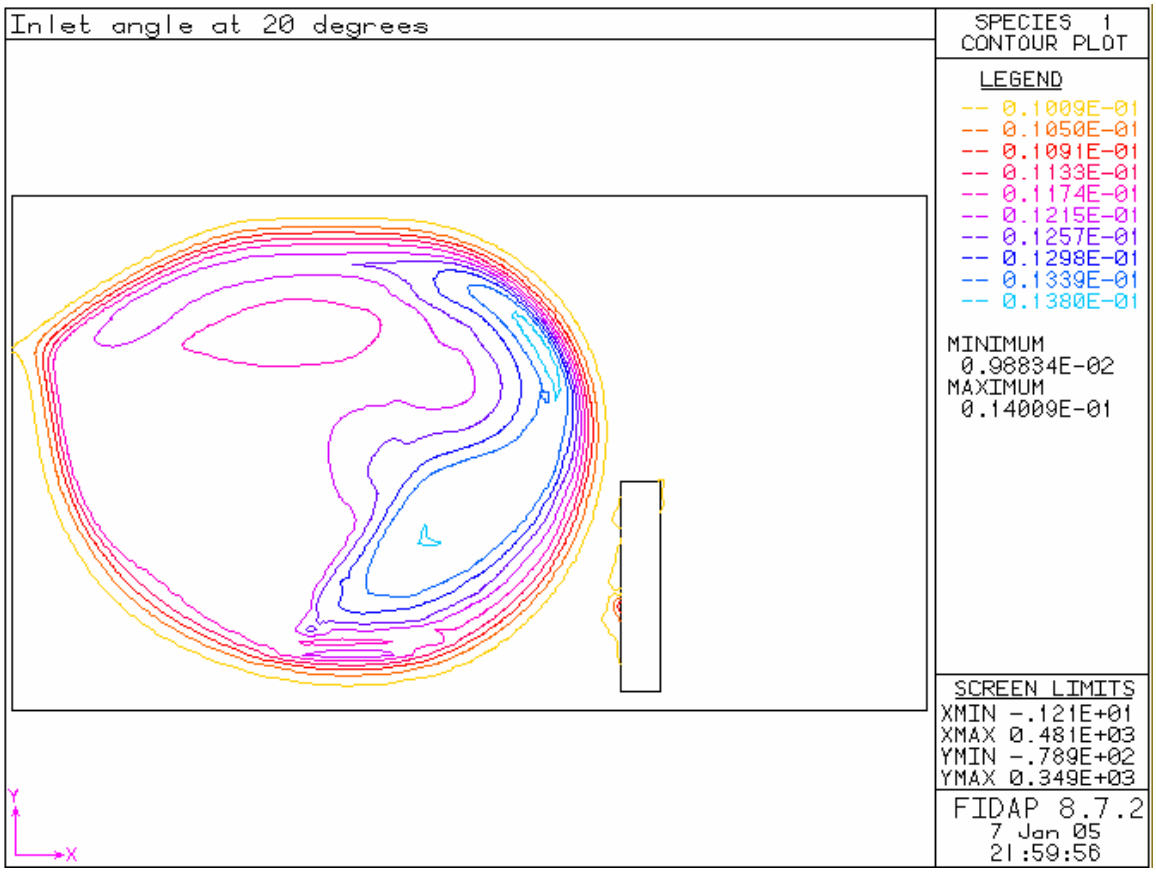

Figure 3-8 Water vapor distribution, inlet angle at 20^{o}

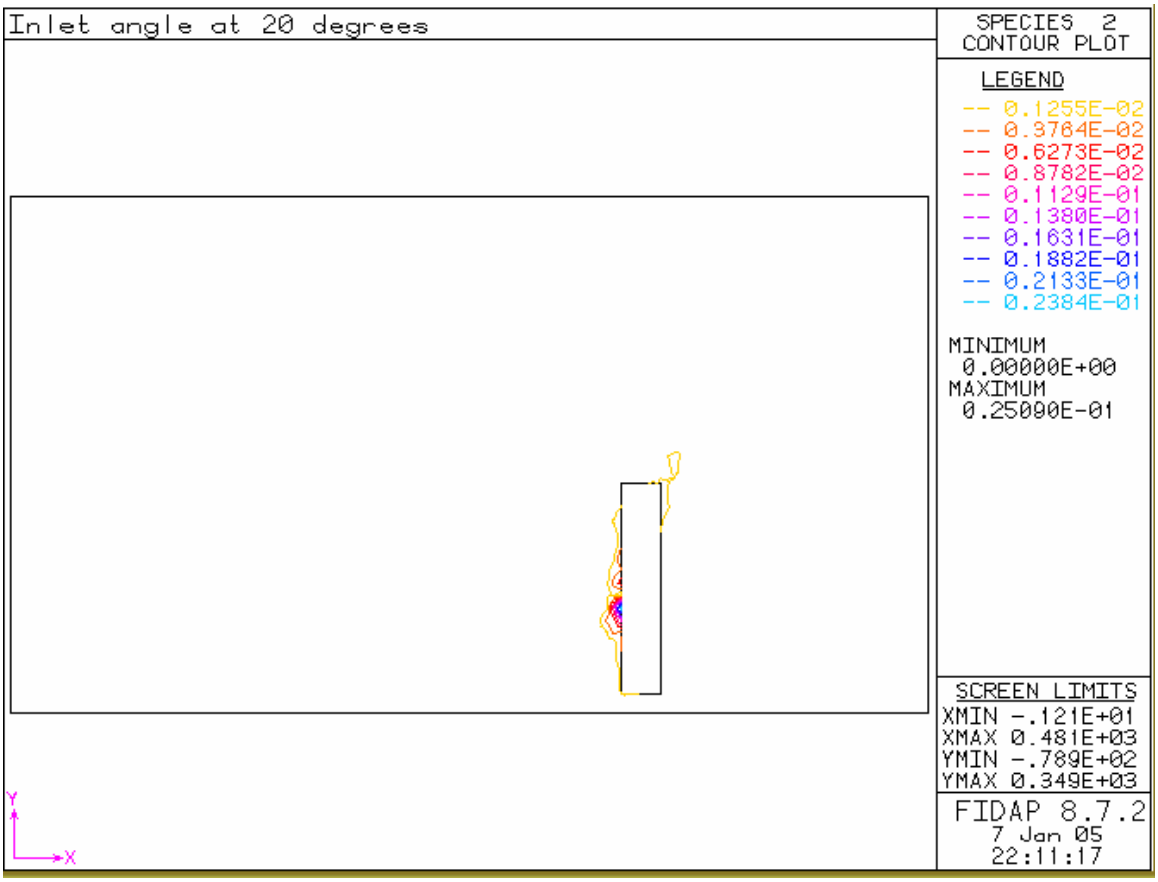

Figure 3-9 Contaminant concentration, inlet angle at 20^{o}

At 40 degrees discharge angle(case3, table 3-1), flow is directed immediately upward making a longer travel along the ceiling with high velocities at the front of the room, between unit and occupant, Fig.3-10. Notice that airflow split under the occupant is significant which allows some of the cold air to travel behind the person.

Figure 3-11 confirms these observations as more cold air is found behind the person; however most of cold air is meanly concentrated between the person and the unit. Immediate surroundings of the person are still fairly warm. Water vapor concentration is low around the occupant indicating a high thermal reading in that region. Even with warm temperature around the occupant, contaminant is removed and transported following the velocity pattern, Fig.3-13. Also contaminant can be found on both sides of the person.

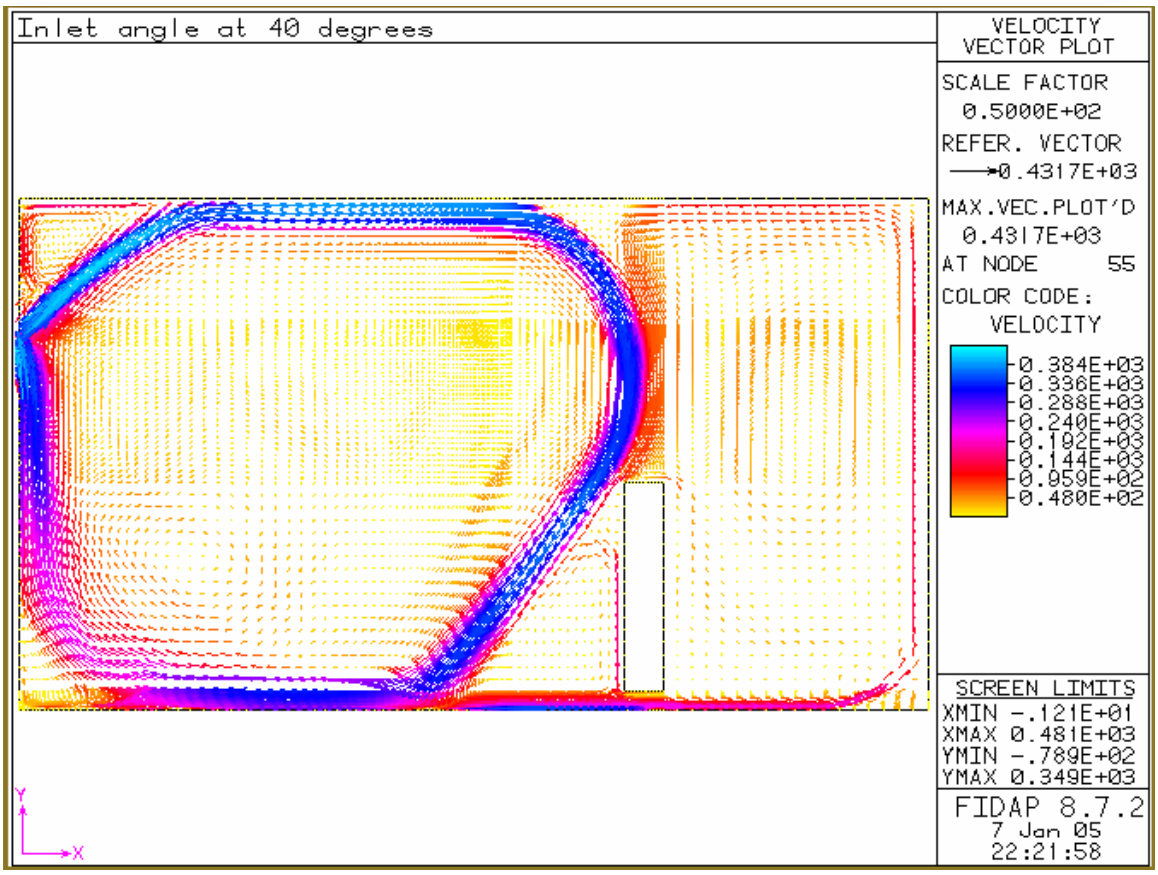

Figure 3-10 Velocity field, 40^0 inlet angle, values of speed are in (cm/s)

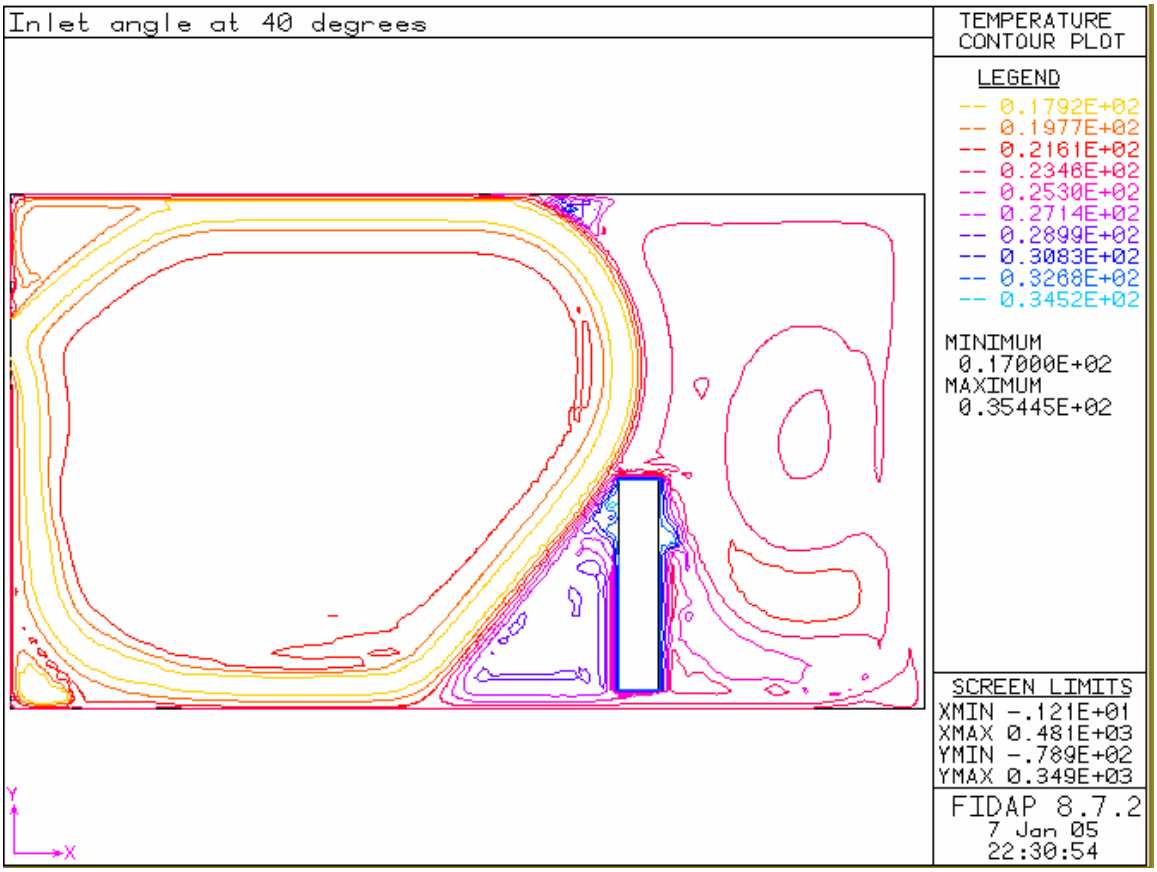

Figure 3-11 Temperature profile, inlet angle at 40^{o}

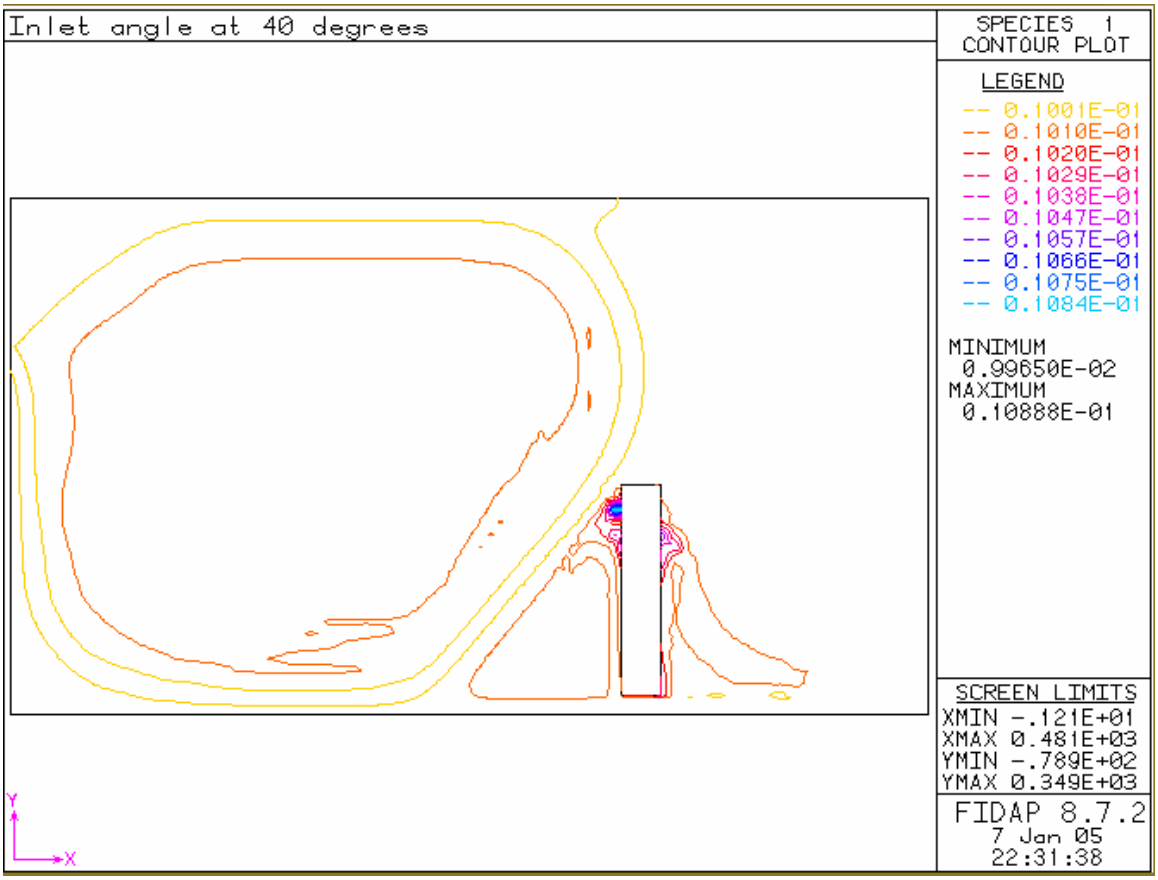

Figure 3-12 Water vapor distribution, inlet angle at 40^{o}

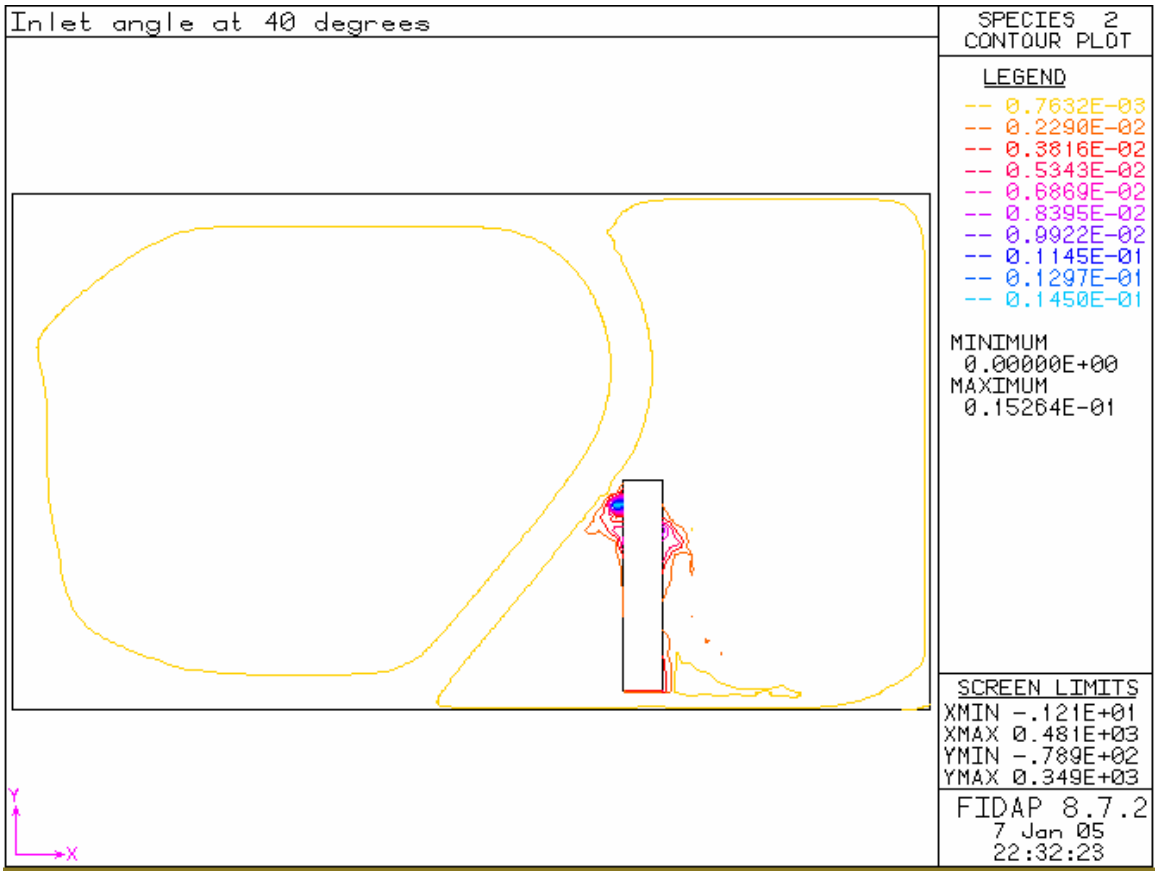

Figure 3-13 Contaminant concentration, inlet angle at 40^{o}

For the second set of simulations, the height of the unit is changed. First, the unit is moved to a height equal to 60% of the total office room height (case4, Table3-1). Notice in Fig.3-14, as airflow enters, it is directly oriented to the ceiling, and the person is directly in the path of the high speed downward flow. Air then splits on the head of the occupant then returns towards the outlet with a portion that travels around the other side of the person.

Figure 3-15 hot air is carried out from the person and from the light fixture, which results in high temperatures, behind the occupant and in the flow path of returned air.

Water vapor is removed from occupant and carried out following the velocity profiles throughout the office room, Fig.3-16. Similar to water vapor, and due to high velocities in front of the occupant, contaminant is removed from the top person to bottom, and high contaminant concentration is also located in the path of the returning air.

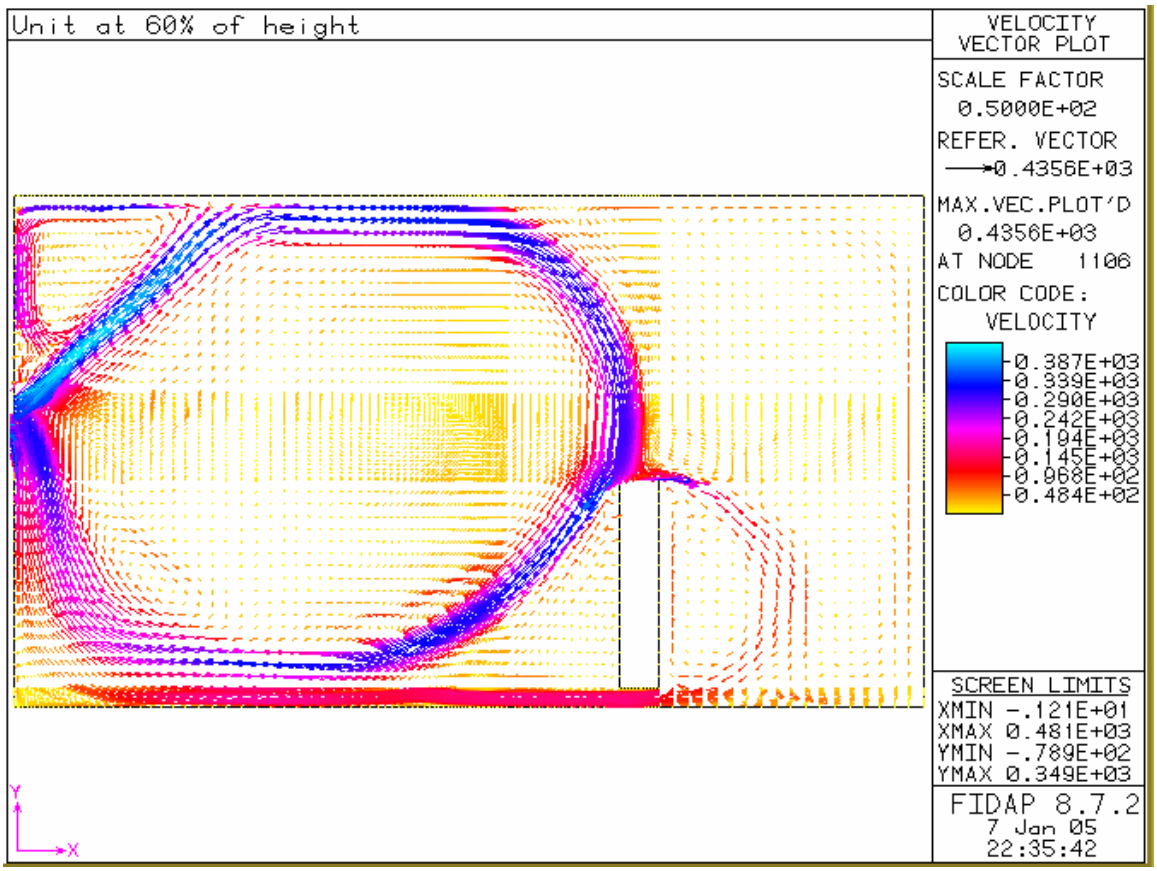

Figure 3-14 Velocity field, unit at 60% of height, values of speed are in (cm/s)

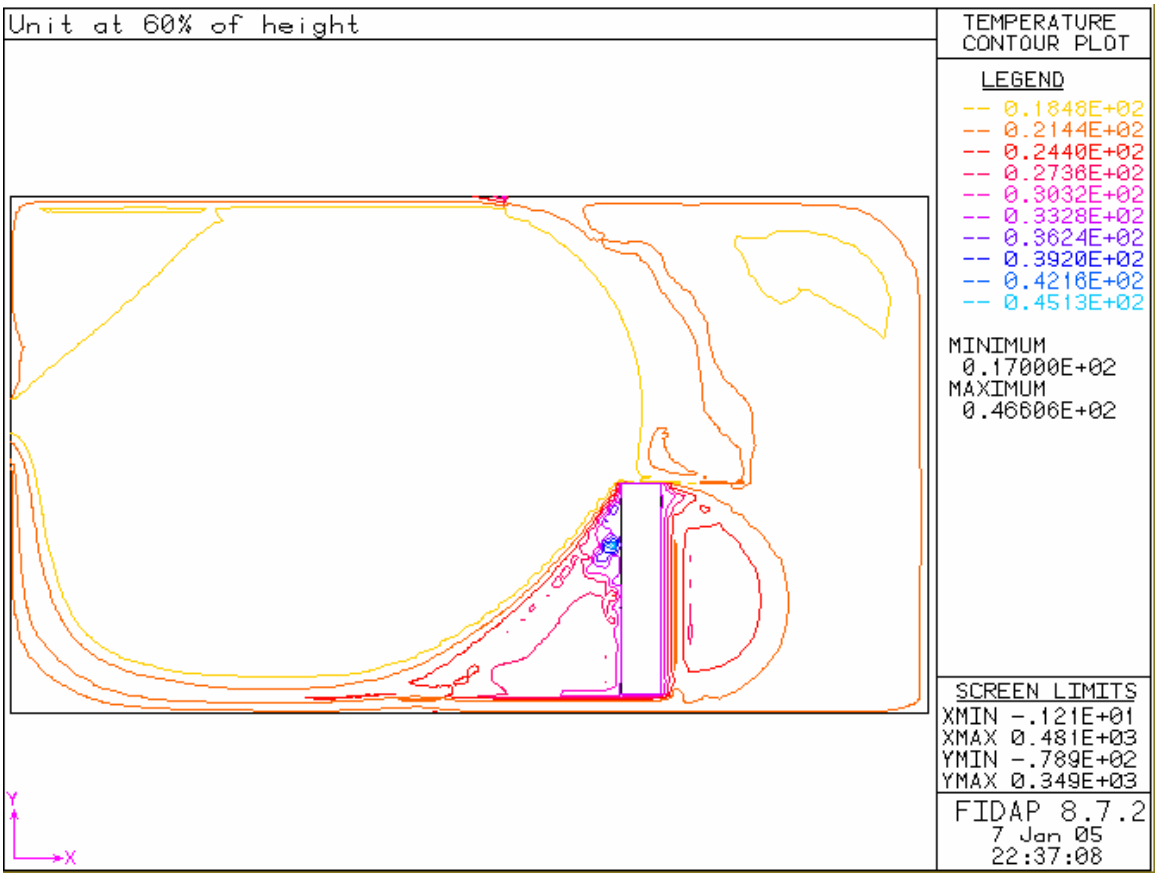

Figure 3-15 Temperature profile, unit at 60%of height

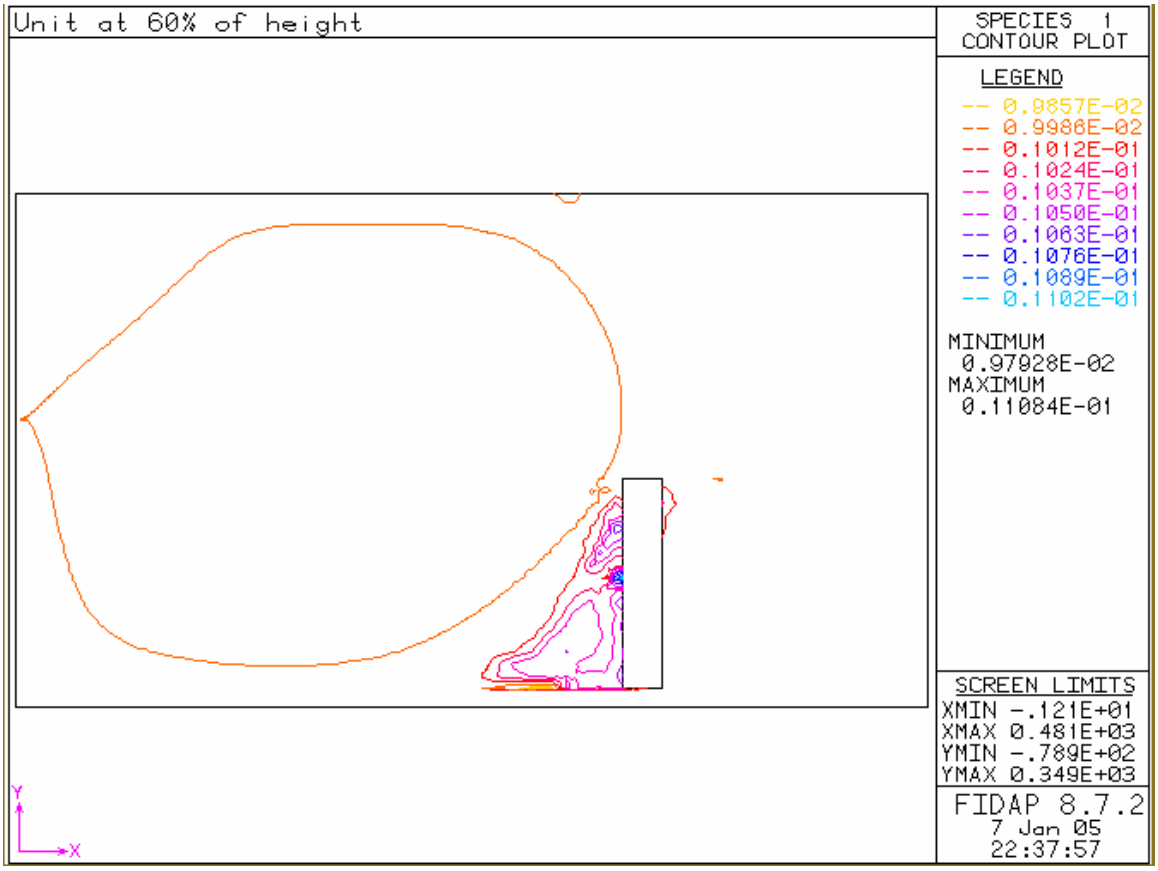

Figure 3-16 Water vapor distribution, unit at 60% of height

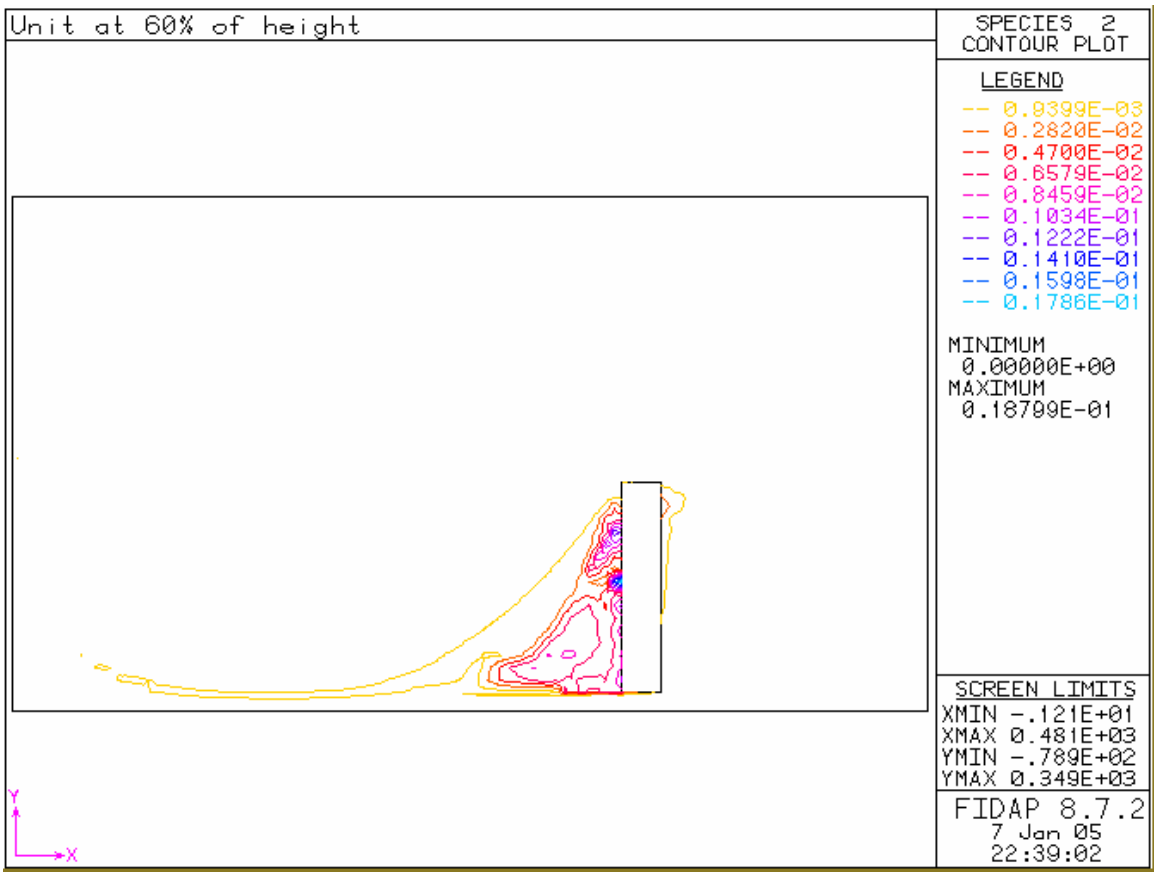

Figure 3-17 Contaminant concentration, unit at 60% of height

The unit is moved now to height equal to 90% of office room height (case 4, Table3-1). From Fig.3-18, the airflow travels at high velocities along the walls then curves towards the floor. The occupant is directly in the flow path. Notice how flow splits on top of the person and is almost evenly divided. Most of the air returns directly to the outlet leaving a significant portion that has to travel around the person before returning. Figure 3-19 shows lower temperatures throughout the office room, notice lower temperatures of the portion that traveled around the person. Also, air from occupant is being cooled before reaching the outlet, opposite to what is shown on Fig.3-15.

Due to colder temperature, more water vapor is noticeable behind the person is this case as Fig.3-20 shows. Notice how the pattern of concentration follows the cold airflow trajectory.

Contaminant in Fig.3-21 is shown to be more efficiently removed compared Fig.3-17, due to high flow velocities experienced by occupant; the concentrations are minimal in the occupant's immediate surroundings

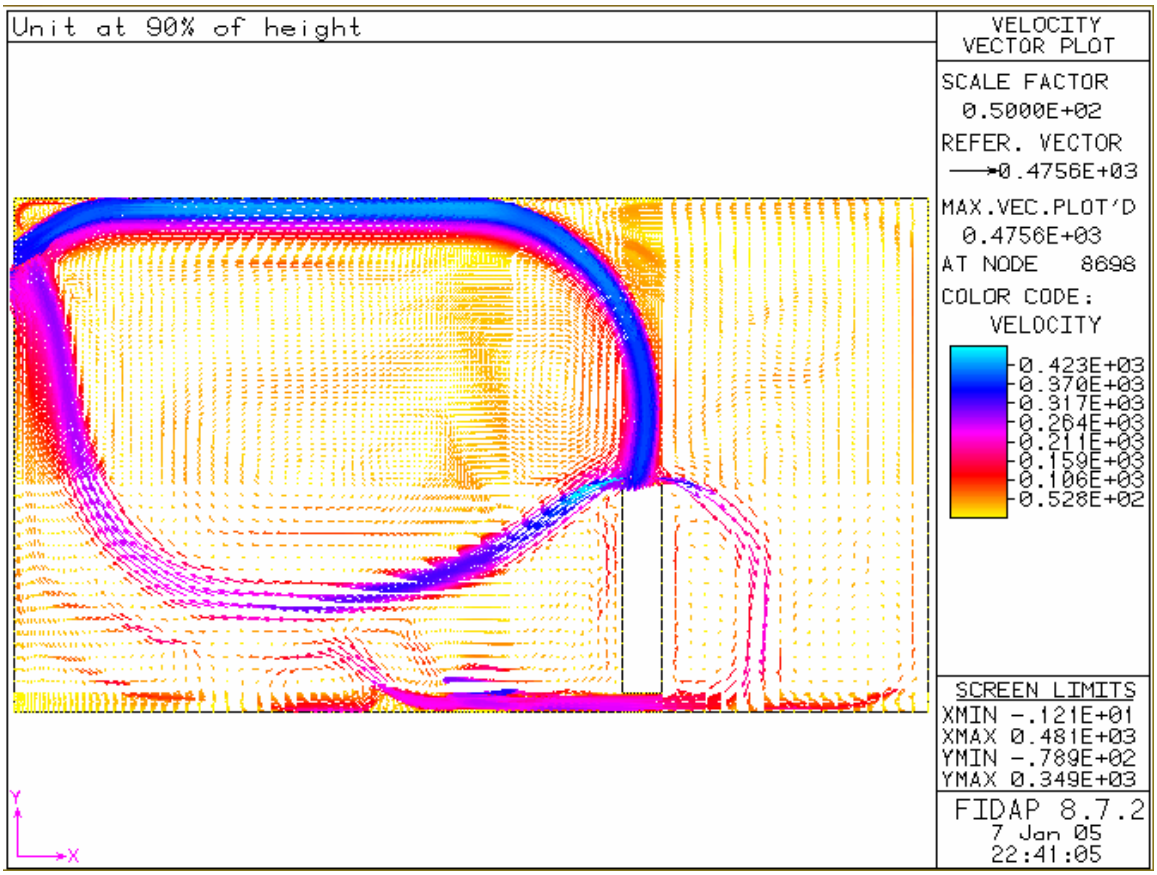

Figure 3-18 Velocity field, unit at 90% of height, values of speed are in (cm/s)

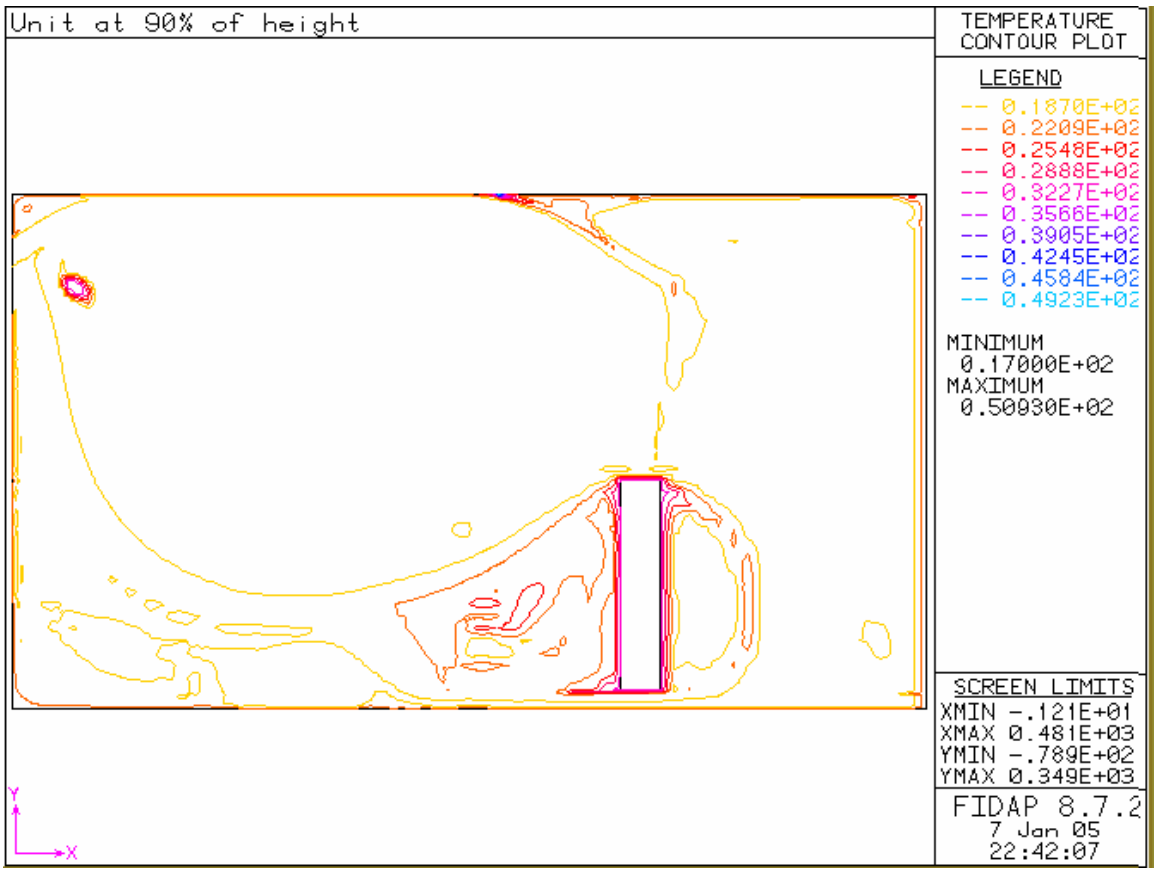

Figure 3-19 Temperature profile, unit at 90% of height

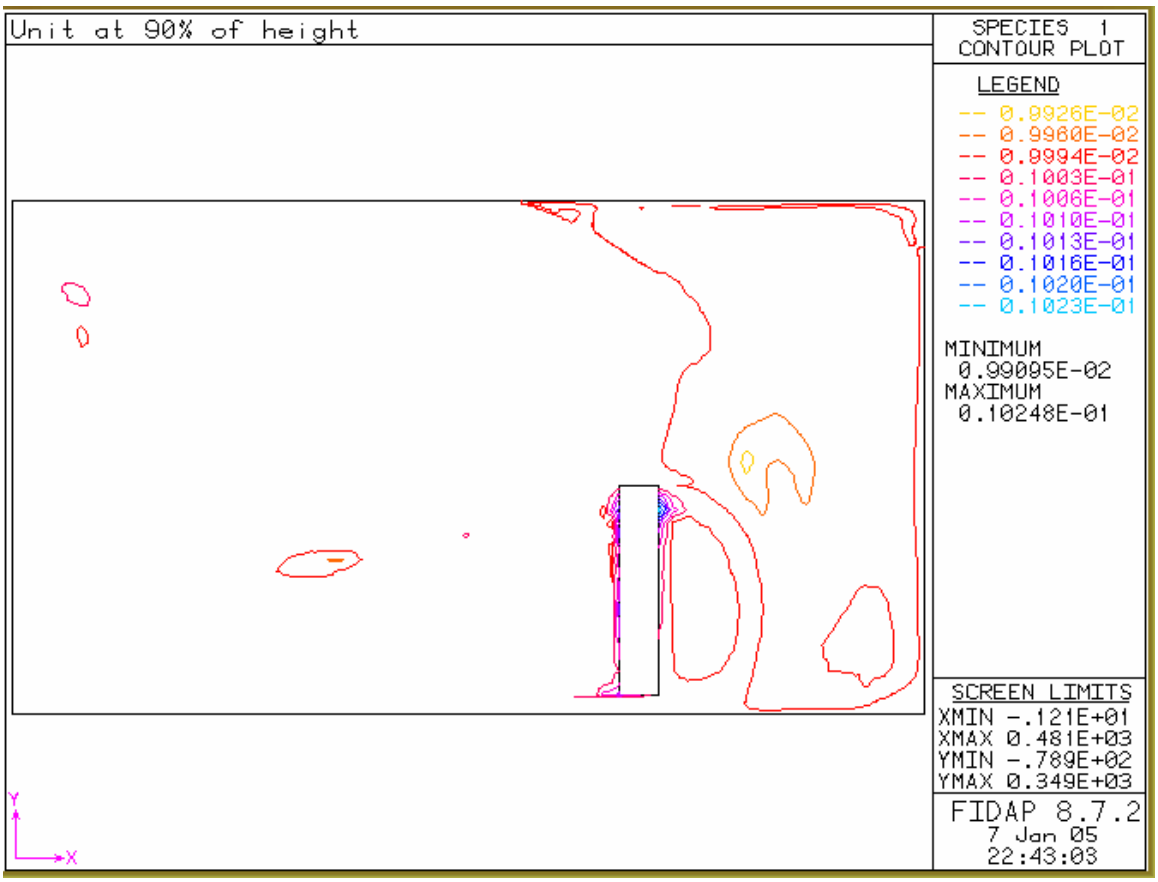

Figure 3-20 Water vapor distribution, unit at 90% of height

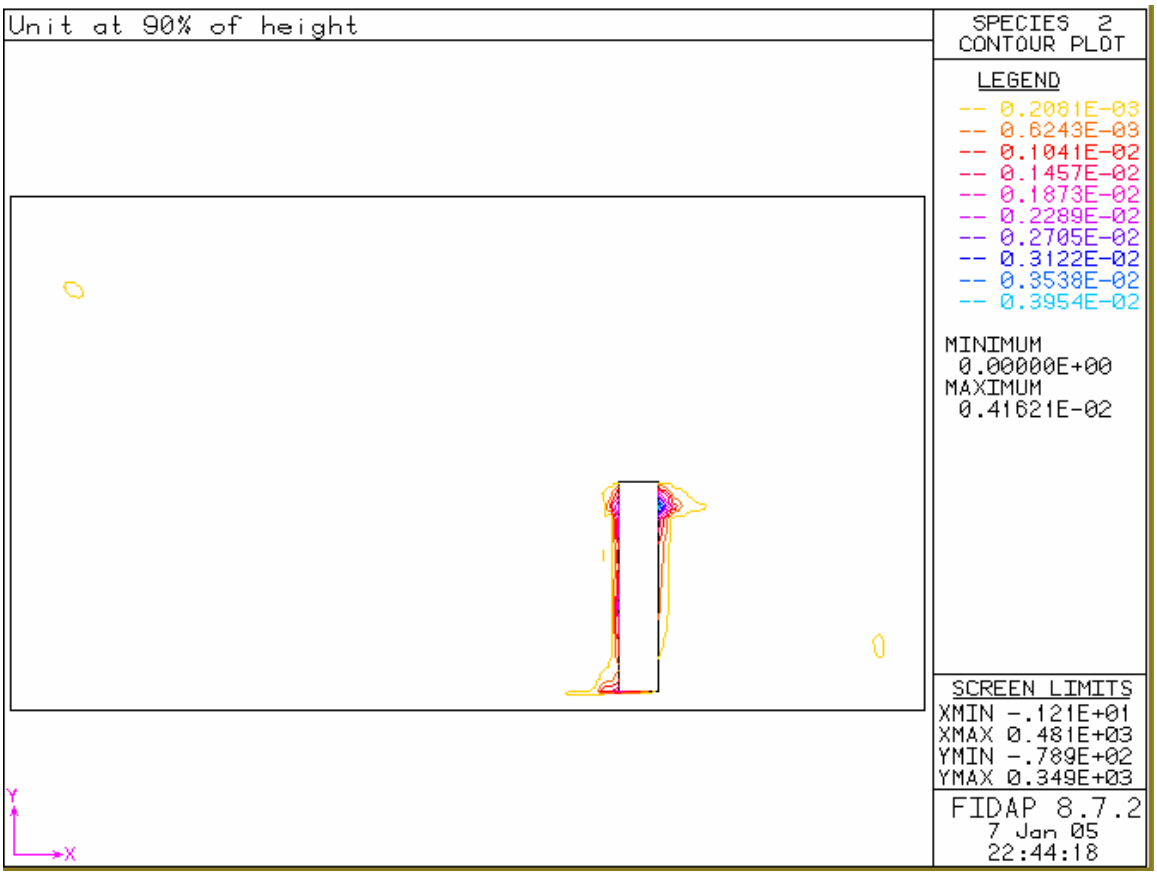

Figure 3-21 Contaminant concentration, unit at 90% of height

Fig.3-23 and Fig.3-24 show the thermal sensation and the predicted mean vote (PMV) as a function of. inlet flow angle for the immediate space around the person. For better prediction of thermal comfort this section focuses on regions expanding 10 centimeters from the person in every direction. However, PMV and thermal sensation take different approaches, thermal sensation correlates comfort level with the length of exposure, temperature, humidity, sex. On the other hand PMV measures the reaction of people to certain conditions, for a particular individual based on activity, air velocity, (metabolic rate), and clothing.

We notice that the thermal sensation is within an acceptable range even when increasing the inlet angle, Fig.3-23. However, the PMV Fig.3-24, indicates the comfort is in the cold side when the angle is low then increases to acceptable comfort as the angle goes up. This shows that not like the PMV, the thermal sensation is independent of the inlet angle. In [7] Similar results were obtained for the temperature the experiment and CFD model Table 3-4. Also they obtained experimentally a comparable PMV= -0.71 and PPD = 16%, versus the present study with PMV = -0.76 and PPD = 17.1%, Table3-5. The difference is meanly because of initial and boundary conditions, like the size of the room, external walls, size of the person, and the inlet angle.

Table 3-4 Comparison of experimental data [7], CFD model [7], and current CFD model

	Temperature [^{0}C]
Experimental data [7]	24.3
CFD [7]	23.3
CFD Current	23.4

Figure 3-22 shows the temperature at a specific height of the room in each of the CFD simulations in addition to the temperature collected using experimental methods [7]. It is noticeable that the pattern of present simulation is lower than the previous one; this can only be explained by the offset parameters chosen for each study.

Table 3-5 Comparison of CFD model [8] and current CFD model

	PMV	PPD %
CFD [3]	0.71	16
CFD	0.76	17

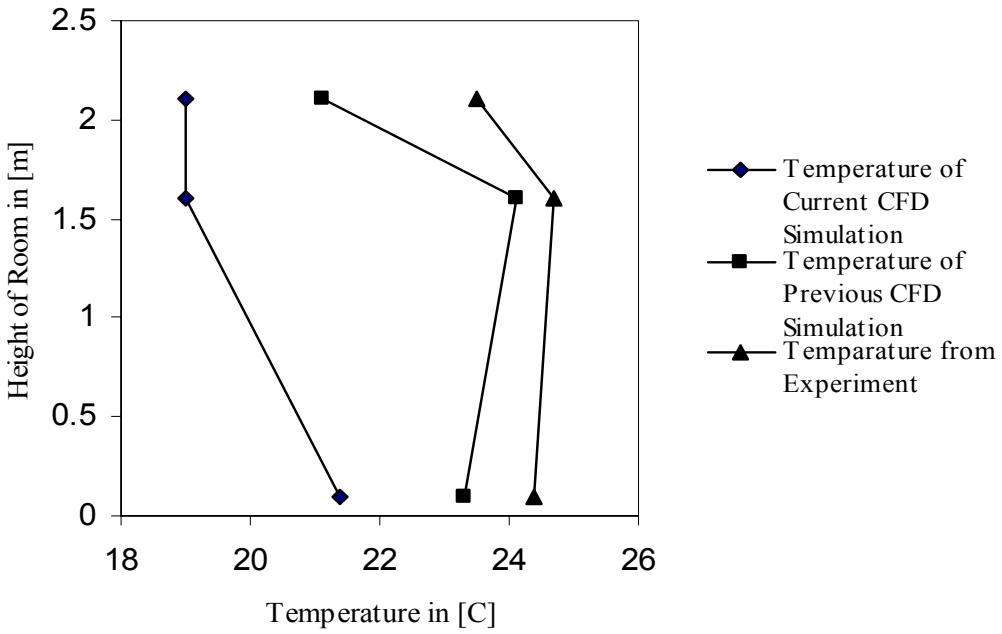

Figure 3-22 Temperature profiles of both simulations and experiment vs. Height

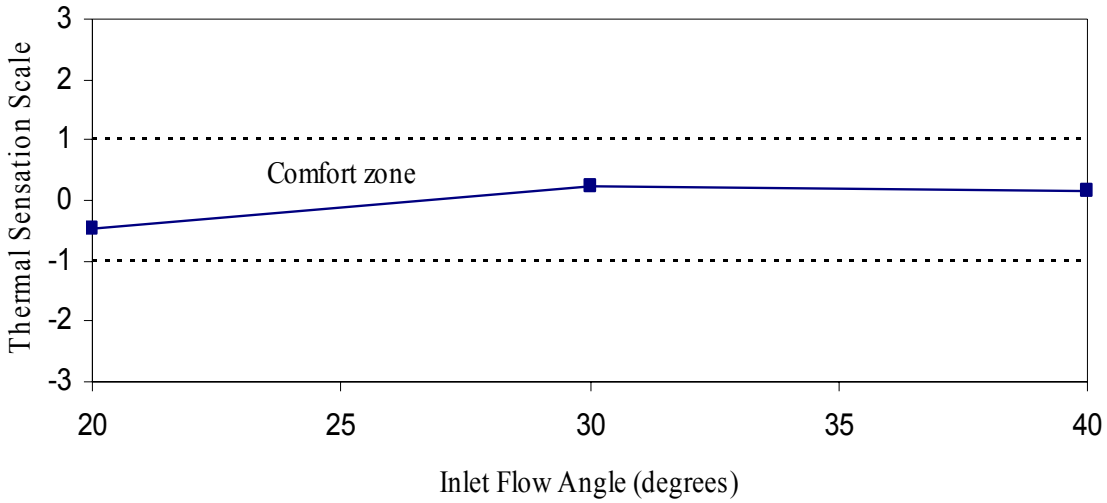

Figure 3-23 Thermal sensation vs. inlet angle

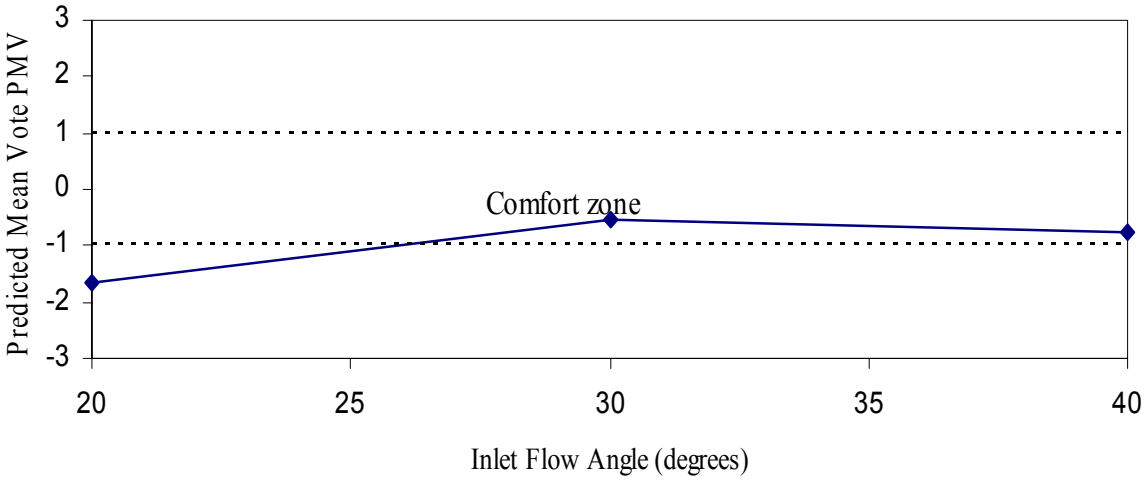

Figure 3-24 Predicted mean vote vs. inlet angle

When varying the height of the air conditioning unit with respect to the base case the thermal sensation shows almost same profile, Fig.3-25. Sensation is cold in both higher and lower cases due cold temperature around the occupant who is located directly in the airflow path. Fig. 3-26 shows PMV very low in high and the low cases due high to velocities. Again, the occupant is in the path of the airflow, he feels great speed air at low temperatures. This should give local thermal discomfort to the occupant especially at unit height of 90% of total office room height. Velocity of airflow in this case is very high coming form the ceiling hitting the occupant straight on thus, creating a very cold zone around him. This observations show in Fig.3-27 and Fig.3-28 where the Percentage Dissatisfied index PPD, which shows the predicted percentage of people that would dissatisfied in such conditions. Since PPD and PMV are directly related, it is only logical that coldest cases invoke the most discomfort for occupants.

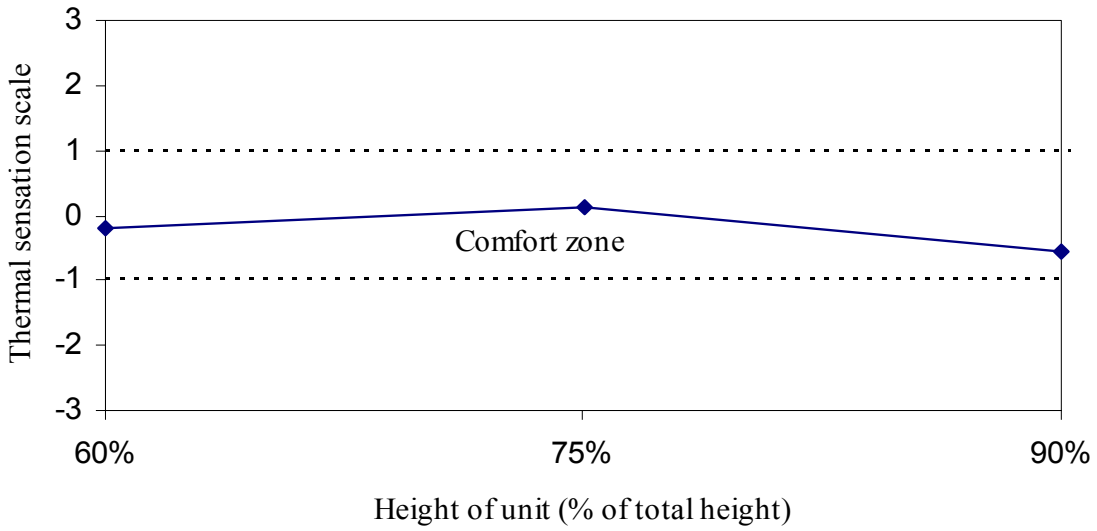

Figure 3-25 Thermal sensation vs. unit height

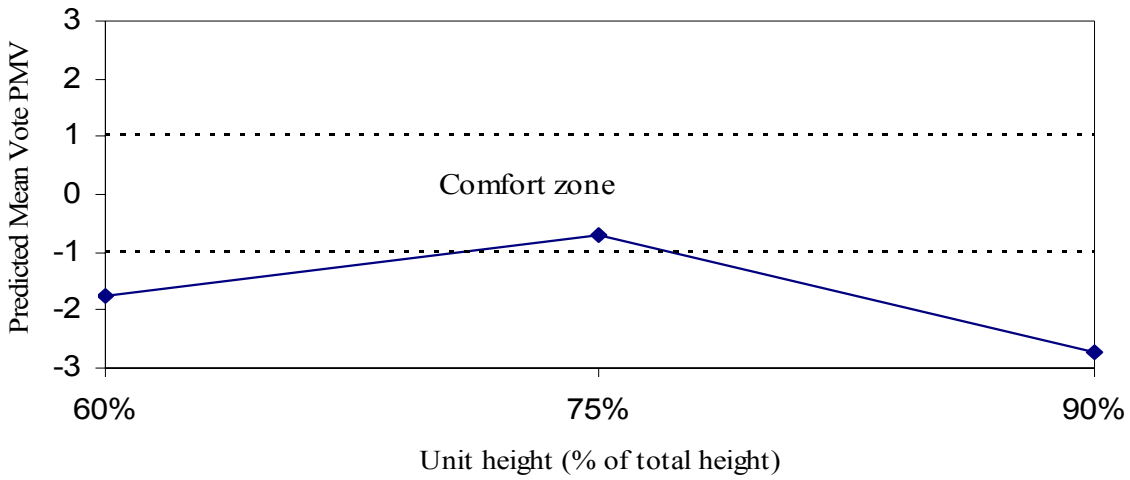

Figure 3-26 Predicted mean vote vs. unit height

Table 3-6 shows that the Thermal sensation, PMV, PPD, relative humidity, and contaminant removal effectiveness. First, the PMV value for position 2 (closer to the unit) is lower than the value for base case; these values are related to the high airflow velocities around the occupant at position 2. Notice a local discomfort PPD of 65% at position 2 compared to only 15% for the base case, a sharp increase on the amount of people that could feel uncomfortable if they only move to the middle of the office room. Even though the thermal sensation shows both case within the comfort zone, the speed of flow so much greater in position 2 thus not preferable for occupants to be in that position

Table 3-6 Conditions of the second position (closer to the unit) compared with base case

	Base Case (Position 1)	Position 2
PMV	-0.6842	-1.80
PPD%	14.8417	64.96
RH%	61.8400	56.55
Thermal Sensation	0.1405	-0.17
CRE	0.0138	0.47

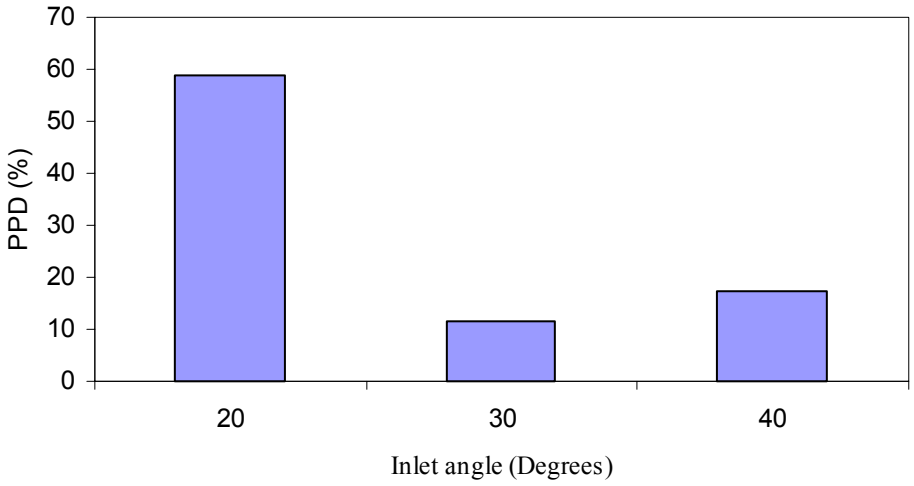

Figure 3-27 Predicted percentage dissatisfied (PPD) vs. inlet angle

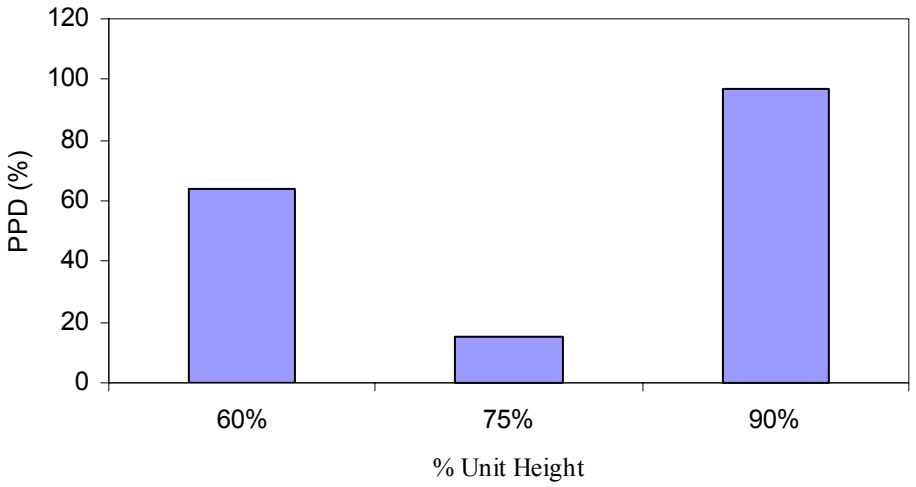

Figure 3-28 Predicted percentage dissatisfied (PPD) vs. unit height

Table 3-7 shows an average relative humidity in every simulation, which in fact is in each case an average value taken for all the local relative humidity using local temperatures and water vapor concentrations

Table 3-7 Simulations and relative humidity

Simulation Number	Inlet Angle	% Unit Height from Total Height	RH %
1	20	75%	69.21
2	30	75%	61.84
3	40	75%	56.61
4	30	60%	66.58
5	30	90%	69.96
6	30	75%	56.55

.

The CRE Contaminant Removal Effectiveness is shown in Table 3-8 as a dimensionless Ratio between the average concentrations of the contaminant in the occupied zone (Breathing Zone) and the contaminant at the outlet. In the first set of simulations, 1 to 3, Table 3-1, where the inlet angle was the variable keeping everything else constant. Notice that at lower inlet angle (case 1) the CRE is higher compared with cases 2 and 3. This is due to fact the more of the occupant's body is in the path of the airflow, which results in more contaminant removed from the surroundings of the occupant. The second set of simulations, 2 (base case), 4 and 5 Table 3-2, for window air conditioner location at high height (90% of total office room height, case 4, Table 3-1) and at low height (60% of total office room height, case 5, Table 3-1), more air is hitting the occupant directly from the ceiling, air speed and temperature around the occupant explain the CRE number being higher then the base case, the high velocity airflow takes more contaminant cases 4 and 5 however, compared to case 1, Table 3-2, low temperatures prevent removing more contaminant. The third set of simulation case 2 (base case) and case 6 from Table 3-1, notice that high airflow velocity around the person allows a better removal of contaminant compared to the base case where the velocity magnitude is smaller.

Table 3-8 Simulations and contaminant removal effectiveness

Simulation Number	Inlet Angle	% Unit Height from Total Height	CRE
1	20	75%	2.75
2	30	75%	0.014
3	40	75%	0.27
4	30	60%	1.108
5	30	90%	1.84
6	30	75%	0.47

From Fig. 3-29, Fig. 3-30 and Table 3-9 show the impact of the window air conditioner location on energy consumption. This following evaluation using Eq.18 is based on a nominal case where the difference between the outside temperature and the average room temperature is 20^0F. Notice that there is energy consumption of around E_i =3.36% for the worst case possible in the first set of simulations (cases 1, 2, and 3) is when the inlet angle is 20^0 Fig.3-29, this is because in case 2 Table 3-2 the relative humidity is maximum out of all three simulations as shown in Table 3-7. On the other hand the energy consumption for the height variation set of simulations (cases 2, 4, and 5 respectively) is around E_i =3.51% for 90% height of the AC unit shown on figure 14. Again, notice that the relative humidity in this case is at its maximum value from as shown in Table3-7.

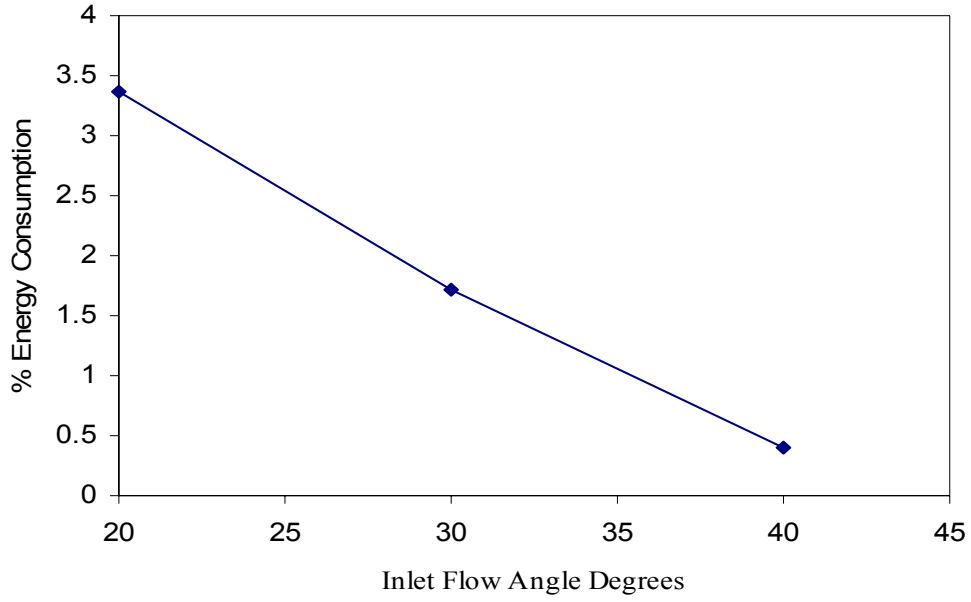

Figure 3-29 % Energy consumption vs. inlet angle

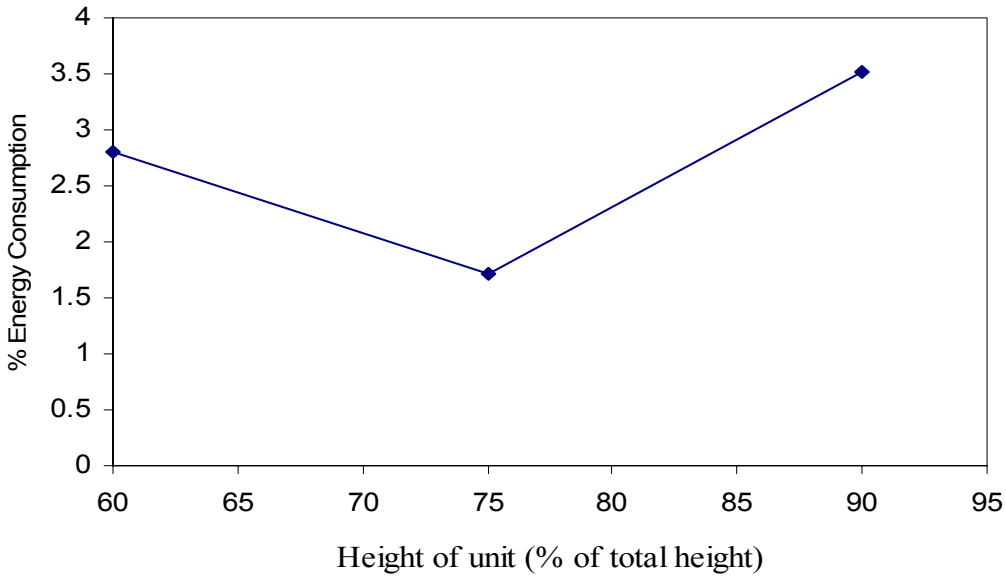

Figure 3-30 % Energy consumption vs. unit height

Table 3-9 shows that the minimum energy expenditure E_i=0.388% is when the occupant is close to the air conditioning unit showing that the average temperature of the

room is lower in this case. This is a plausible result looking at the relative humidity Table 3-7, since the relative humidity is at its lowest in when the person is in the middle of the room.

Table 3-9 Changing occupant position and % energy Consumption

Base Case	% Energy Consumption
Position 1	1.713
Position 2	0.388

Chapter 4 - Three Dimensional Simulation of Window Air-Conditioner in Office Rooms

4.1 Introduction

The chapter provides a detailed analysis of three-dimensional mixed convective flow induced by a window air conditioning system. It also intends to extend the understanding of location of wall-mounted units and their effect on human comfort. It is very important that computational models be made in three-dimensional simulations, doing so, all the relevant characteristics of fluid flow and heat transfer can be captured and analyzed. Temperature, relative humidity, contaminant concentration, and velocity profiles of both horizontal and vertical cross sections are studied and compared. In addition, when modeling three-dimensional simulations, fewer assumptions have to be made, this makes results more compatible to actual encountered cases.

Other studies in energy and environmental analysis were conducted using 3D modeling in order to have a better understanding of rooms cooled by wall type air conditioners, comparing and evaluating different CFD softwares for the same simulation [16]. Also studies have focused on only air conditioning diffuser angles and their influence on comfort level in computer rooms [17].

4.2 CFD Model

In this chapter, the CFD software Fluent was used in two phases. First, GAMBIT was utilized to make the model office room with a unit, an occupant, and a light fixture. Also, GAMBIT was used mesh the model. Then FIDAP was used to analyze the office room using all assumptions and boundary conditions. Modeled room size was 4.8m (length) x 3.7m (width) 2.7m (height) and unit was at manufacturing ratio dimensions between inlet and outlet. Also the light fixture was modeled in the center of the ceiling and with standard size.

The turbulent model used to numerically compute all properties was Mixing-length model with segregated solution scheme. Due to the size of the office room, mixing-length model was chosen because it's high precision and reduced memory use and computation time.

The room was modeled as a 3D cube as shown is Figure 4-1 with and air conditioning unit at one vertical side, and a person represented by a smaller vertical cube positioned at an offset from the center. Also, the light fixture is represented by a section area on the upper horizontal plane of the cube (ceiling).

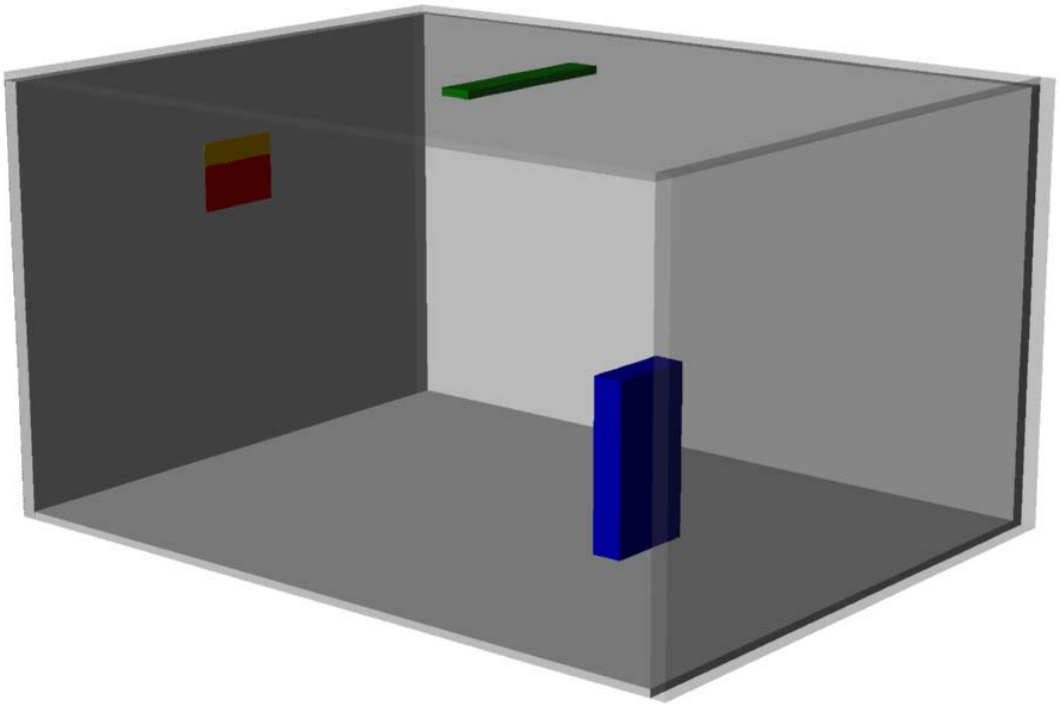

Figure 4-1 Layout of the 3D simulated office room

Table 4-1 shows corresponding dimensions of the simulated office room,

Table 4-1 Simulation dimensions

Name	Length	Name	Length
L	4.8	L5	0.2
L1	3.2	L6	1.1
L2	2.7	L7	1.2
L3	1.7	L8	0.2
L4	0.3	L9	2.4

Table 4-2 gives the boundary conditions used form this simulation, these values of temperature, fluxes, and concentrations are taken from a typical application for a wall mounted air conditioning unit used to cool an office.

Table 4-2 Simulation boundary conditions

Entity	Temperature and Heat Flux	Velocity m/s	Water Vapor Concentration	Contaminant Concentration
Inlet	T=19 ^{o}C	3.50	c1 = 0.011	c2= 0
Walls	T=24 ^{o}C	0	0	
Person	T = 34 ^{o}C	0	Flux=5E-7 kg/(m.s^2)	Flux=1E-5 kg/(m.s^2)
Light	Flux= 50 W/m^2	0	0	0
Outlet	T=0 C Flux=0	0	0	0

Velocity and temperature were calculated first by solving the coupled equations, and then species concentrations (water vapor, and contaminant gas) were studied with known a velocity field. Relative humidity is computed by inputting the temperature pressure, water vapor concentration and executing for every cell of the studied space using Temperature, pressure, and water vapor concentration using the method outlined by ASHRAE [12]

The simulations were done in three runs, where inlet angles were set at 20^{o}, 30^{o}, and then 40^{o}. First, the simulation with a 30^{o} inlet angle then 20^{o} and 40^{o} respectively. On the output files six cross-sectional (planes) were studies as Table 4-3 shows, the six planes studied, three horizontal and three vertical, and their location with respect to the office room.

Table 4-3 Cross-sectional planes examined

Plane	Orientation	Coordinates in [m]
1	Vertical	Y = 1.85
2	Vertical	Y = 0.975
3	Vertical	Y = 2.825
4	Horizontal	Z = 1.35
5	Horizontal	Z = 0.675
6	Horizontal	Z = 2.025

The examination of these six planes will allow a detailed analysis of the heat transfer and thermal comfort associated with air movement and temperature inside the office room.

4.3 Results and Discussion

4.3.1 Simulation with 30^{o} inlet angle

Temperature distribution throughout the room is analyzed first in the three vertical planes shown in Fig.4-2, Fig.4-3, and Fig.4-4. In Fig.4-2 the temperature rises around the light fixture and the occupant, the heat transfer from the light is very significant because of the high local temperature. The same is true around the occupant where the surrounding air gets warmer as it get closer to the person. Fig.4-3 and Fig.4-4 are identical in describing the temperature profile as expected by the symmetry of the simulation and the position of the planes studied, the temperature magnitude is on the low side since from both ends; the two studied planes do no intersect with the person and the light fixture

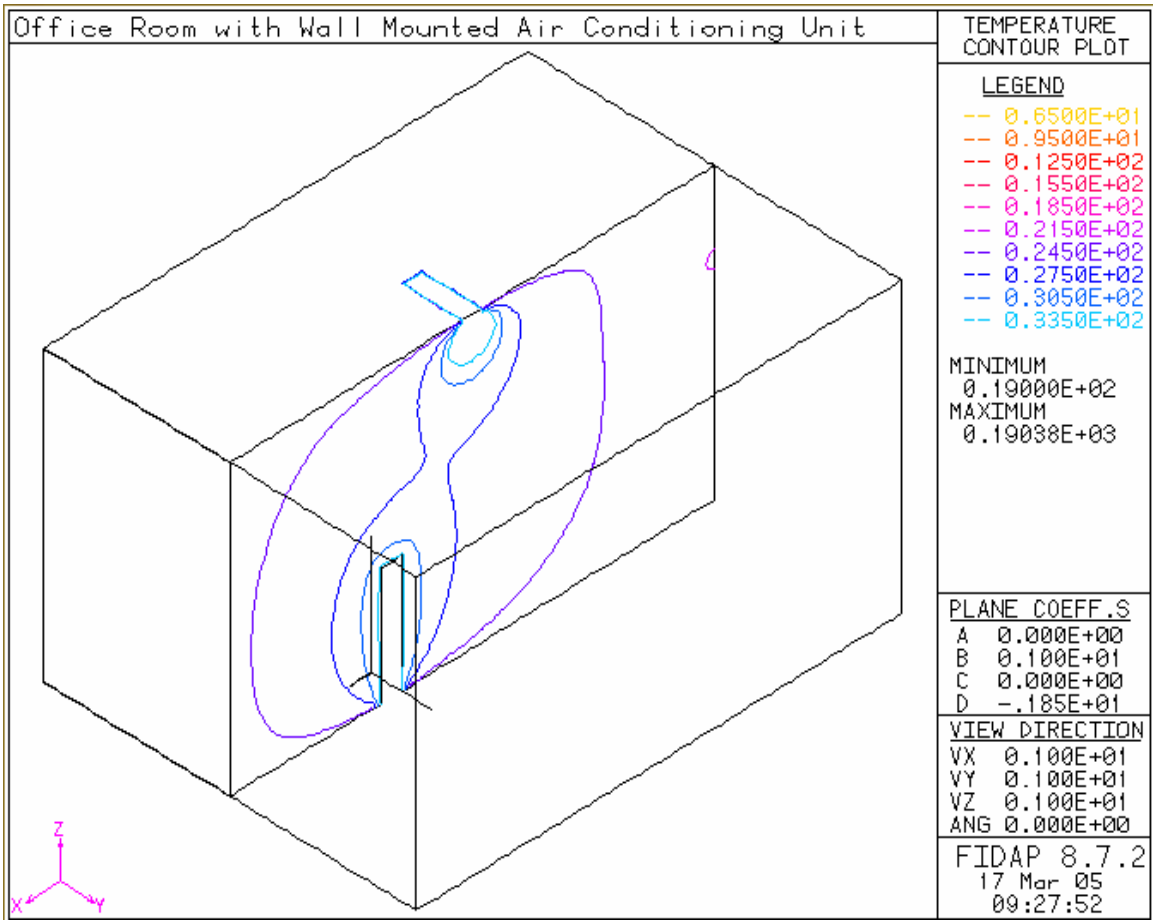

Figure 4-2 Temperature profile on plane 1, inlet angle of 30^{o}

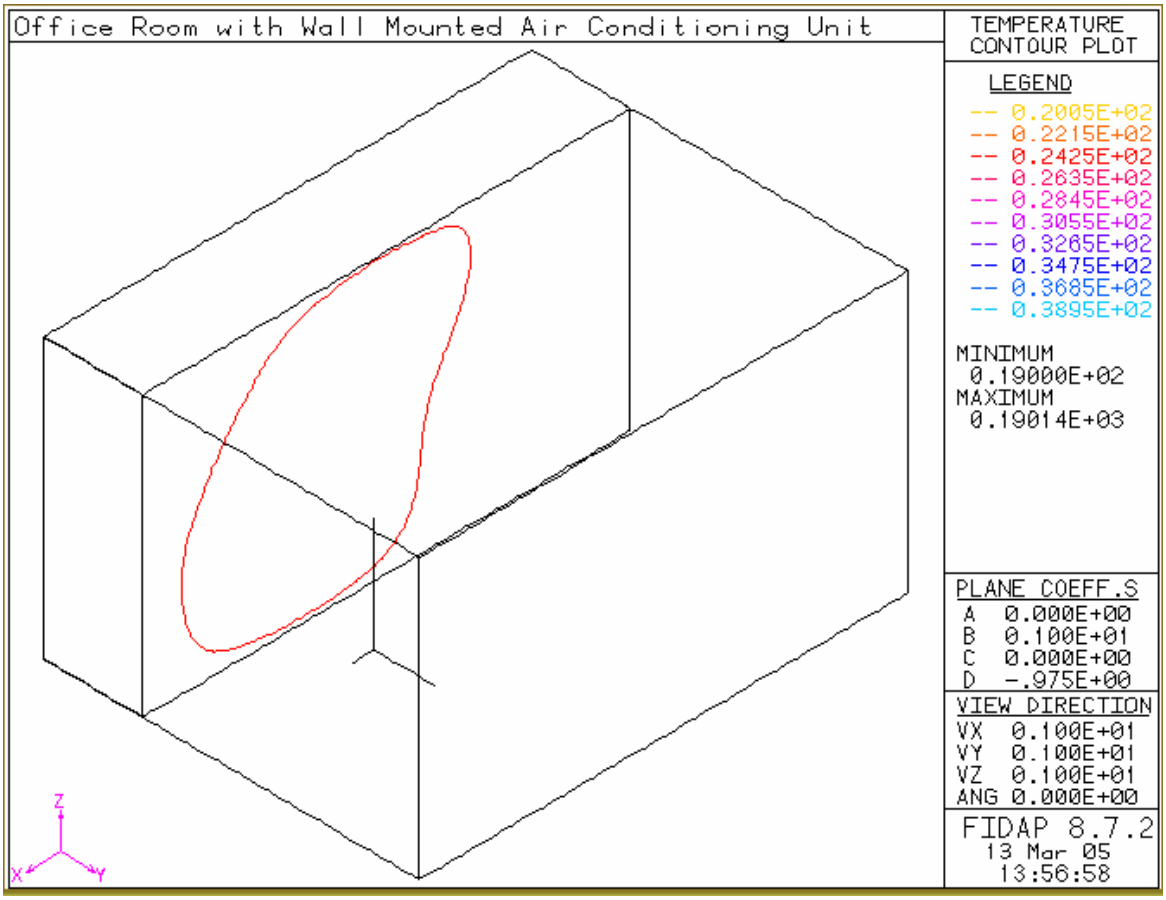

Figure 4-3 Temperature profile on plane 2, inlet angle of 30^{o}

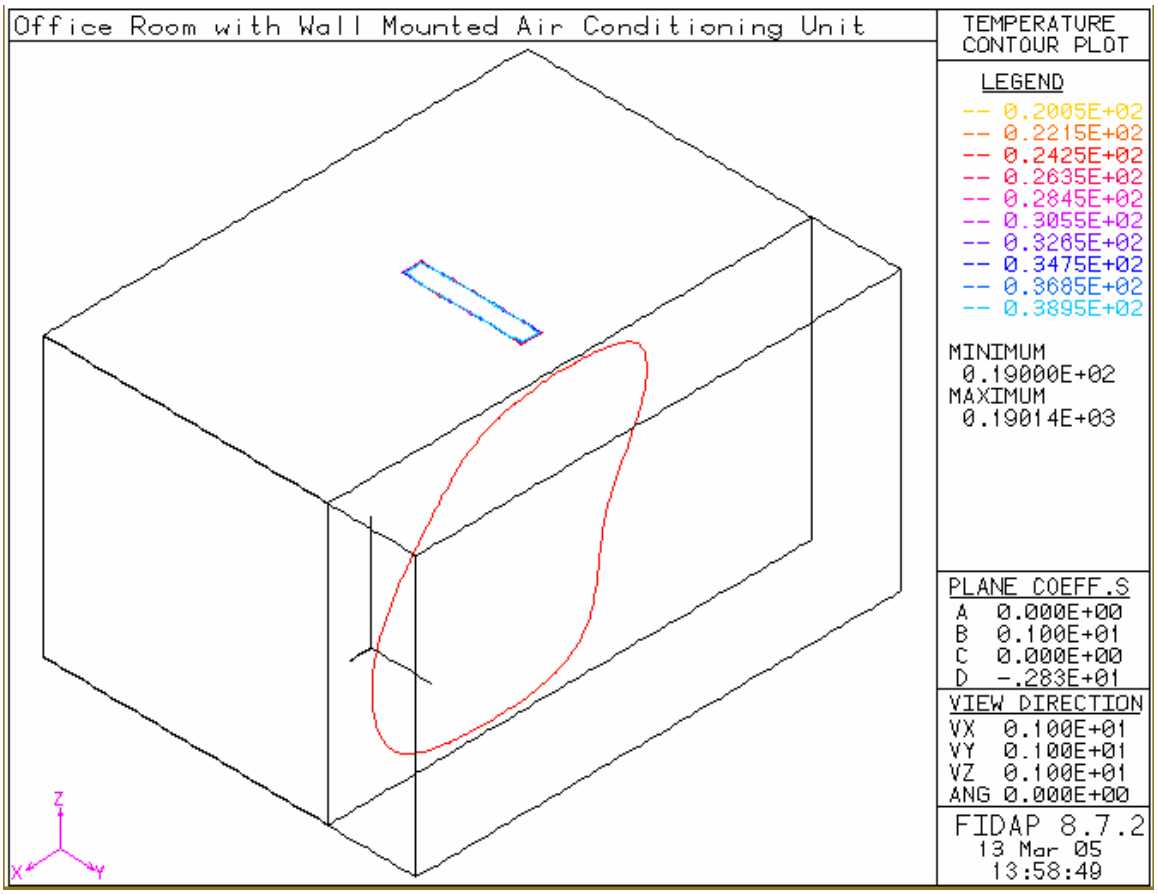

Figure 4-4 Temperature profile on plane 3, inlet angle of 30^{o}

Figures 4-5. 4-6 and 4-7 show the distribution of the contaminant on the three vertical planes 1, 2, 3, first Fig.4-5 shows that the contaminant's most significant concentrations are meanly around the person since the person is the only source of that flux. Notice that contaminant distribution around the person is uneven, which is due to the airflow direction shown in Figure 4-8. Since the air direction is meanly from top to bottom, the occupant releases contaminant which is then pushed downward away from the head of the occupant which explains why more contaminant is found towards the back and bottom of the office room, also contaminant is found around the occupant. Fig.4-5 shows very minimal concentrations in the adjacent plane, plane 2. The scale of the Fig.4-5 had to be changed to show the concentrations of contaminant in plane 2. The symmetry of the model dictates the concentrations in plane 3, which is the case in this simulation.

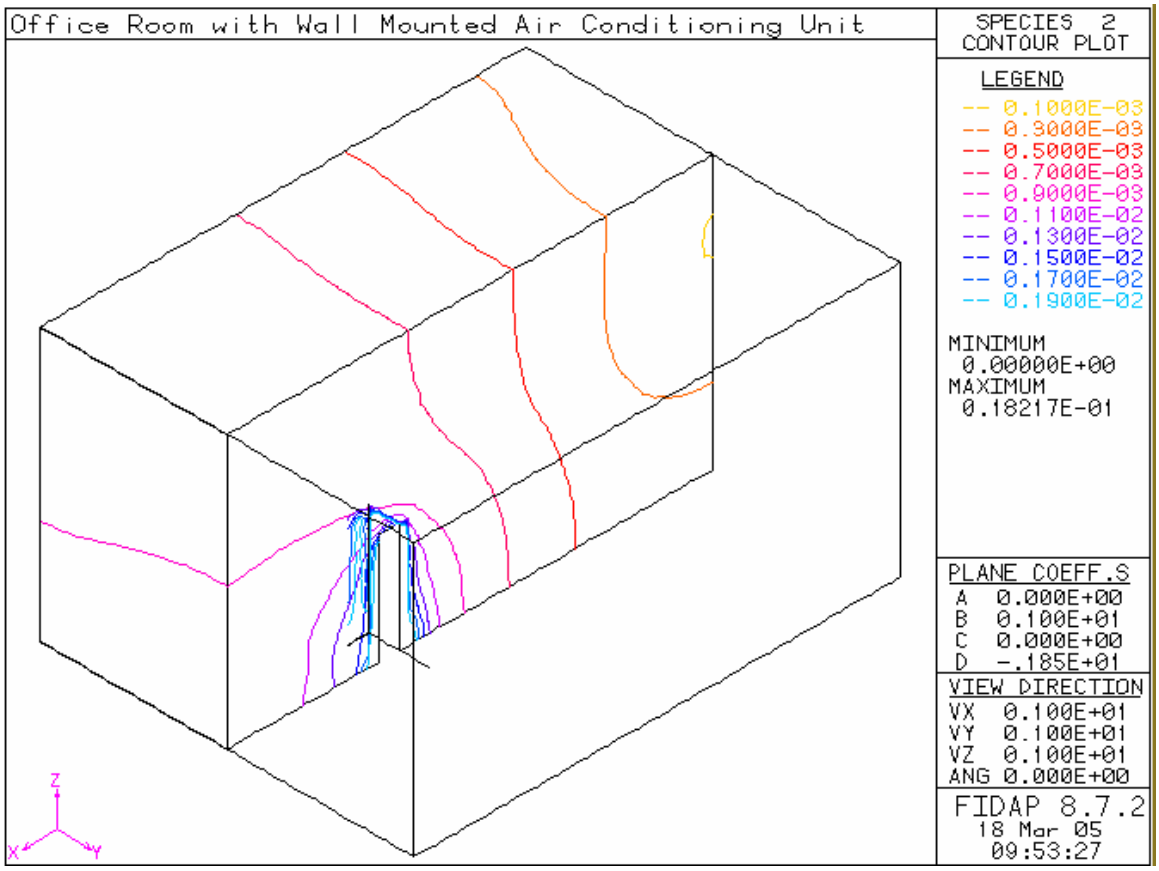

Figure 4-5 Contaminant profile on plane 1, inlet angle of 30^{o}

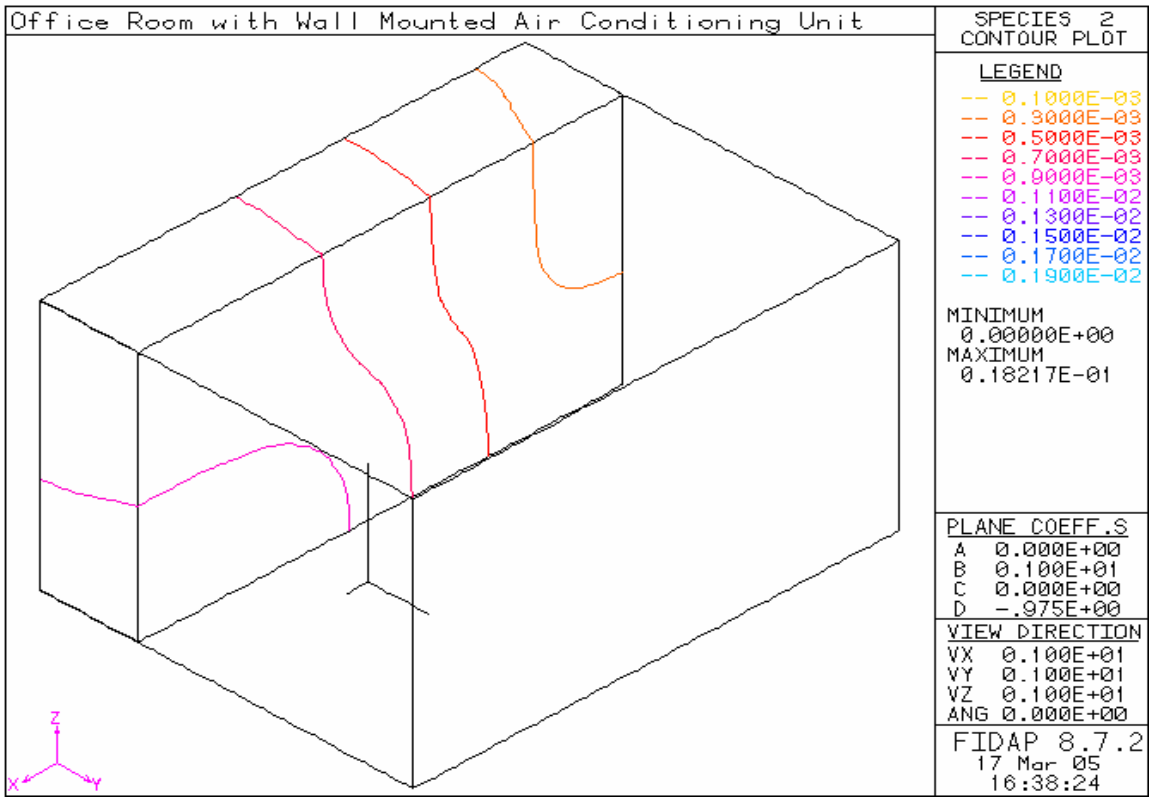

Figure 4-6 Contaminant profile on plane 2, inlet angle of 30^{o}

Chapter 1

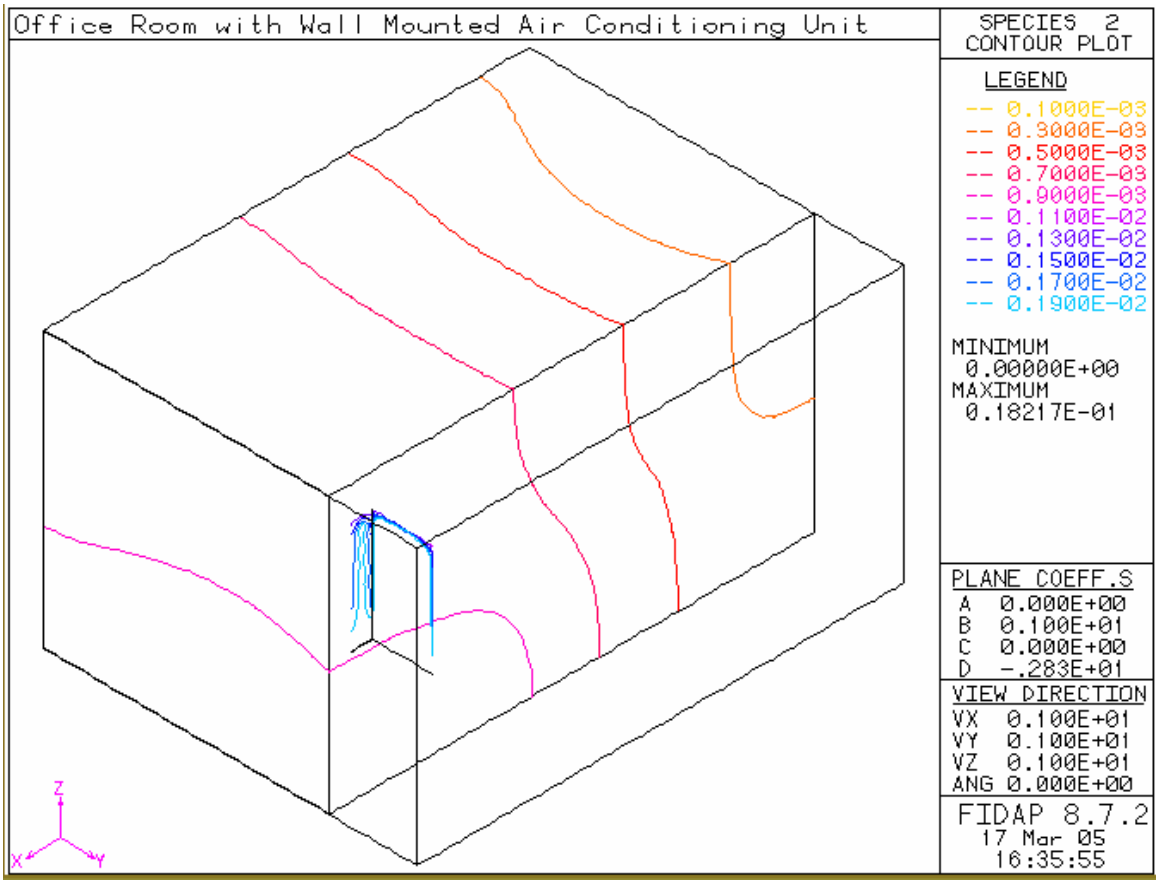

Figure 4-7 Contaminant profile on plane 3, inlet angle of 30^{o}

Velocities around the occupant on the vertical planes 1, 2, 3 are displayed in Fig.4-8, Fig.4-9, and Fig.4-10. Again Fig.4-9 and Fig.4-10 are very similar in showing the velocity profile on the vertical planes 2 and 3 because of the symmetry of the simulation on both sides of the office room. Fig.4-8 shows how the flow circulates around the person, notice that the inlet angle is 30^0 which drive airflow to the ceiling of the room however from Fig.4-8 we see that the angle is slightly higher than 30^o because air entering the room is pushed upward by the air from the previous circulation.

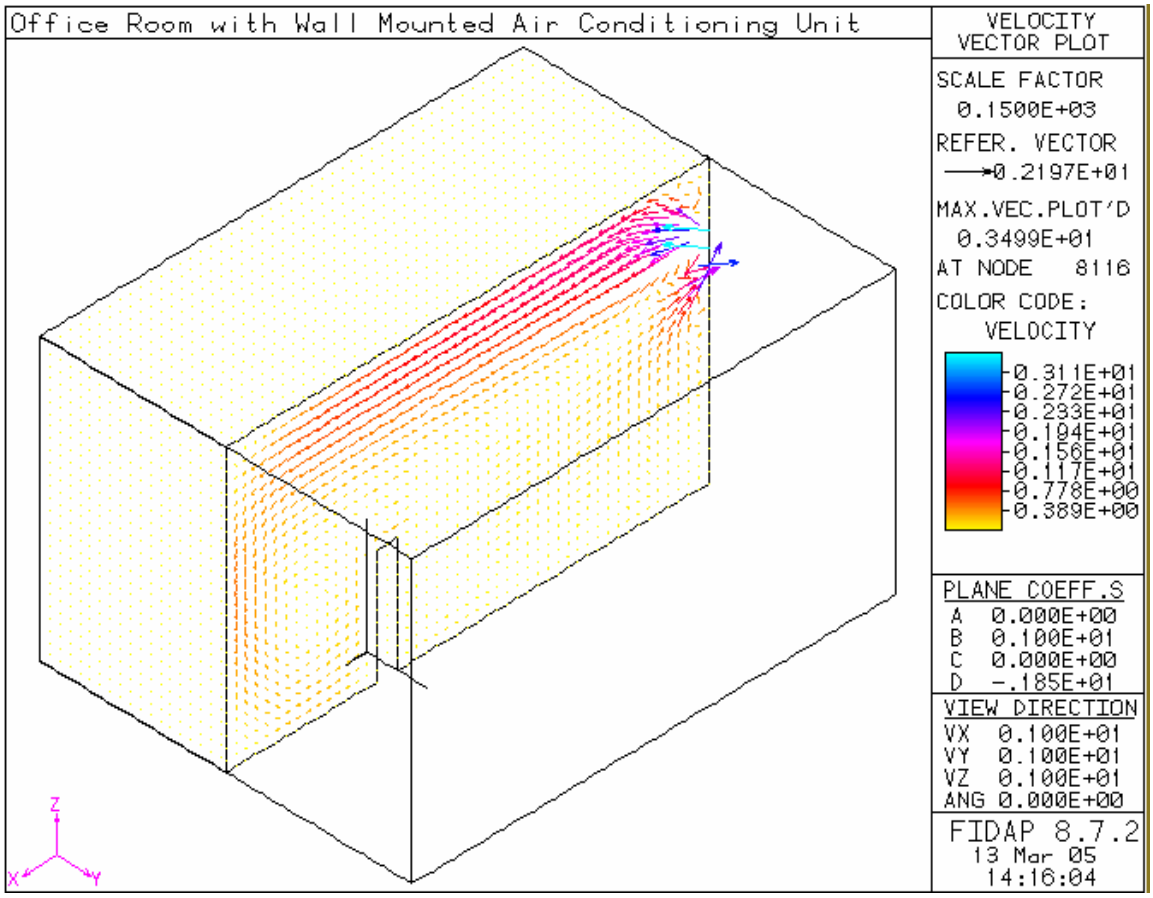

Figure 4-8 Velocity profile on plane 1, inlet angle of 30^o

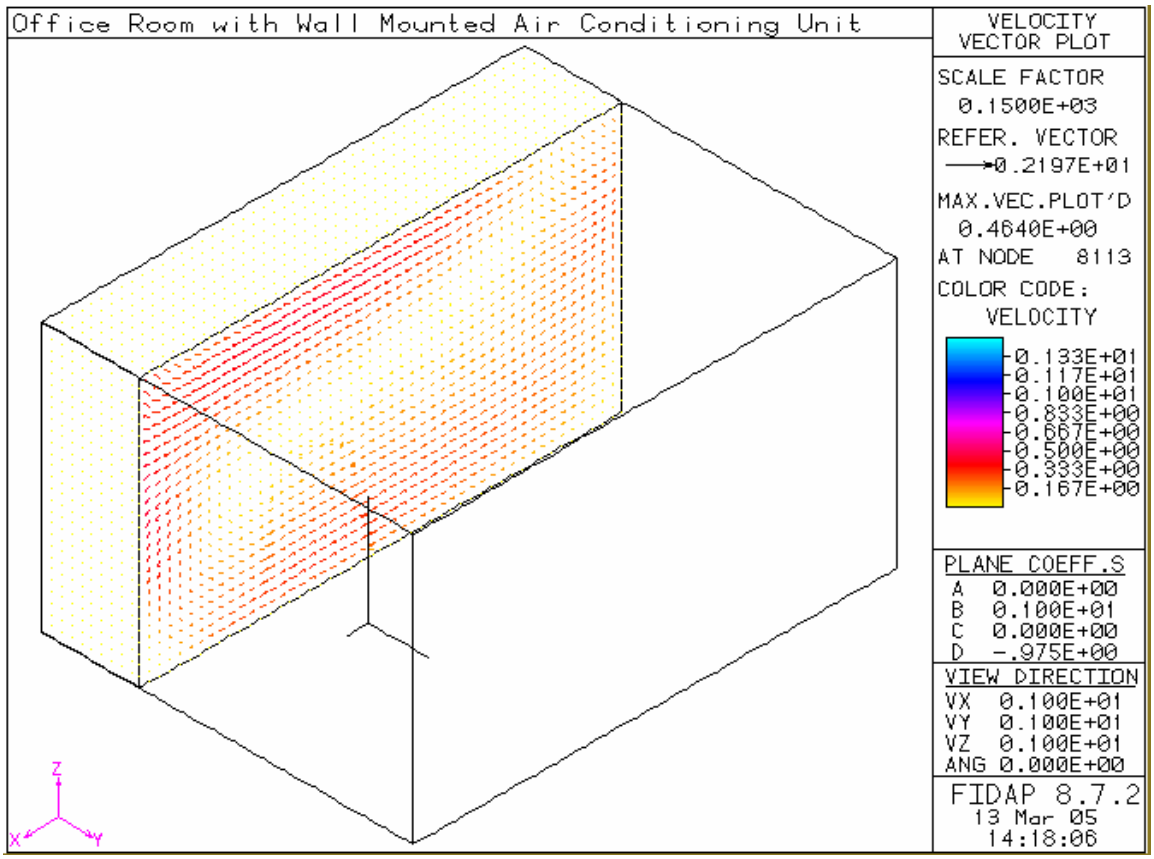

Figure 4-9 Velocity profile on plane 2, inlet angle of 30^{o}

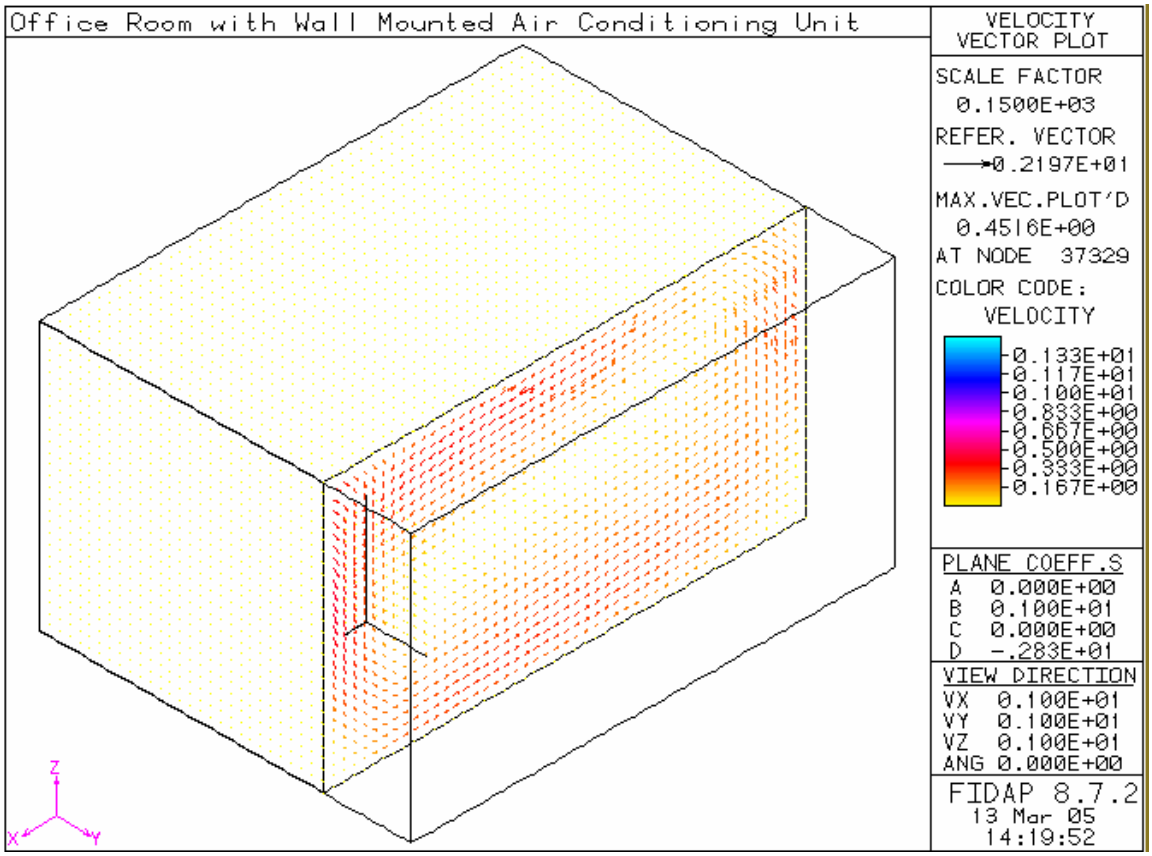

Figure 4-10 Velocity profile on plane 3, inlet angle of 30^{o}

Figure 4-11, Figure 4-12, and Figure 4-13 describe the temperature distribution in the horizontal planes 5, 4, and 6 respectively, as we can see the temperature gets colder as the air gets away from the occupant, Fig.4-11. Plane 5 intersects with the occupant a distance that allows for a significant convective heat transfer, this gives clear idea about the temperature directly surrounding the occupant and how much does the person's temperature affects the immediate surrounding air around him or her.

At the middle of the room the temperature has similar distribution with exception that plane 4 does not intersect with the occupant, the convective heat transfer is mildly less than in plane 5 however, it is noticeable that immediately above the person the air temperature is high, Fig.4-12.

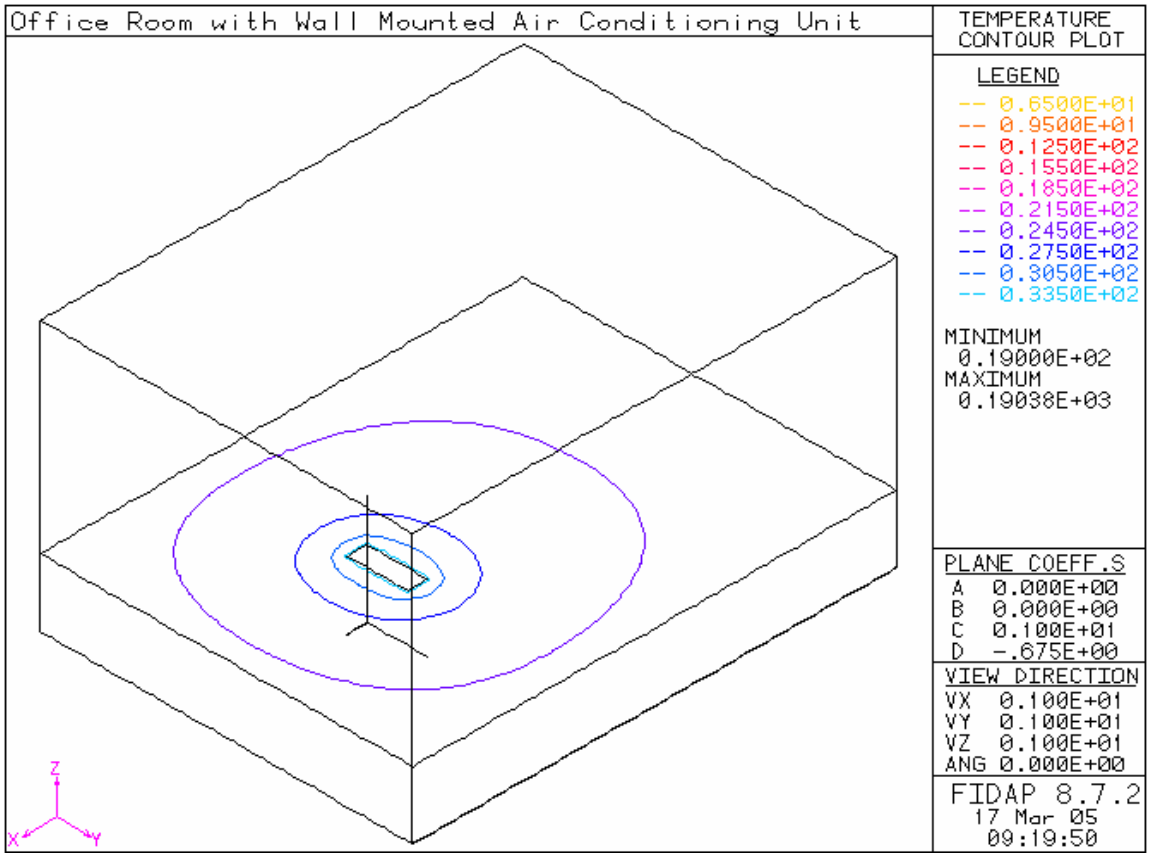

Figure 4-11 Temperature profile on plane 5, inlet angle of 30°

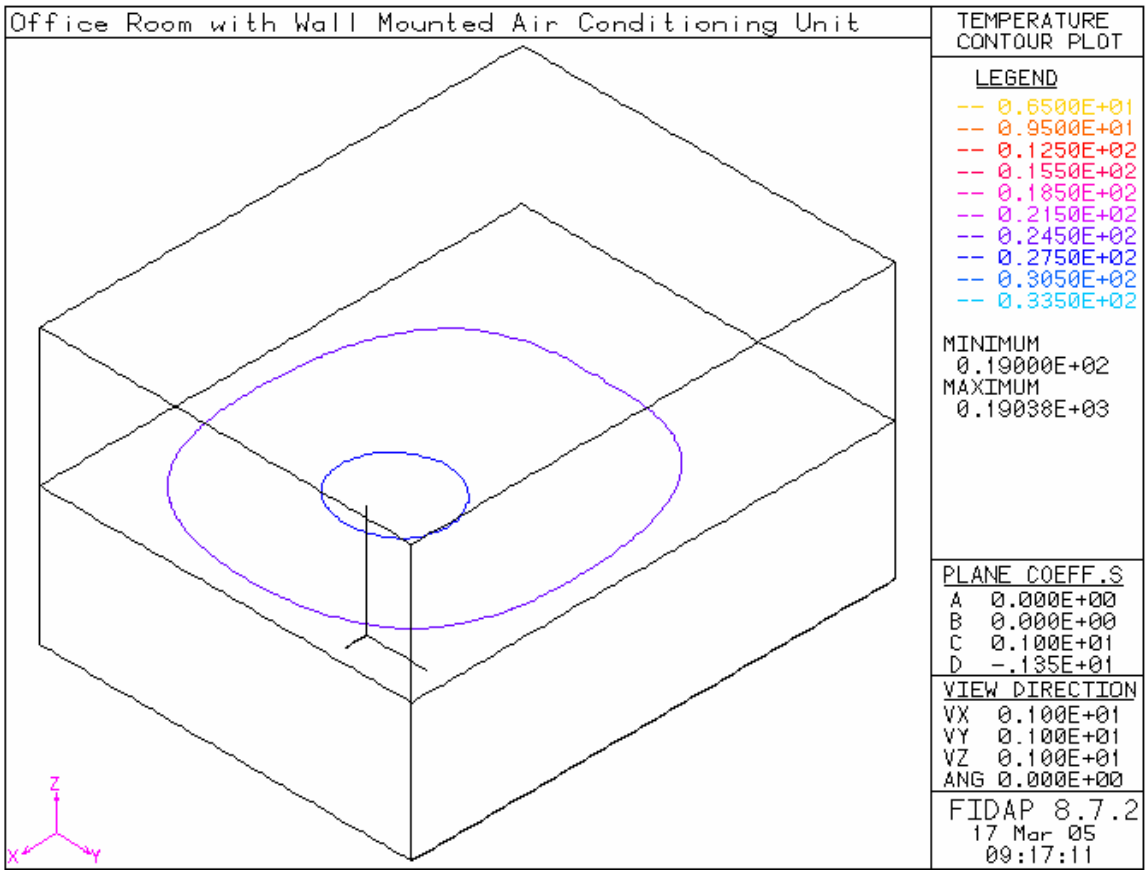

Figure 4-12 Temperature profile on plane 4, inlet angle of 30^{o}

Plane 6 shown in Fig.4-13 shows the same pattern as in plane 4, only this time the high temperature is influenced by the closeness of the light fixture. Notice how the circular high temperature profile is closer to the person and has a slight offset in the direction of the light. It is not immediately above the occupant. The light fixture has great influence on the heat transfer in the high section of the room, even if cooling air moves towards the occupant, the high temperature is around the light which is located in the center of the ceiling.

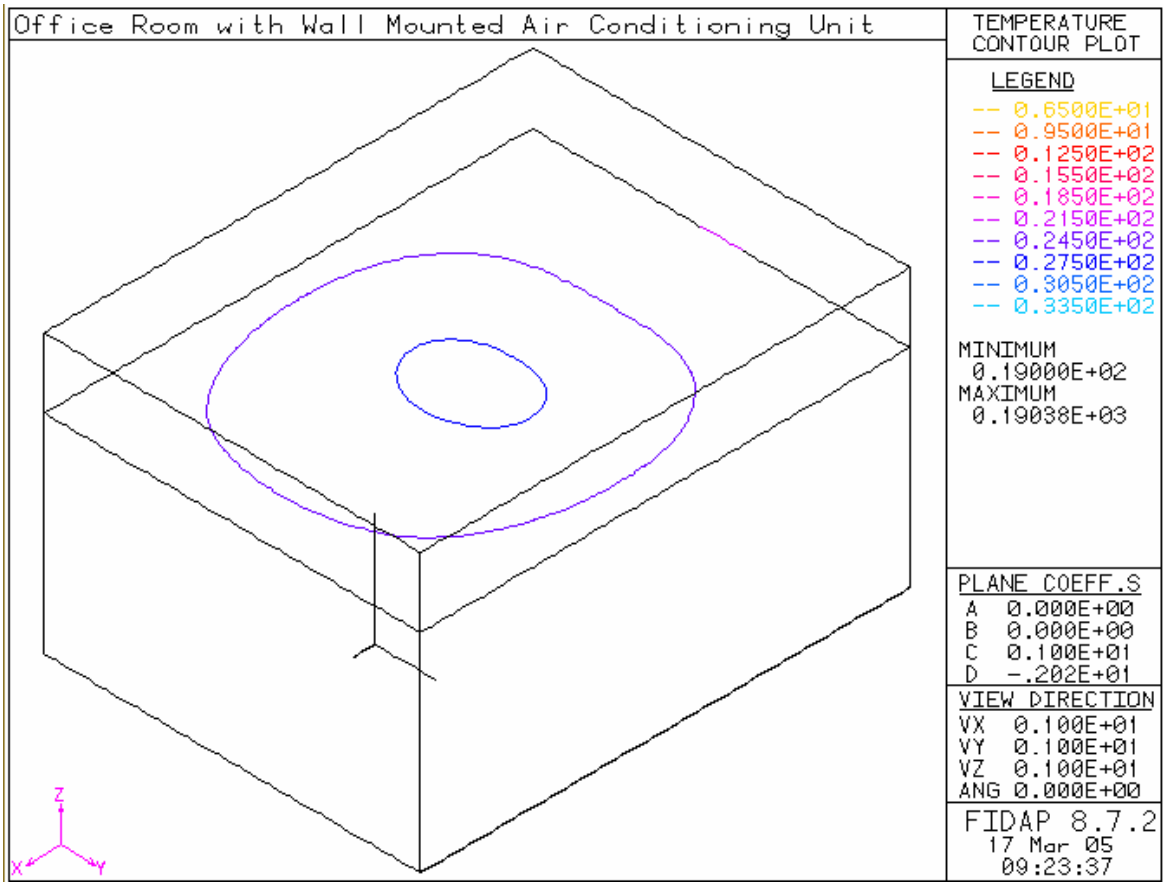

Figure 4-13 Temperature profile on plane 6, inlet angle of 30^{o}

Contaminant distribution of the office room analyzed by horizontal planes shows as first predicted, the contamination secretion from the person is uneven. High concentrations are found towards the bottom back section of the room as Table.4-6 shows. It is clear from comparing Fig.4-14, Fig.4-15 and Fig.4-16 that the concentration of contaminant within the office room diminished as the height increases. This is explained by the airflow movement inside the room and around the occupant, which is meanly directed downwards.

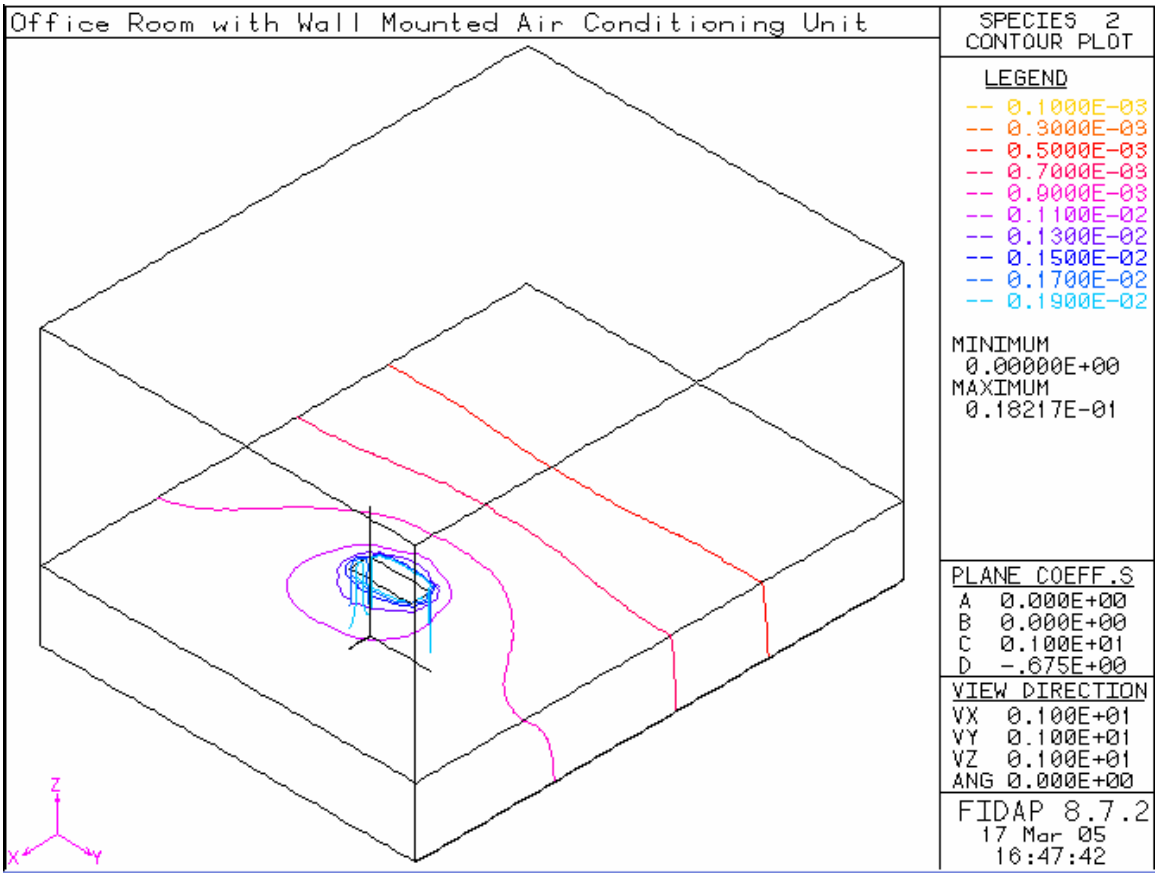

Figure 4-14 Contaminant profile on plane 5, inlet angle of 30^{o}

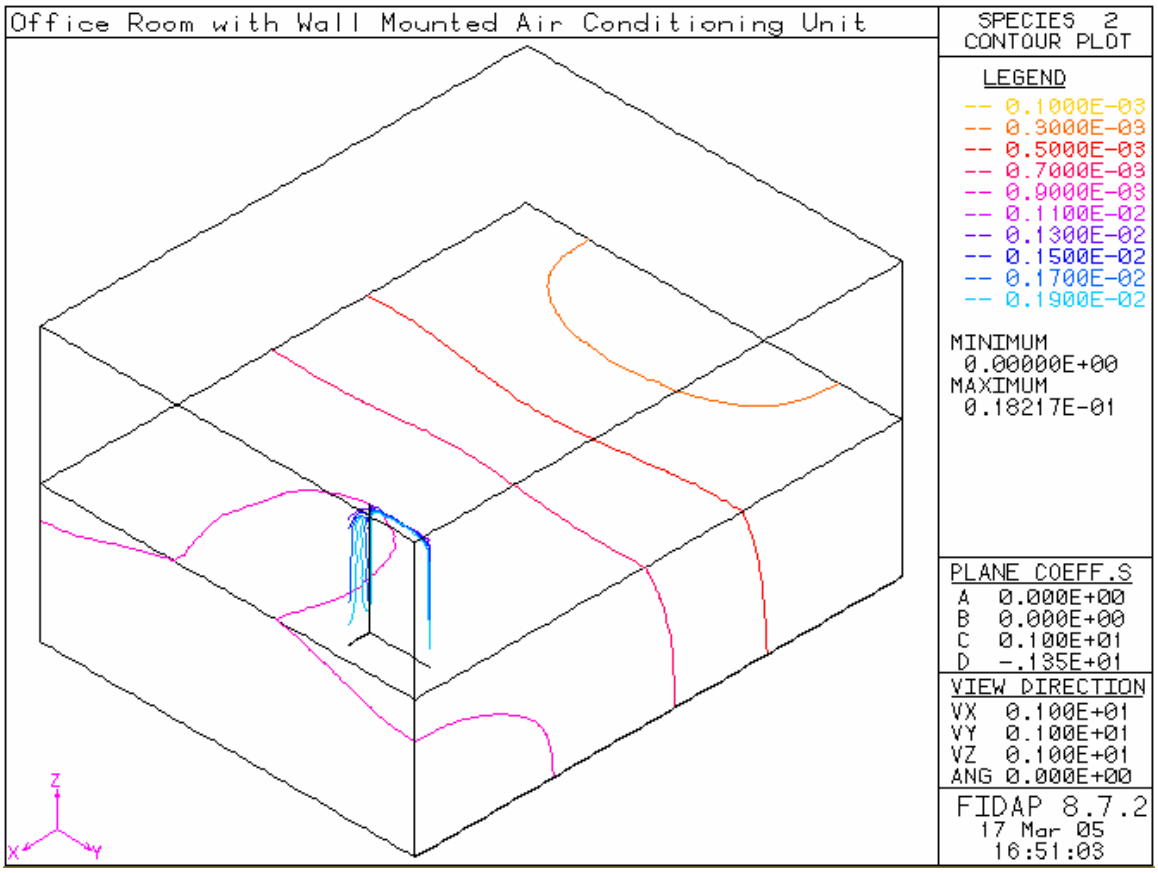

Figure 4-15 Contaminant profile on plane 4, inlet angle of 30^{o}

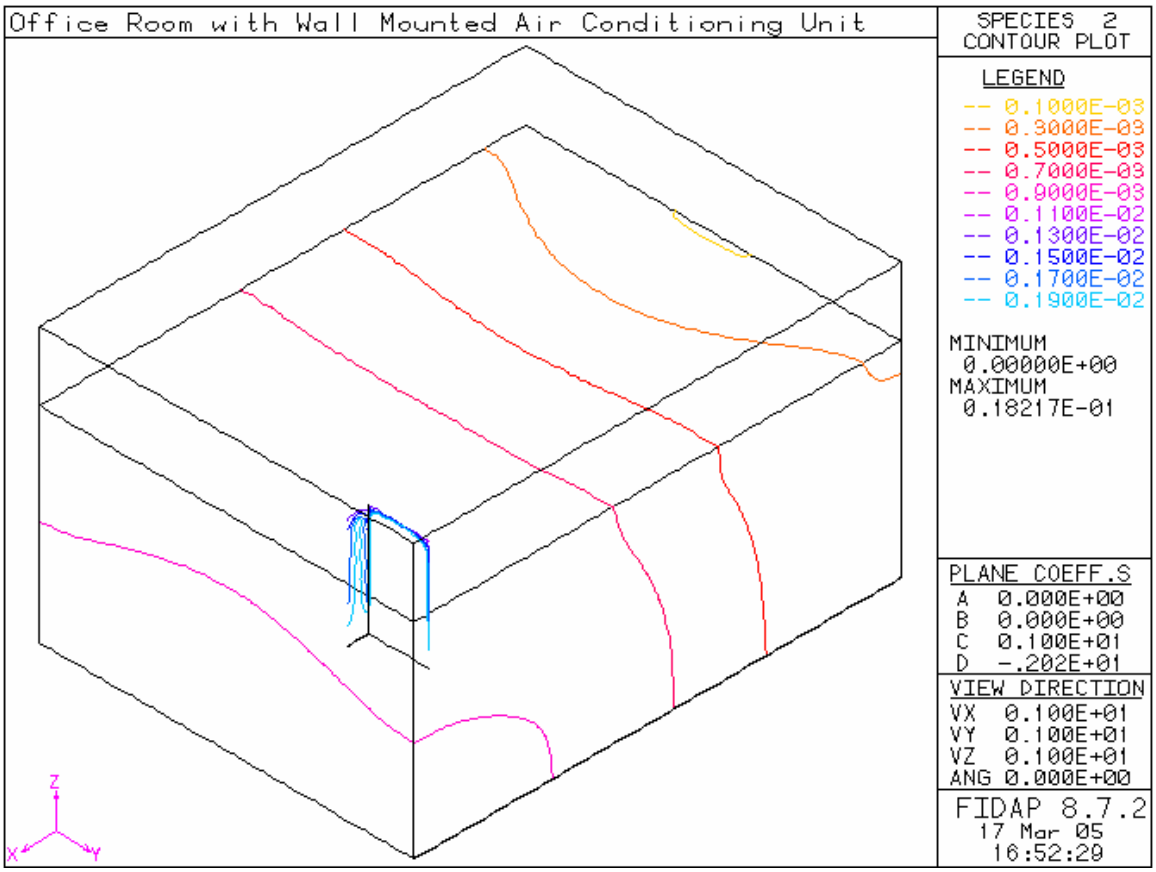

Figure 4-16 Contaminant profile on plane 6, inlet angle of 30^{o}

As the airflow enters the office room and circulates around the person, it follows a specific trajectory as shown in Fig.4-17, Fig.4-18, and Fig.4-19 for planes 4, 5 and 6. The high speed airflow goes around the person from the top and two sides; as the height decreases Fig.4-17 effectively shows that high speed air shown in Fig.4-19 is evenly dispersed around the room's ceiling and walls before being guided downward. Notice the circulation pattern around the person; it explains the temperature and the contaminant distribution in the office room.

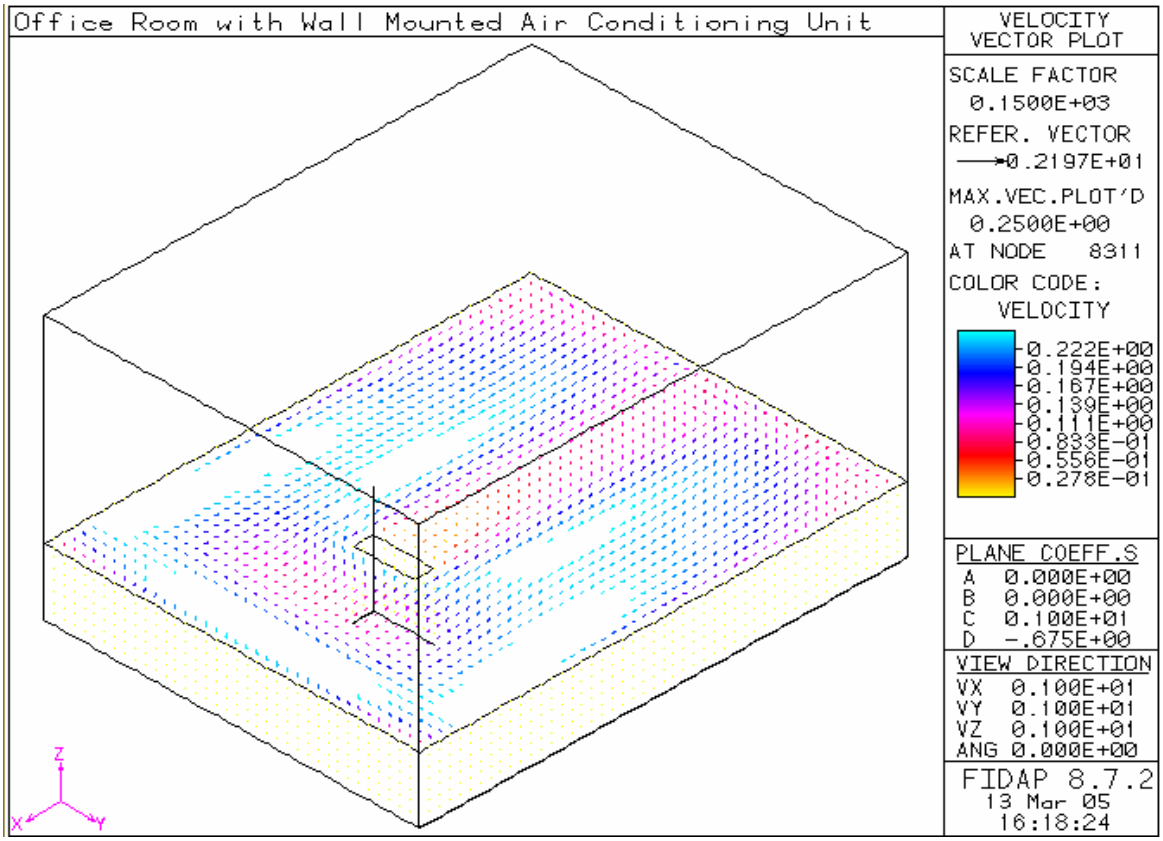

Figure 4-17 Velocity profile on plane 5, inlet angle of 30^{o}

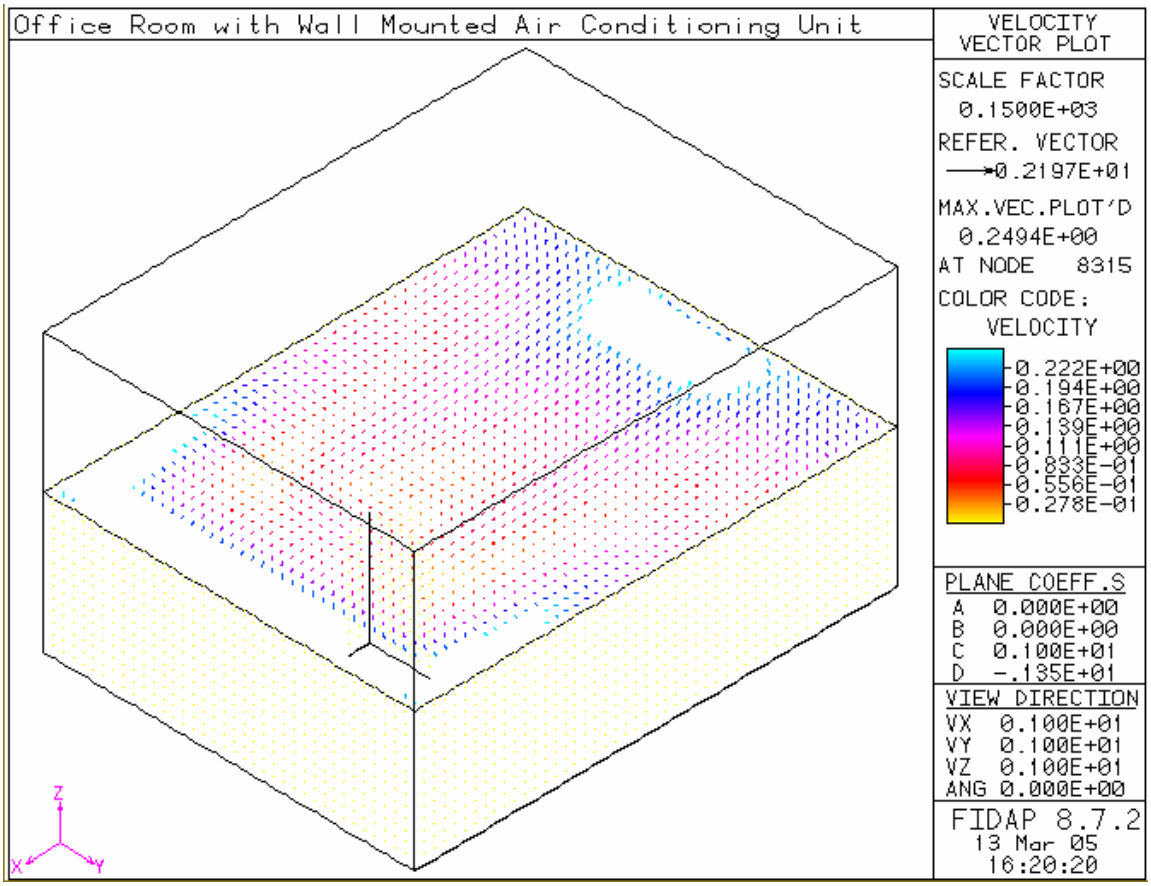

Figure 4-18 Velocity profile on plane 4, inlet angle of 30^{o}

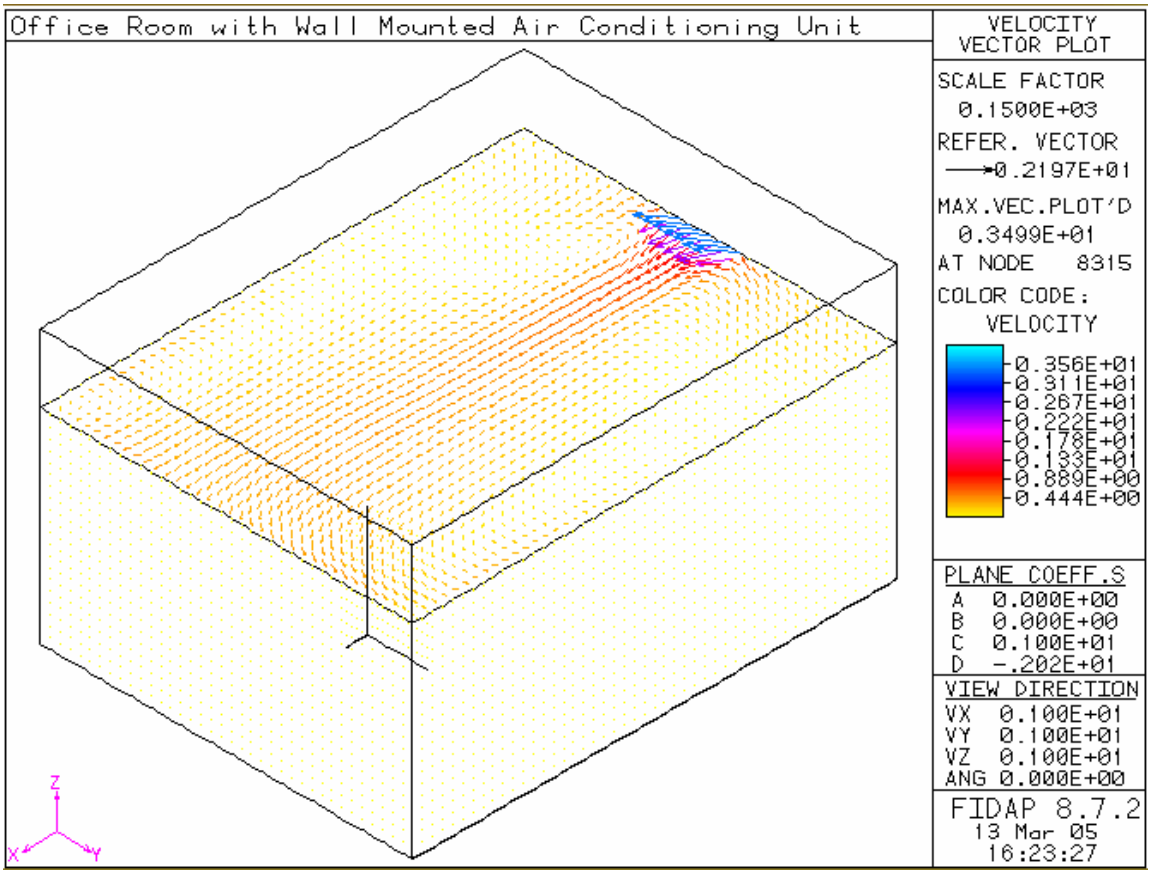

Figure 4-19 Velocity profile on plane 6, inlet angle of 30^{o}

Relative humidity is a very important factor of indoor human thermal comfort especially in office rooms cooled by wall-mounted units. Table 4-4 shows values of average relative humidity in the studied planes. Knowing the symmetry of the simulation and, in agreement with Fig.4-21 and Fig.4-22 the values of relative humidity are very acceptable. Notice that values of relative humidity in the vertical planes 3 and 4 in Table 4-4 are equals and the profiles shown in Fig.4-21 and Fig.4-22 agree to the numerical values. Even though the numerical value of relative humidity in the center plane 2 is lower than the adjacent planes, Table 4-4. Fig.4-20 shows a high relative humidity around the light and the person with is explained by the heat transfer magnitude at these

locations due to high temperatures. Fig.4-2 agrees with this profile. Further more due to high temperature, the relative Humidity decreases considerably as the airflow get closer to the occupant.

Table 4-4 Relative humidity in the studied planes

Planes	Relative Humidity %
1	39.58
2	59.85
3	59.80
4	55.85
5	56.69
6	58.02

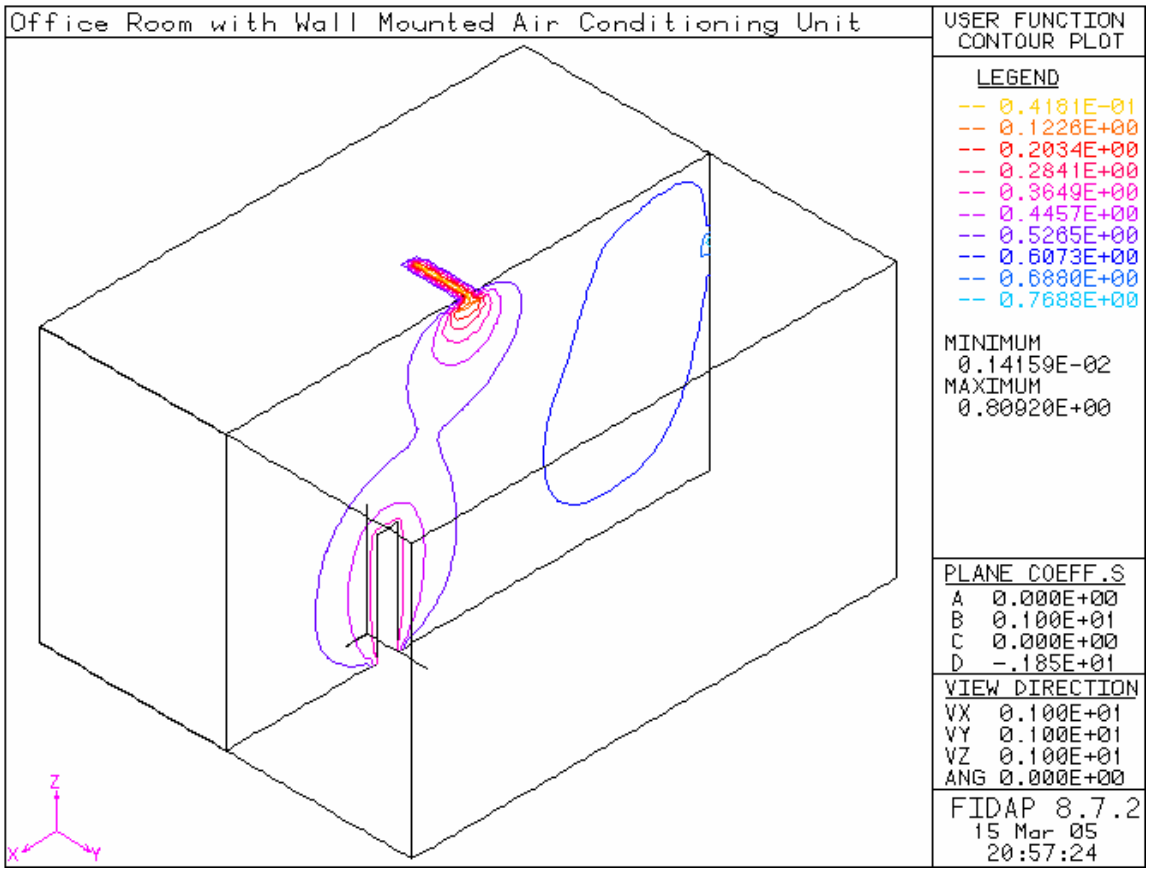

Figure 4-20 Relative humidity on plane 1, inlet angle of 30^{o}

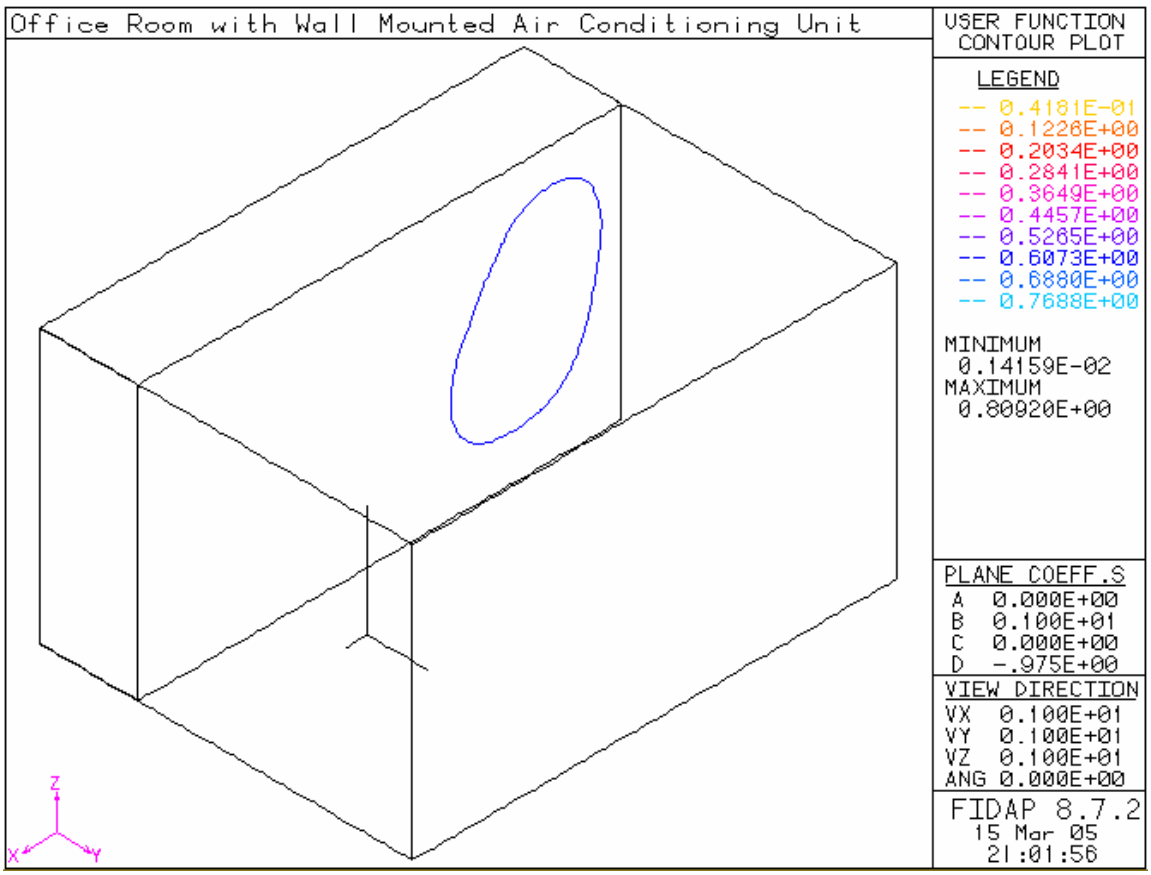

Figure 4-21 Relative humidity on plane 2, inlet angle of 30^{o}

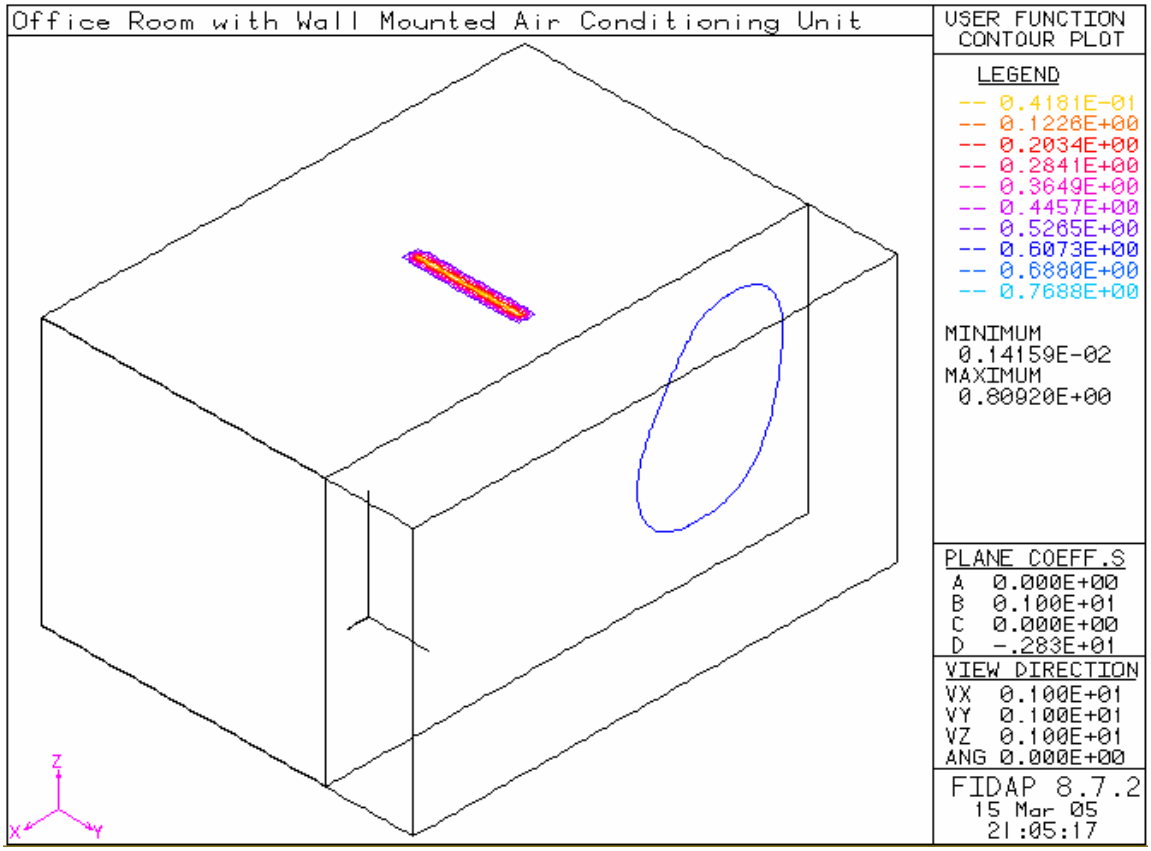

Figure 4-22 Relative humidity on plane 3, inlet angle of 30^{o}

As Table 4-4 shows the numerical value of the average relative humidity in the horizontal planes 4, 5, and 6 increase as height increases. Cool airflow velocity in the upper planes of the room is very high which explains the increase in average relative humidity in the high sections of the office room. However, as predicted by the temperature profile Figures 4-11, 4-12, and 4-13, the relative humidity is greater around the person. The heat around the occupant is presumed transferred at a high constant rate that heats air surrounding it, raising its temperature thus decreasing the immediate relative humidity. Fig.4-24 and Fig.4-25 show planes that do no intersect with the occupant, yet as temperature in Fig.4-12 and the convective heat transfer ratio predict it, the relative humidity is low immediately above the person and as the air get closer to the light fixture.

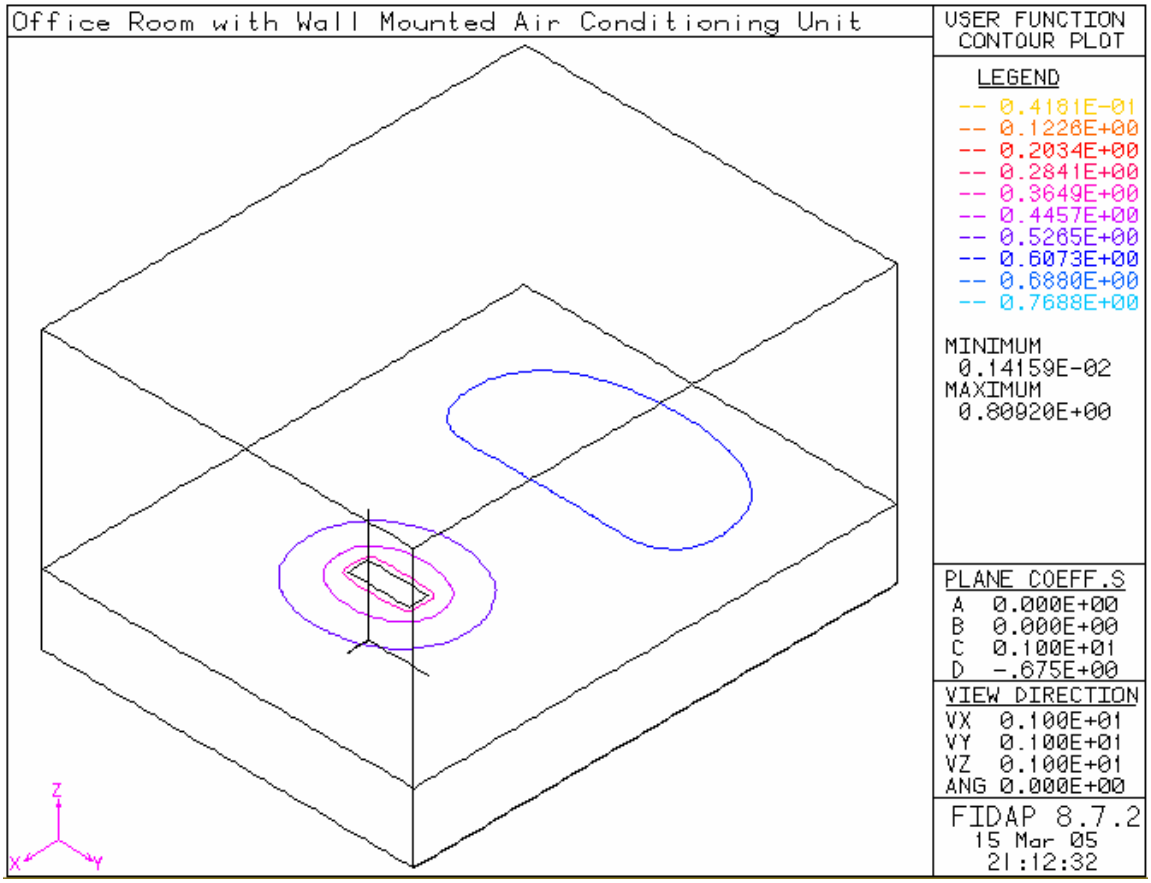

Figure 4-23 Relative humidity on plane 5, inlet angle of 30^{o}

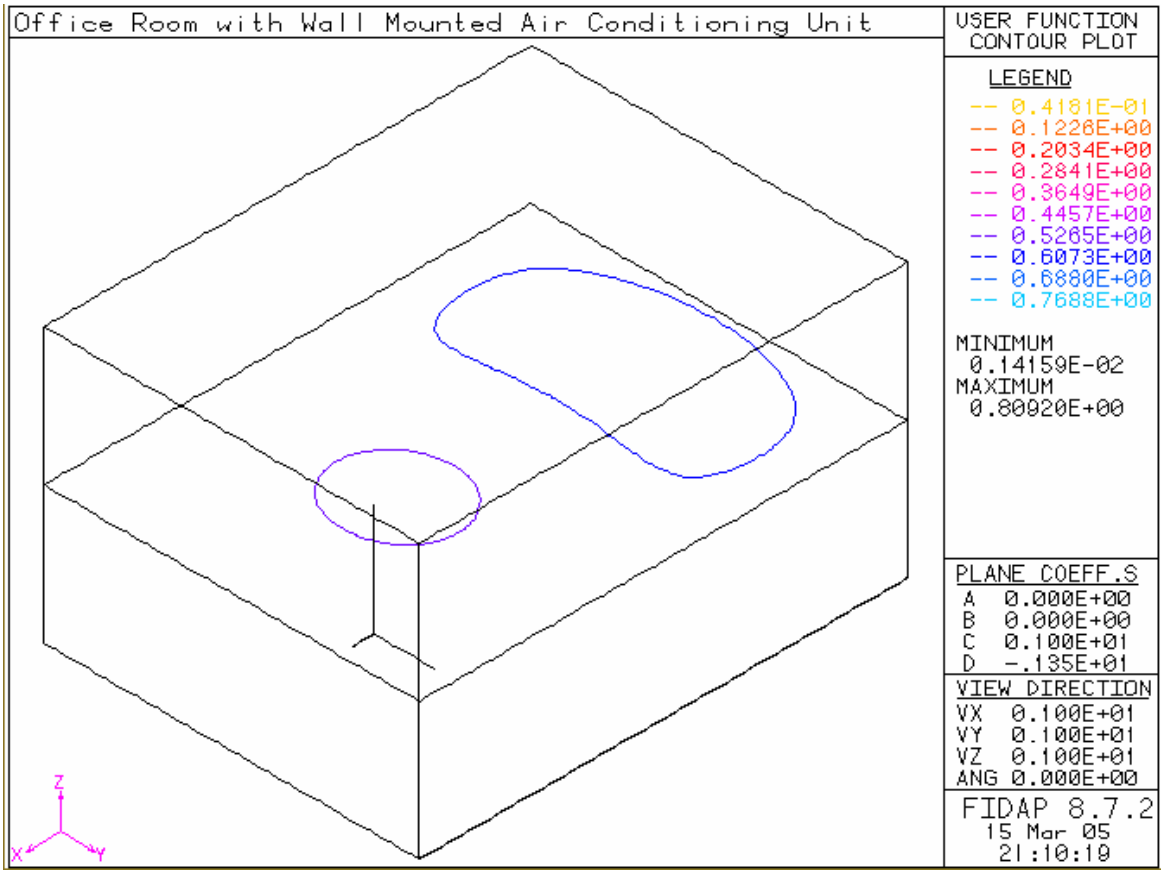

Figure 4-24 Relative humidity on plane 4, inlet angle of 30^{o}

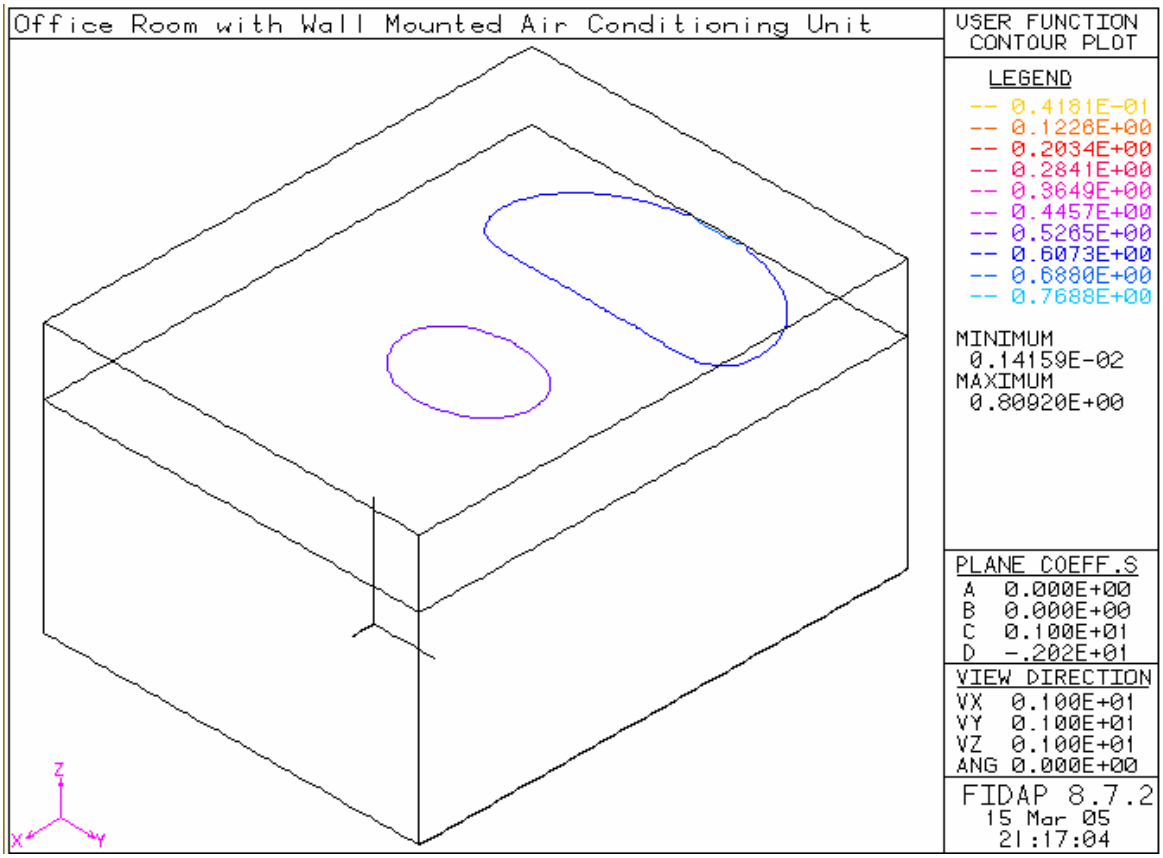

Figure 4-25 Relative humidity on plane 6, inlet angle of 30^{o}

Table 5-5 compares the values of average relative humidity and temperature in this three-dimensional model, to a reduced two-dimensional model using the same boundary conditions (chapter3). The relative humidity and temperature are inversely proportional, this shows in Table 4-5, and the values are very close. The small the difference in numbers is due to the assumptions made for both cases and the difference in precision of solution since two turbulent models were used to solve for each case. Also to get the same results in 3-D model as in 2-D model one has to assume all entities are extended to full length of the office room.

Table 4-5 Comparison of relative humidity and temperature in 30^{o} inlet angle 2-D and 3-D models

Simulated Models	Average Relative Humidity %	Average Temperature ^{0}C
Three Dimensional	58.47	24.4
Two Dimensional	62.86	22.1

Figure 4-26 shows the averages temperature values for present study In comparison with the three dimensional CFD modeling done in [8], with respect to height of the office room, the temperatures compared are from three points with the same coordinate in all three cases. Fig.4-26 shows the two CFD models are in agreement with the temperature pattern as the height increases, as stated above the fluid's temperature is low at height that include the airflow trajectories. The experimental data has similar results except that the temperature in this case grows proportionally to the height. Discrepancies in this case are explained by difference in solution schemes and different initial boundary conditions

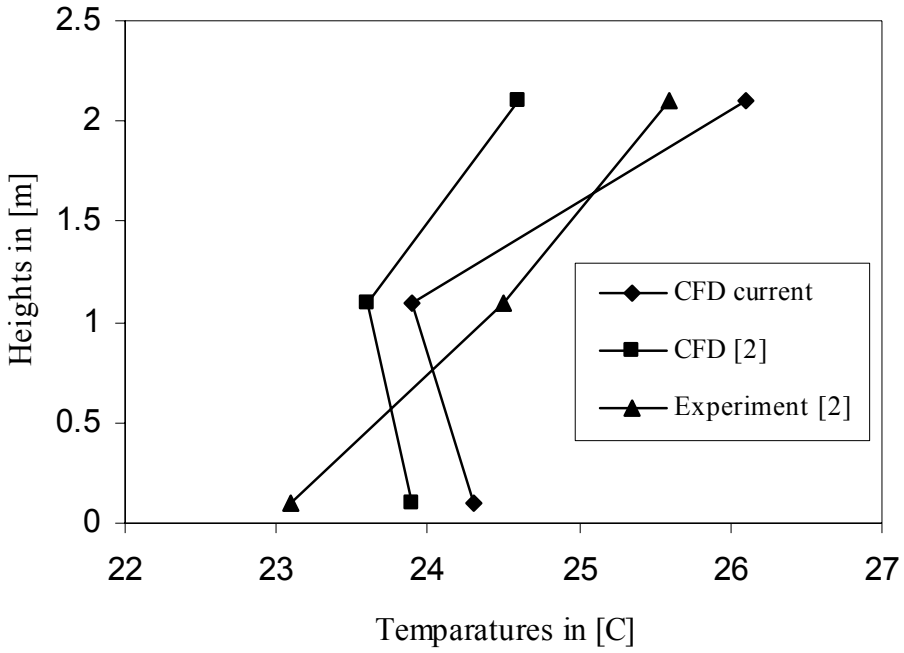

Figure 4-26 Temperature profiles for both simulations vs. height

Table 4-6 compares the contaminant concentrations in the 6 planes studied also shows the value of CRE in each plane. As predicted by Figures 4-14, 4-15, and 4-16, it is clear from Table 4-6 especially in planes 4, 5, and 6 (Horizontal planes) that the concentration of contaminant increases as the height of the office room decreases. The concentration on vertical planes 1, 2, and 3 is very straightforward because the highest concentration is on the plane that intersects the occupant (plane1).

CRE values are directly proportional to concentration values as CRE is a ratio of these concentrations with the amount cleared by airflow through the outlet.

Table 4-6 Concentration of contaminant and CRE, for 30^{o} inlet angle

Studied planes	Contaminant concentration	CRE
1	0.00404	4.29E-4
2	0.00104	0.001669
3	0.00104	0.001669
4	0.000851	0.002041
5	0.000782	0.002217
6	0.000986	0.001861

Theses numbers agree with the velocity profile as the CRE is highest in the middle plane (plane 1) where there is more air circulating at high velocity since plane 1 intersects with unit. As stated before the symmetry of the office room horizontally makes the plane 2 and plane 3 have the same characteristics.

4.3.2 Simulation with 20^{o} inlet angle

Temperature profiles are shown in Fig.4-27, Fig.4-28, and Fig.4-29 for vertical planes; it is noticeable that the low temperatures are around the walls and the ceiling. Warm temperatures exist at the proximity of the light fixture and around the person as in the case of 30^{o} inlet angle. However, lower values are noticed in this case. At planes 2 and 3 temperatures profiles are very similar due to the vertical symmetry of the office room.

Figures 4-39, 4-40, and 4-41 show temperature profiles on the horizontal planes 4, 5, and 6 respectively. Around the person in Fig.4-39, we see that the temperature lower

between the person and the unit however, even when close to the person Fig.4-40, the profile is still wide due to high velocities which keep local temperatures colder. Plane 6 Fig.4-41 shows the air temperature are cold around the wall and even more so in the middle and away from the light.

Table 4-7 shows the comparison of the overall average temperatures and relative humidity in this 3-D simulation with it counterpart in Chapter 3. As predicted the 3-D simulation show a lower relative humidity and lower temperature due to the high number of nodes analyzed.

Table 4-7 Comparison of relative humidity and temperature in 20^{o} inlet angle 2-D and 3-D models

Simulated Models	Average Relative Humidity %	Average Temperature ^{o}C
Three Dimensional	70.89	21.22
Two Dimensional	75.99	20.15

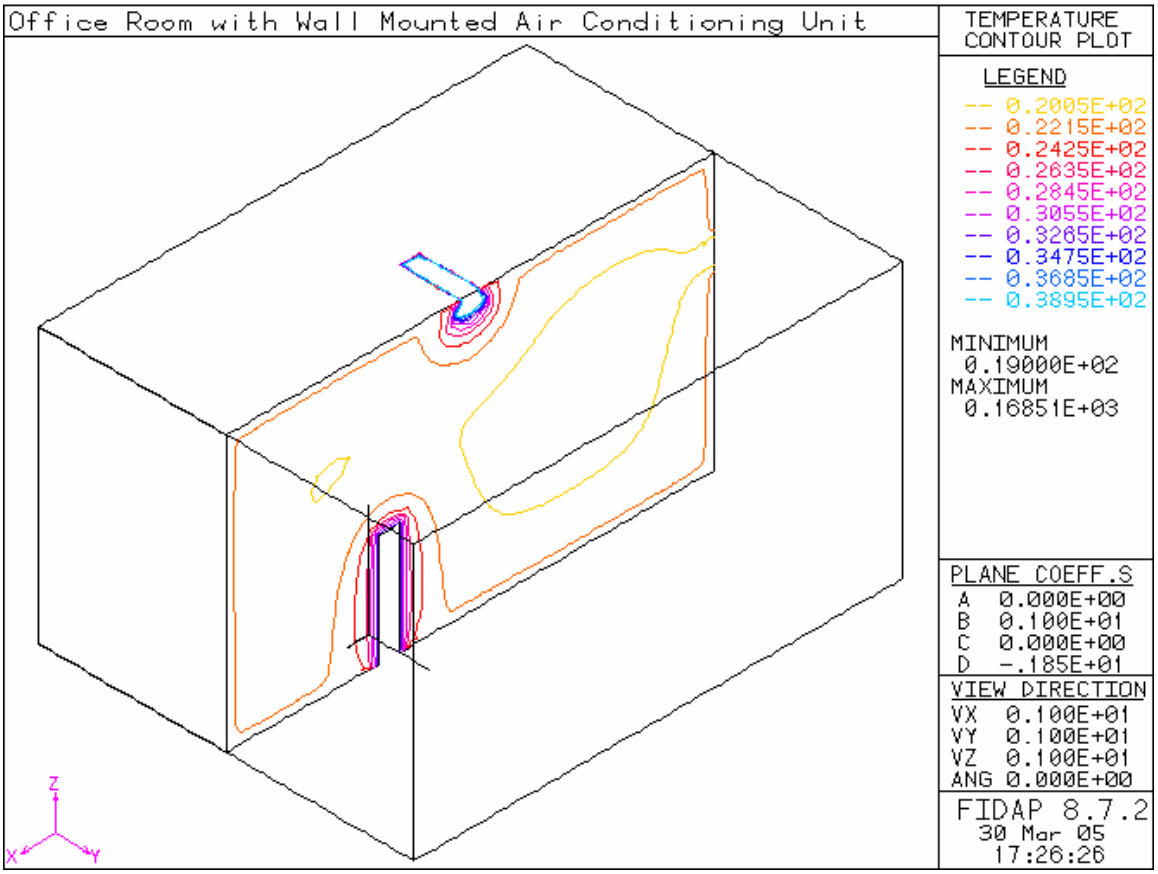

Figure 4-27 Temperature profile on plane 1, inlet angle of 20^{o}

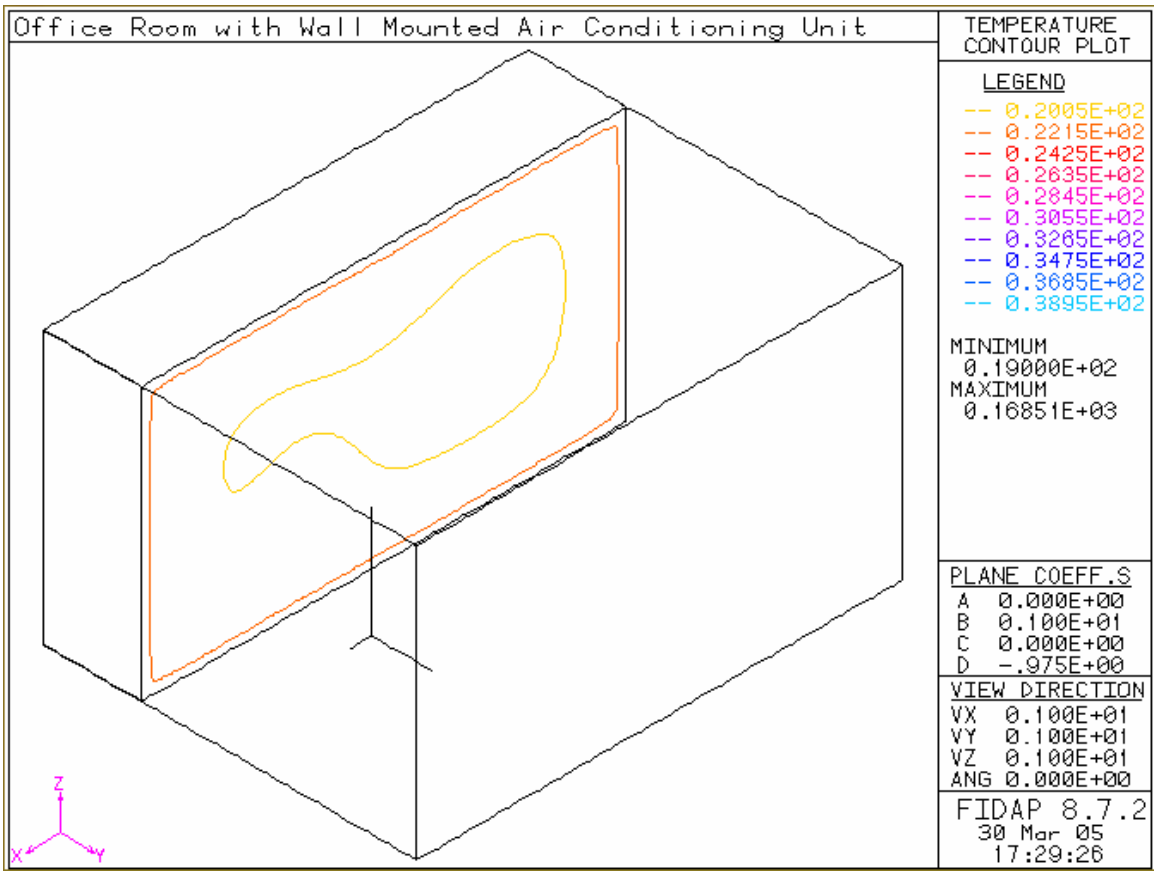

Figure 4-28 Temperature profile on plane 2, inlet angle of 20^{o}

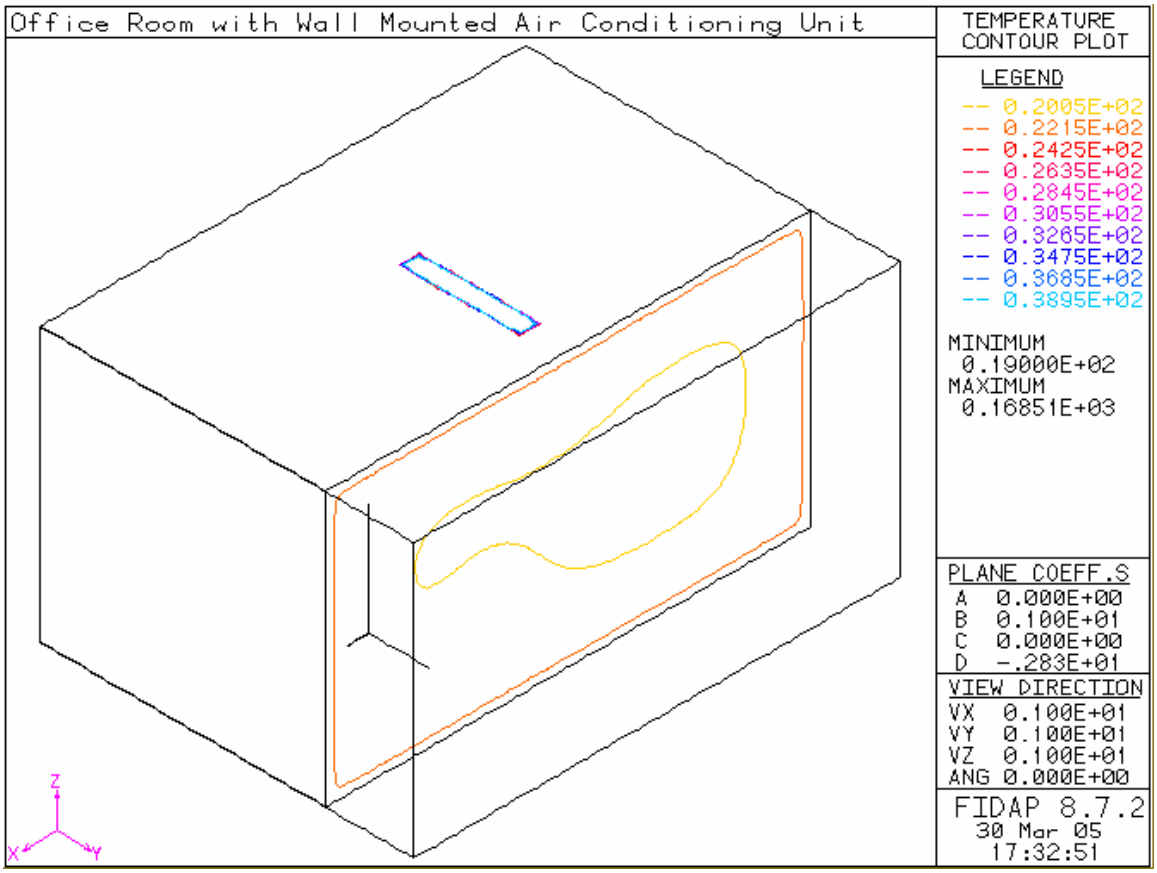

Figure 4-29 Temperature profile on plane 3, inlet angle of 20^{o}

Figures 4-30, 4-31 and 4-32 show the distribution of the contaminant on the three vertical planes 1, 2, 3, first Fig.4-30 shows that the contaminant's most significant concentrations are mainly around the person since the person is the only source of that flux. Since the air direction is mainly from top to bottom, the occupant releases contaminant which is then pushed downward away from the head of the occupant which explains why more contaminant is found towards the back and bottom of the office room, also contaminant is found around the occupant. Fig.4-31 shows very minimal concentrations in the adjacent plane, plane 2. The symmetry of the model dictates the concentrations in plane 3, which is the case in this simulation.

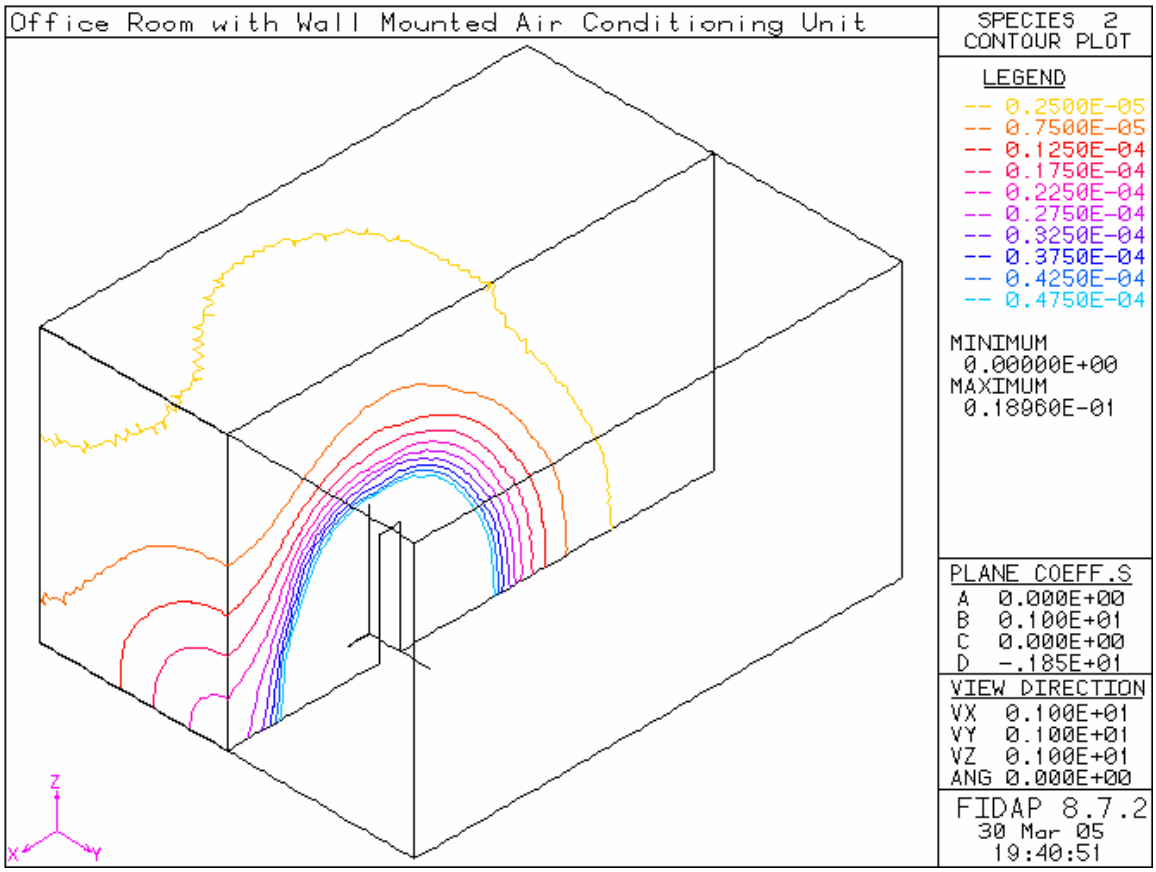

Figure 4-30 Contaminant profile on plane 1, inlet angle of 20^{o}

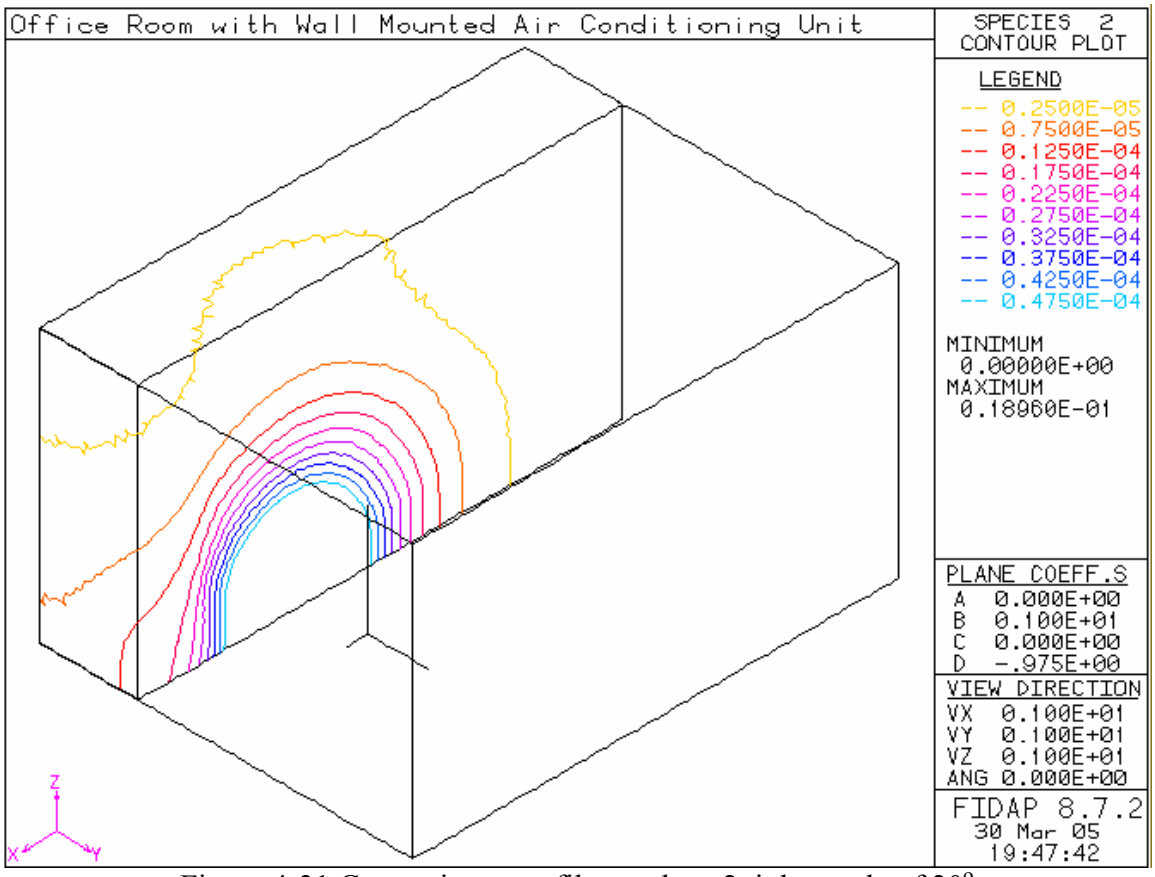

Figure 4-31 Contaminant profile on plane 2, inlet angle of 20^{o}

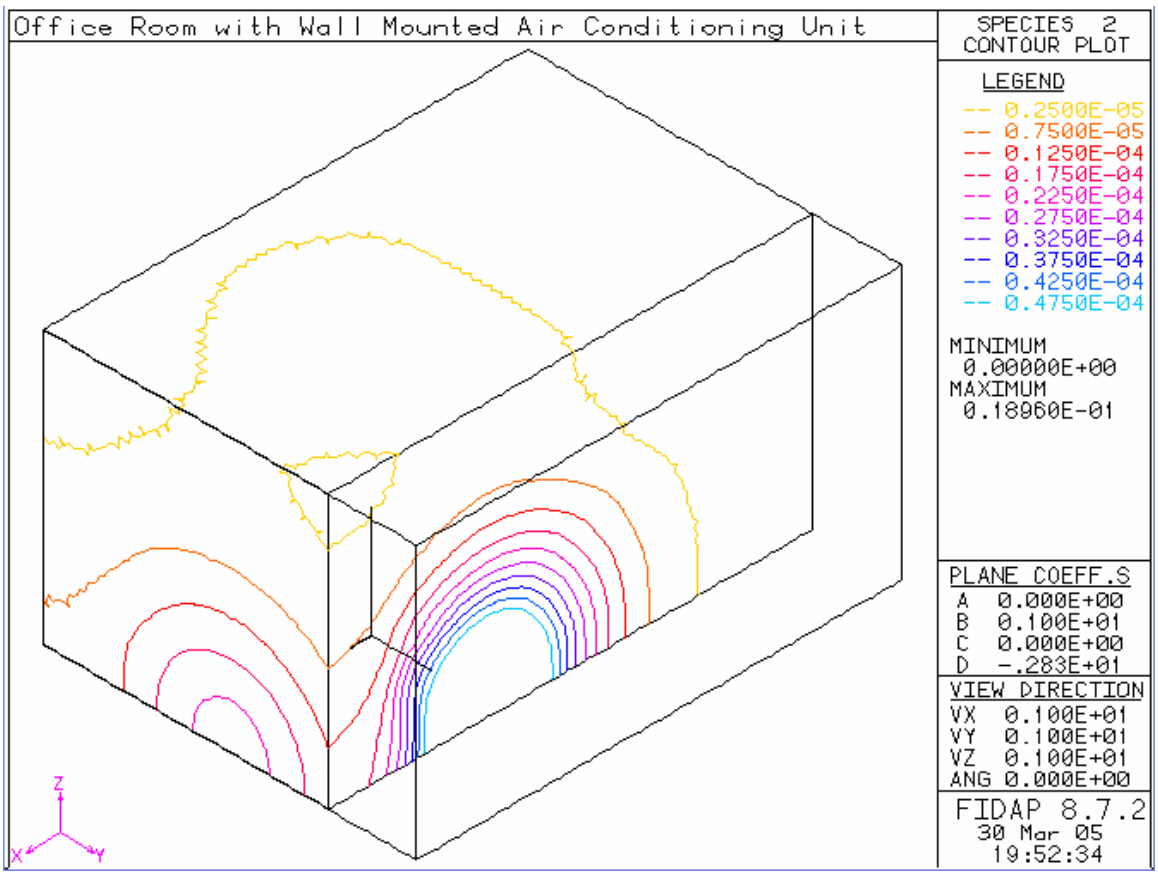

Figure 4-32 Contaminant profile on plane 3, inlet angle of 20^{o}

Fig.4-33 shows how the flow circulates around the person, notice that the inlet angle is 20^{0} which drive airflow to the ceiling of the room however from Fig.4-33 we see that the angle is slightly higher than 20^{o} because air entering the room is pushed upward by the air from the previous circulation. Figures 4-34 and 4-35 are similar in describing airflow behavior due to the symmetry of the office room.

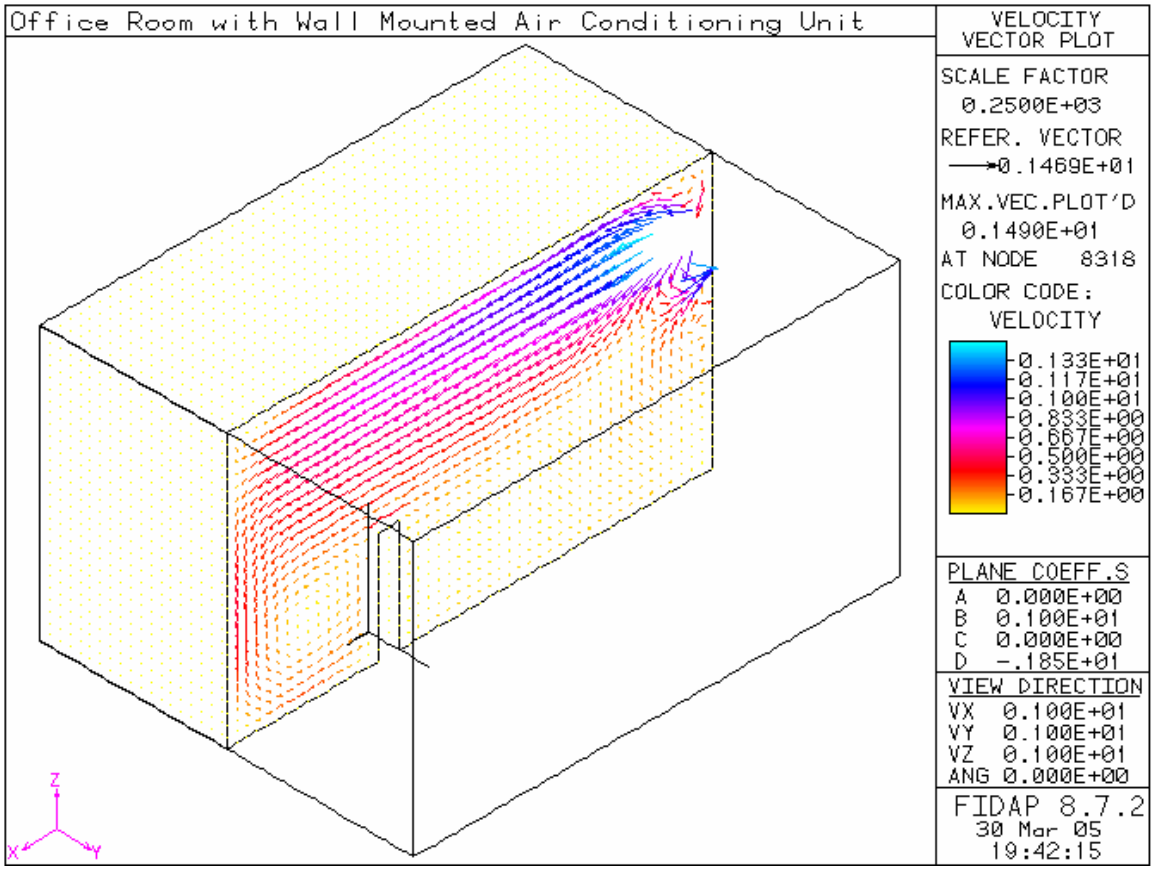

Figure 4-33 Velocity profile on plane 1, inlet angle of 20^{o}

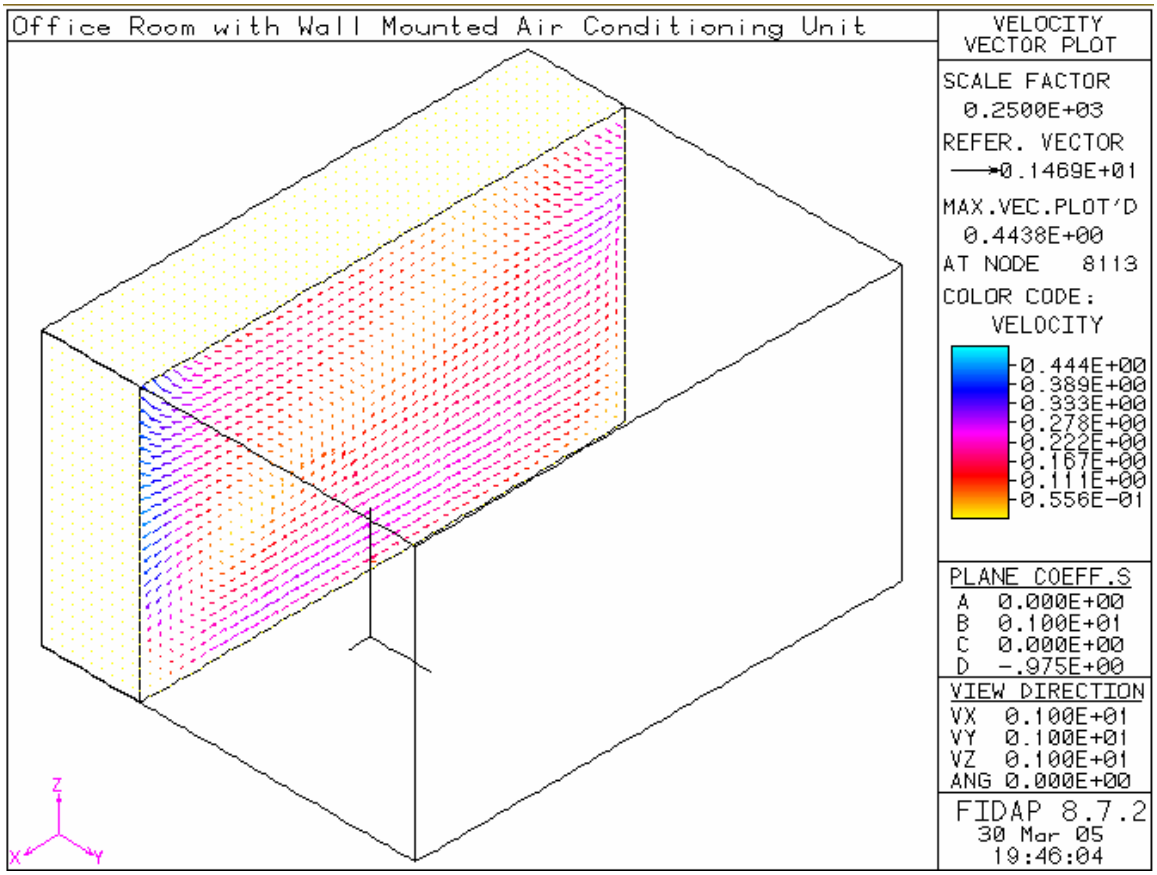

Figure 4-34 Velocity profile on plane 2, inlet angle of 20^{o}

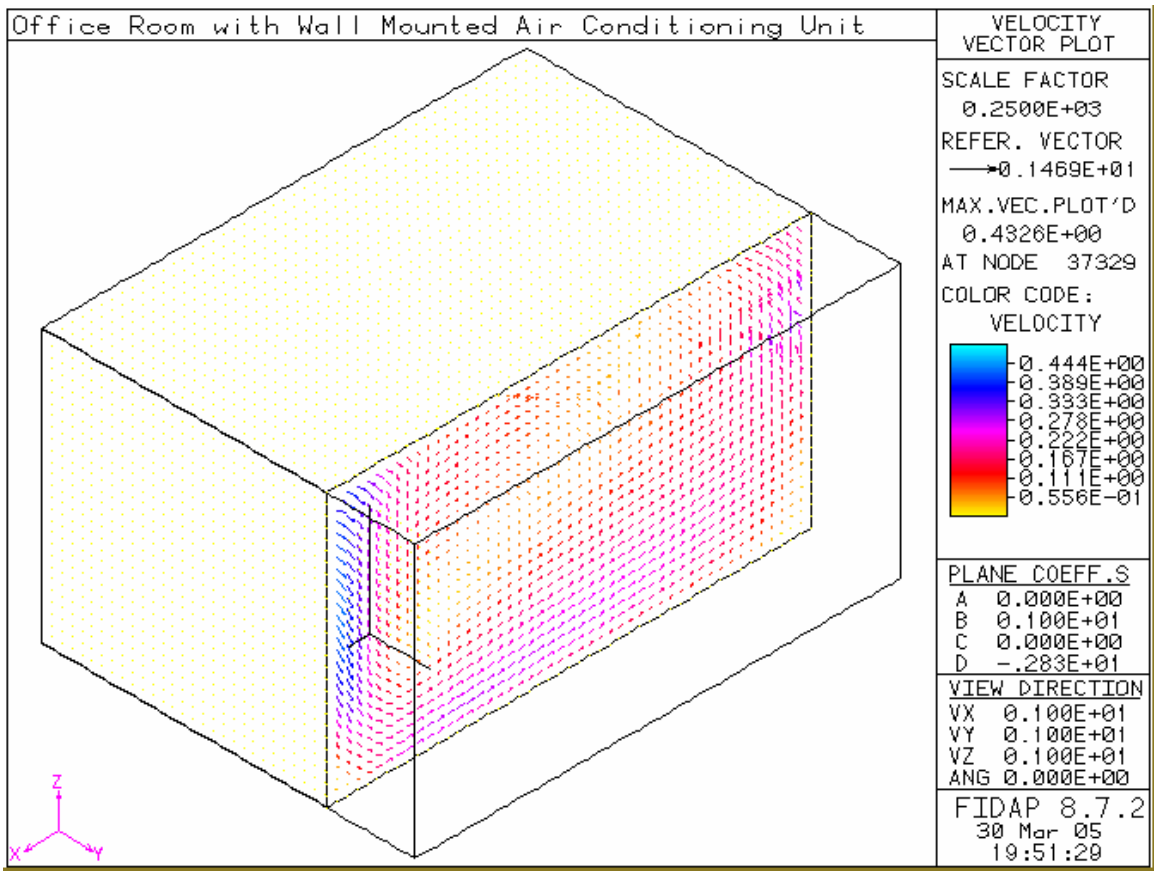

Figure 4-35 Velocity profile on plane 3, inlet angle of 20^{o}

As Relative humidity is inversely proportional to temperature, Fig.4-36, Fig.4-37, and Fig.4-38 show a profile similar to temperature. Relative humidity gets lower as airflow approaches the person and the light fixture, and as predicted is lower and constant on both sides of the room.

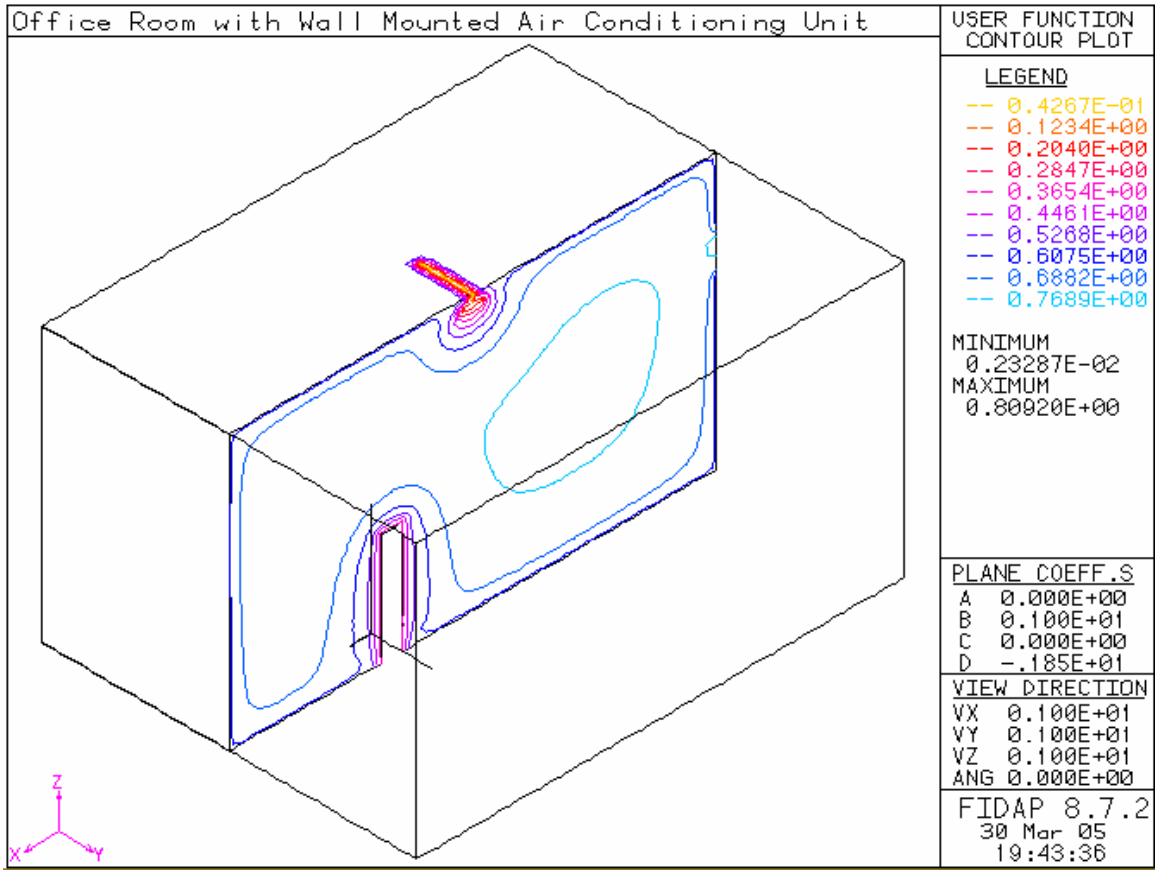

Figure 4-36 Relative humidity on plane 1, inlet angle of 20^{o}

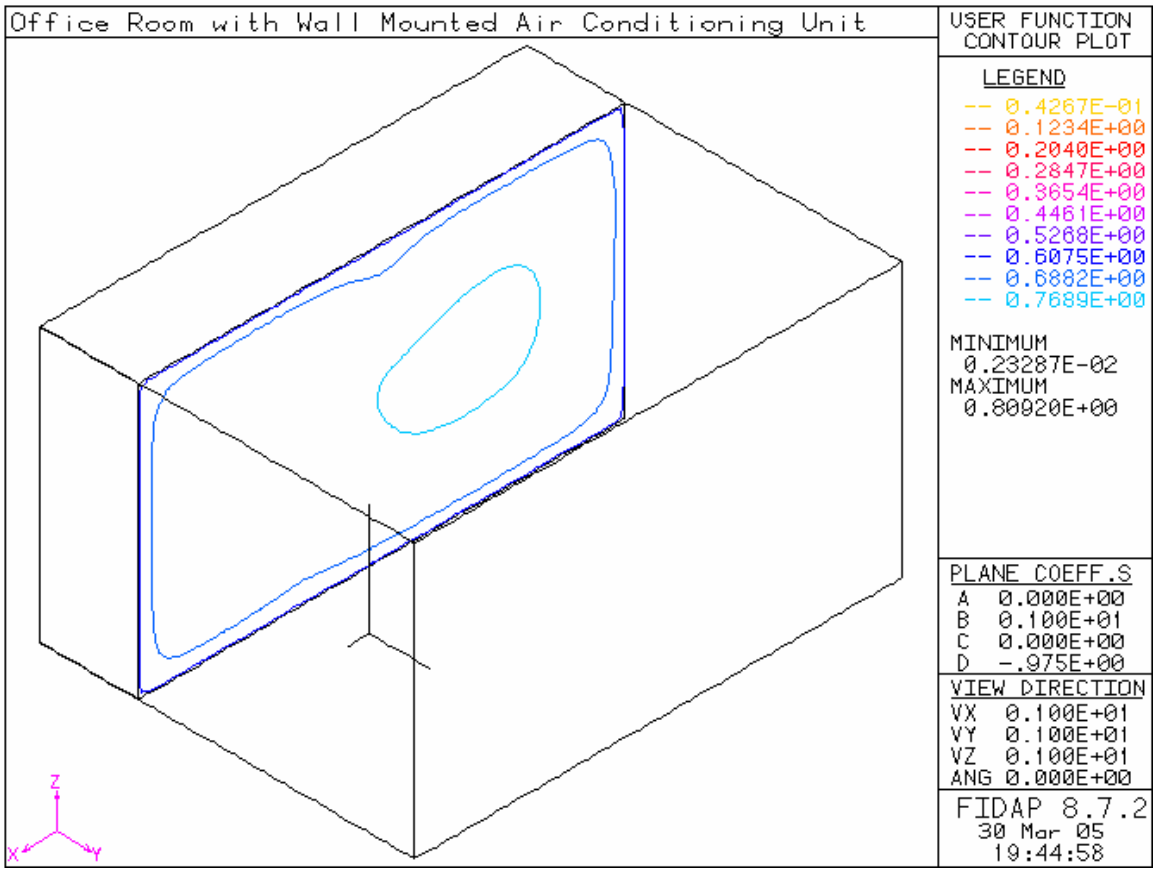

Figure 4-37 Relative humidity on plane 2, inlet angle of 20^{o}

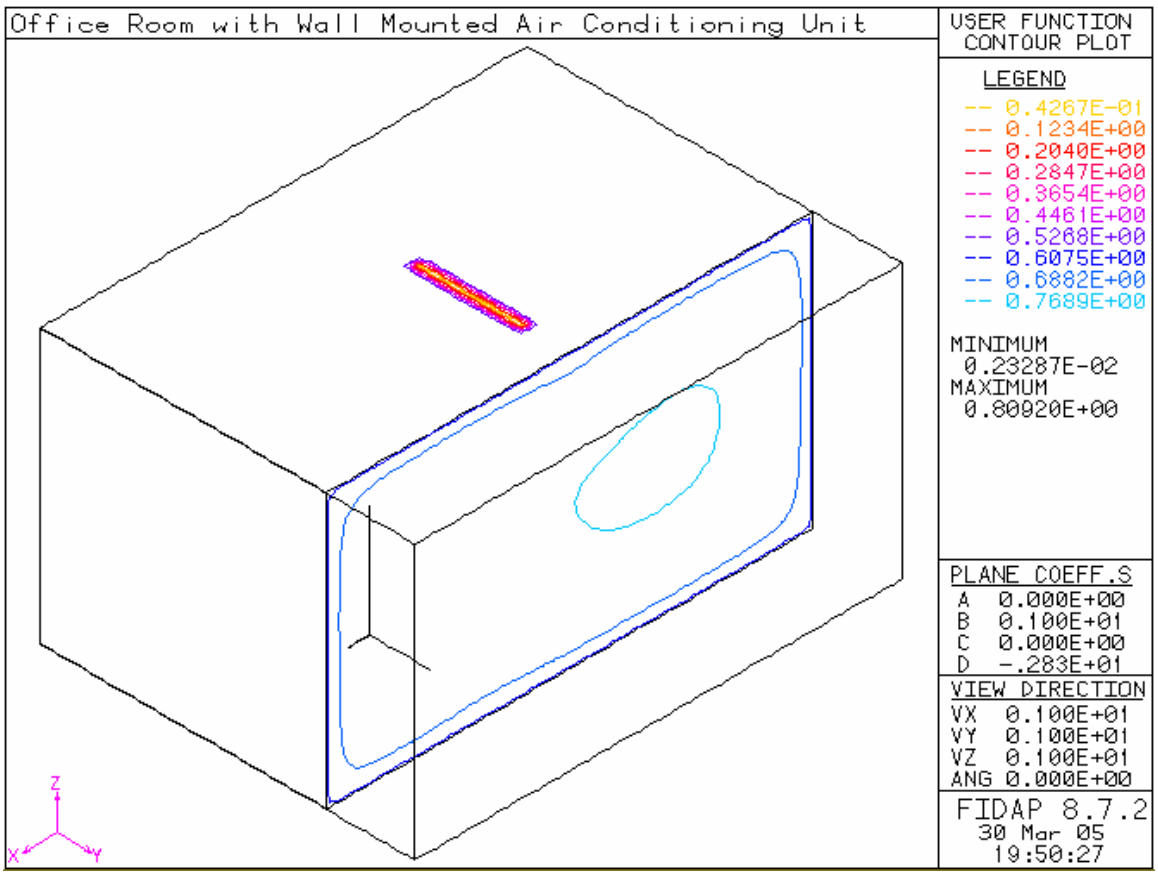

Figure 4-38 Relative humidity on plane 3, inlet angle of 20^{o}

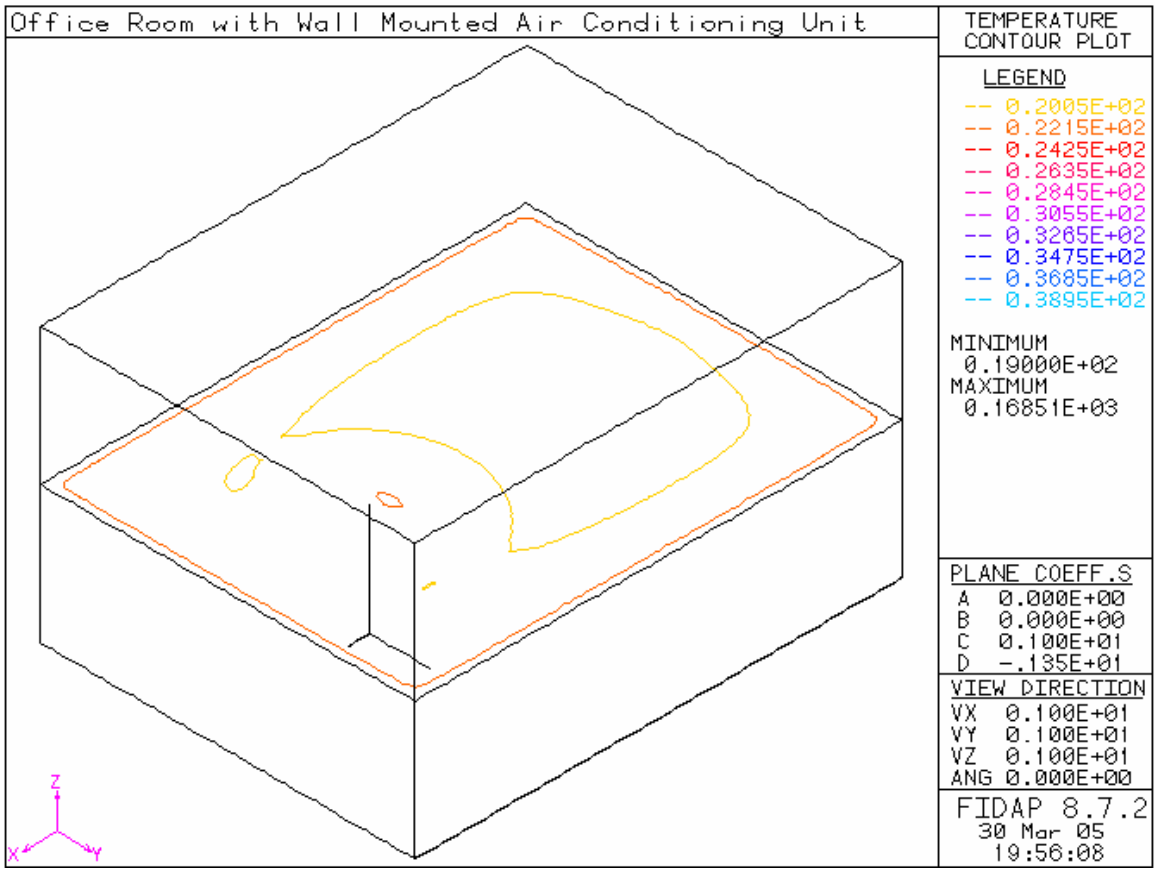

Figure 4-39 Temperature profile on plane 4, inlet angle of 20^{o}

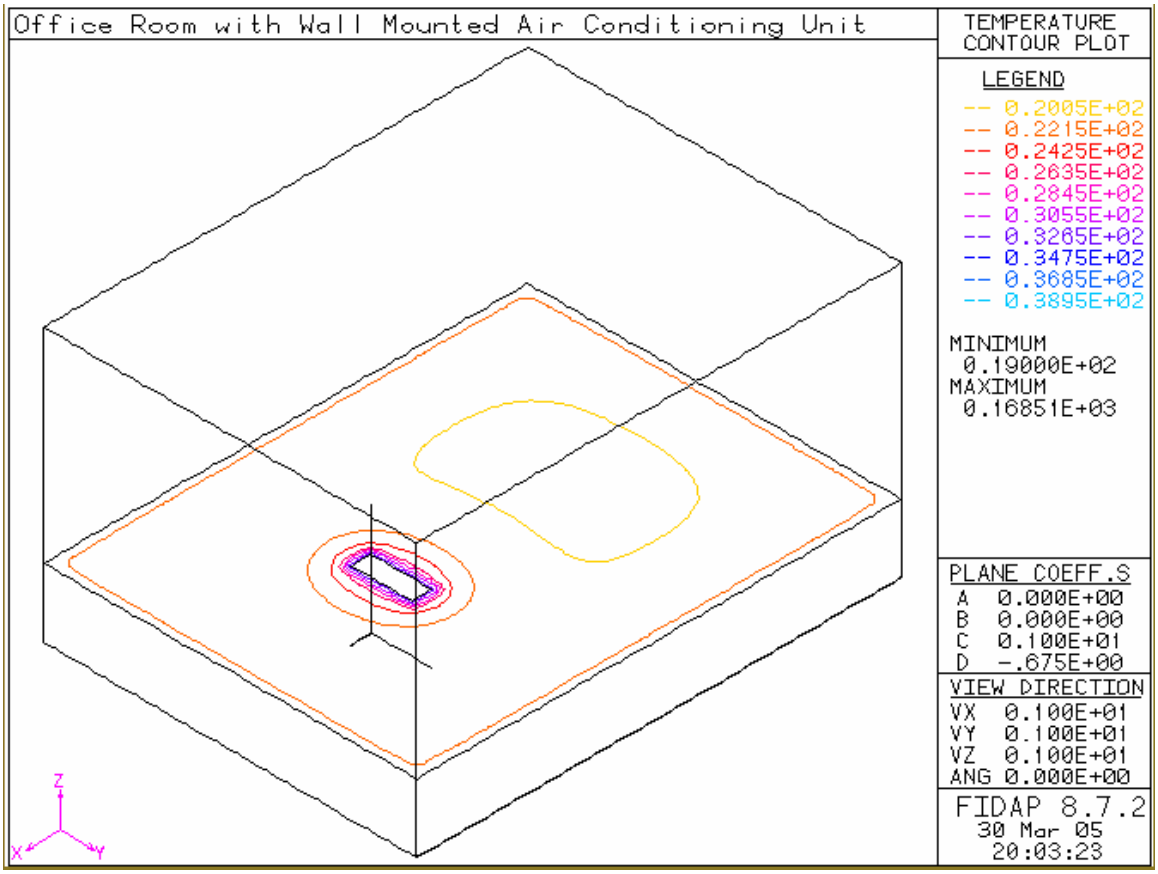

Figure 4-40 Temperature profile on plane 5, inlet angle of 20^{o}

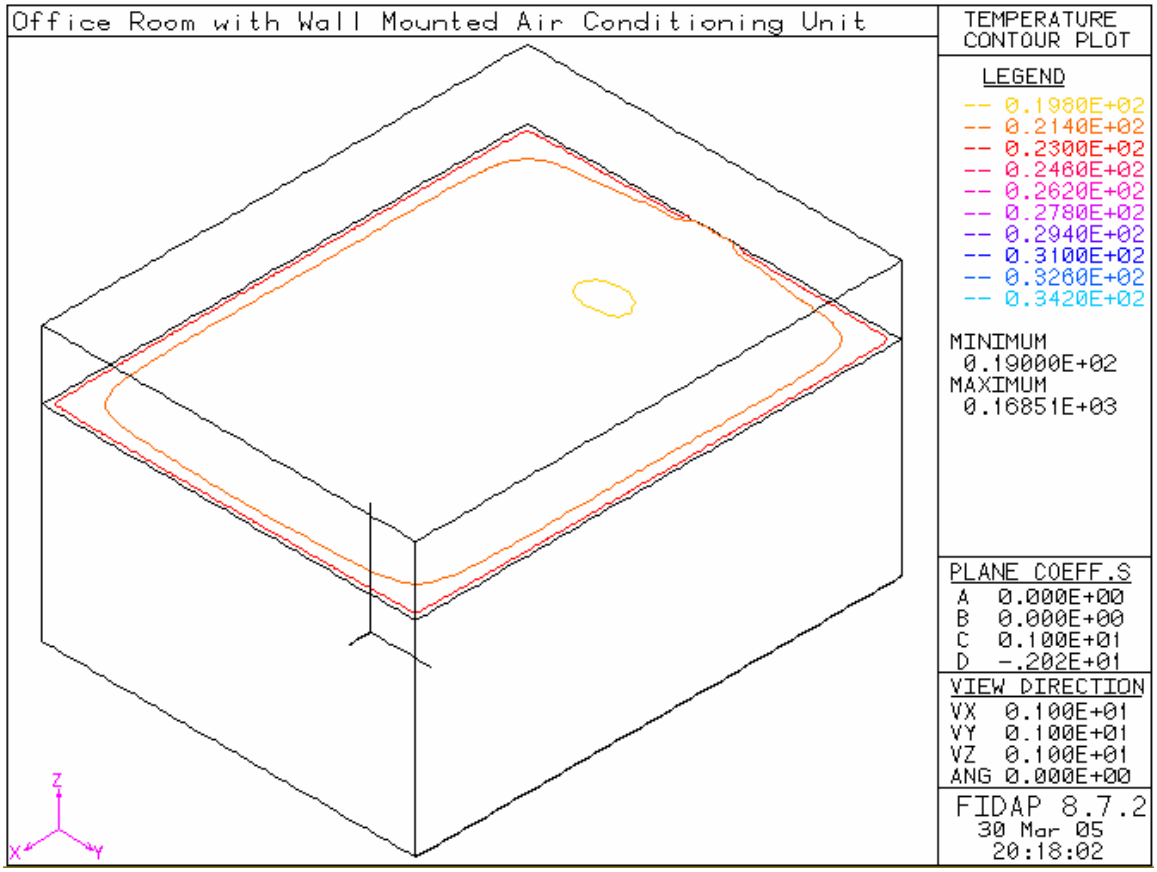

Figure 4-41 Temperature profile on plane 6, inlet angle of 20^{o}

Contaminant distribution of the office room analyzed by horizontal planes shows as first predicted, the contamination secretion from the person is uneven. High concentrations are found towards the bottom back section of the room as Table 4-8 shows. It is clear from comparing Fig.4-42, Fig.4-43 and Fig.4-44 that the concentration of contaminant within the office room diminished as the height increases. This is explained by the airflow movement inside the room and around the occupant, which is meanly directed downwards.

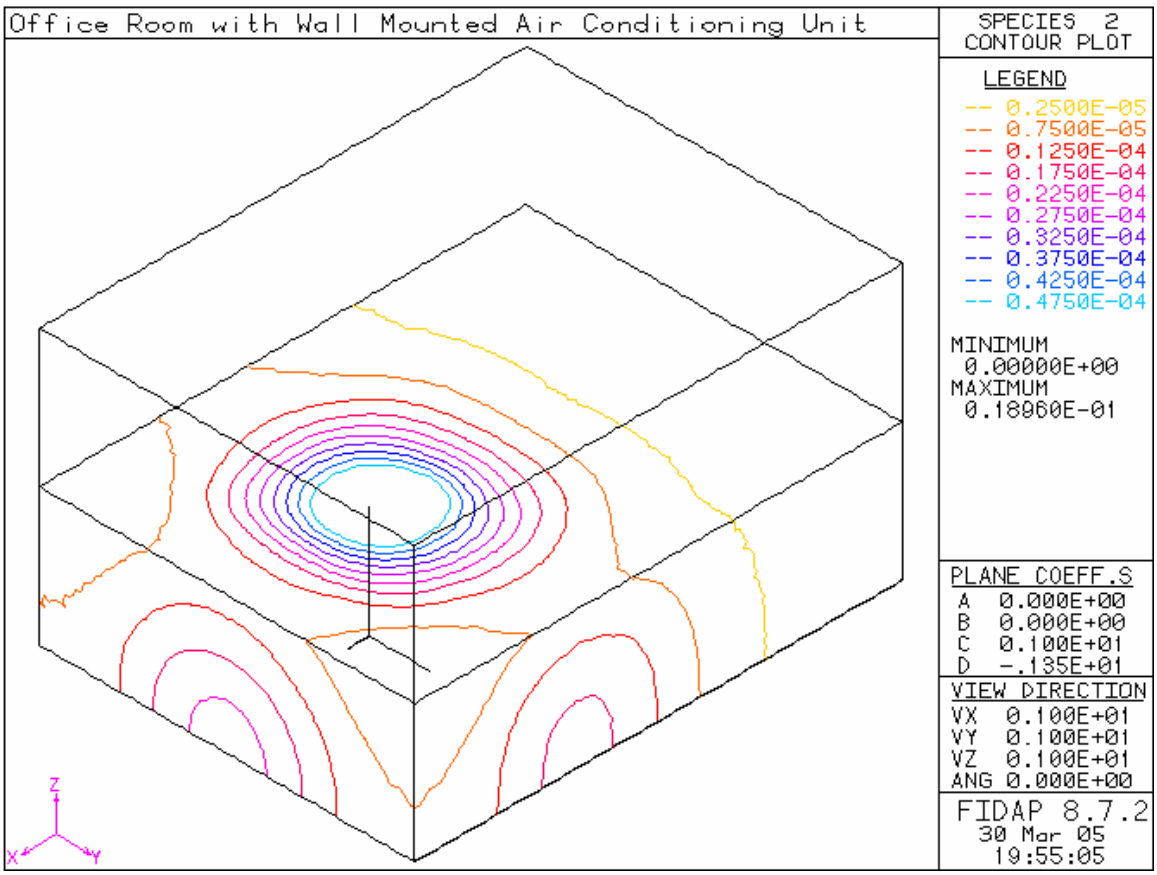

Figure 4-42 Contaminant profile on plane 4, inlet angle of 20^{o}

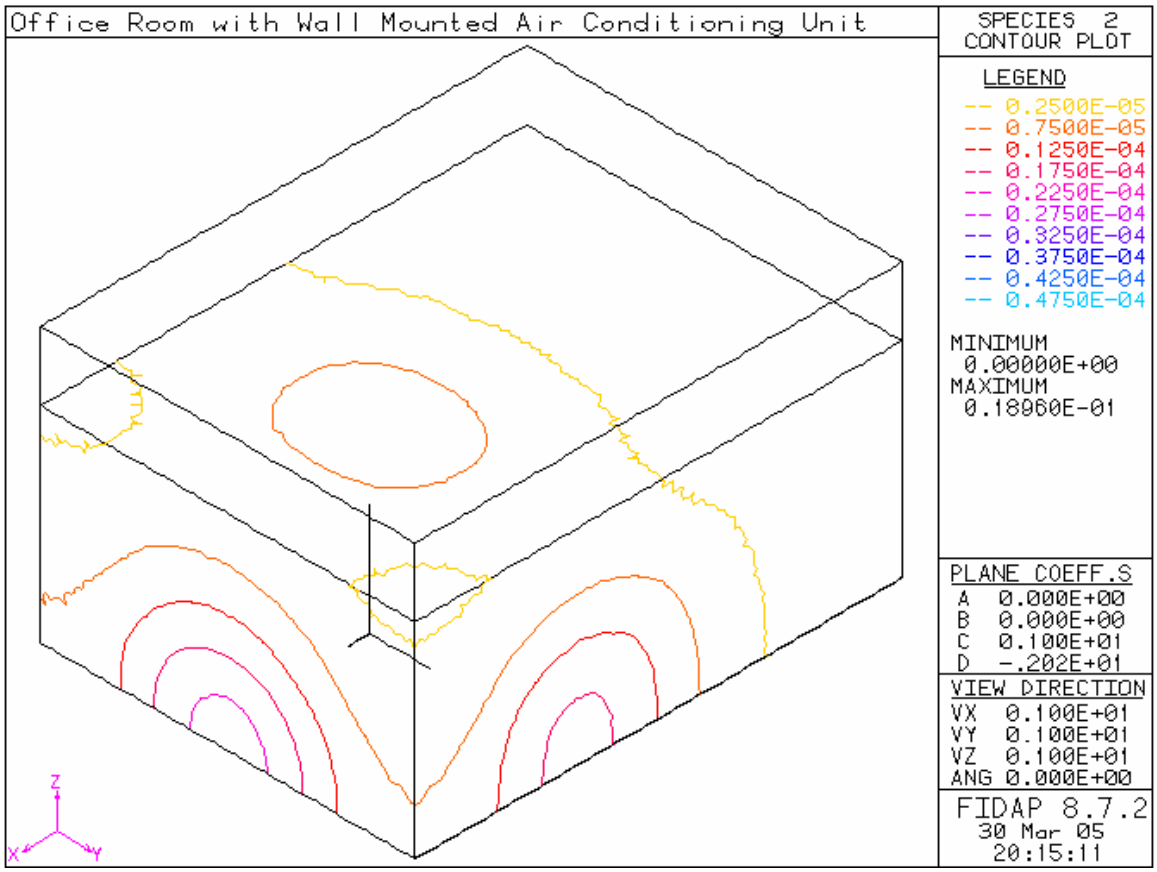

Figure 4-43 Contaminant profile on plane 6, inlet angle of 20^{o}

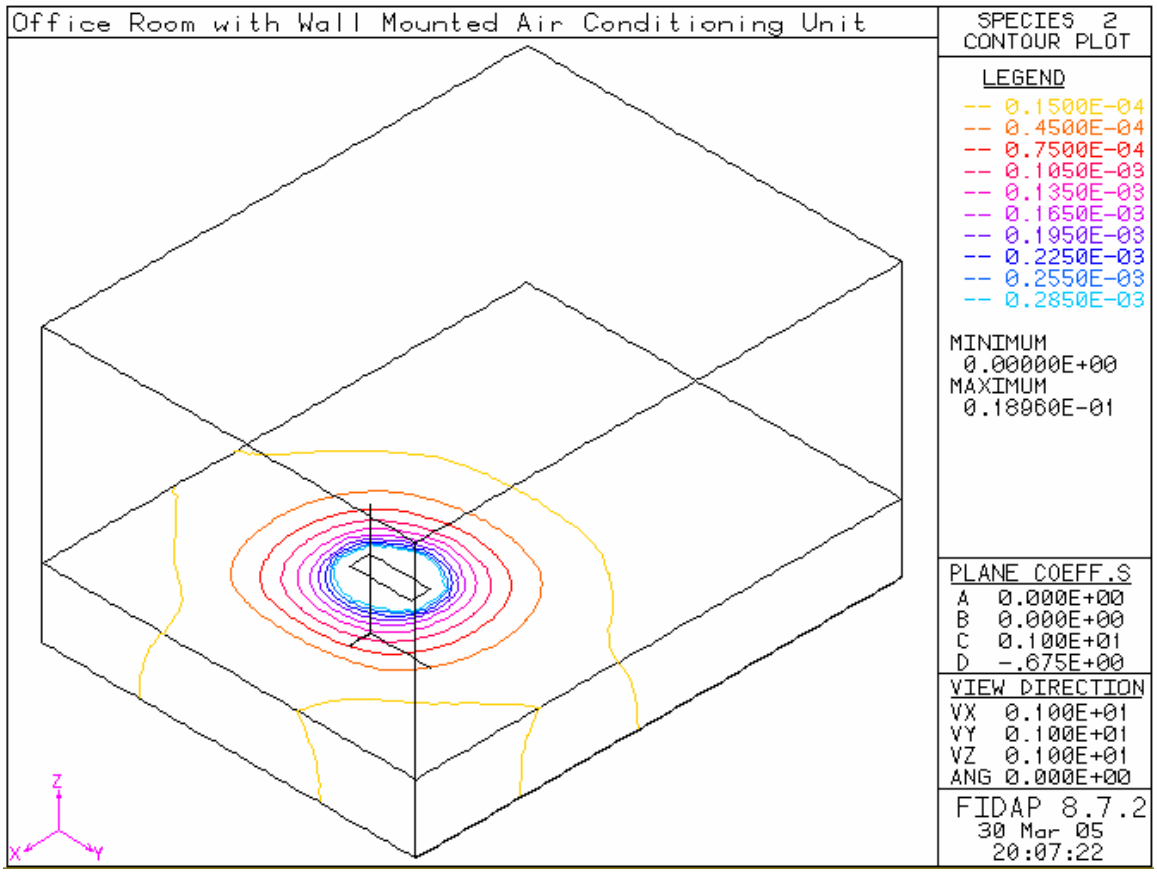

Figure 4-44 Contaminant profile on plane 5, inlet angle of 20^{o}

Table 4-8 shows that contaminant is being cleared very rapidly from plane 1 however, it agrees with predictions that the contaminant is concentrated at the bottom levels of the room.

Table 4-8 Concentration of contaminant and CRE, for 20^{o} inlet angle

Studied planes	Contaminant concentration	CRE
1	3.27E-3	2.41E-5
2	6.94E-6	0.011345
3	6.94E-6	0.011345
4	0.000701	0.00125
5	0.000672	0.001305
6	0.000756	0.00116

Looking at the horizontal planes, high speed airflow goes around the person from the top and two sides; as the height decreases Fig.4-45 effectively shows that high speed air shown in Fig.4-46 is evenly dispersed around the room's ceiling and walls before being guided downward. Notice the circulation pattern around the person; it explains the temperature and the contaminant distribution in the office room.

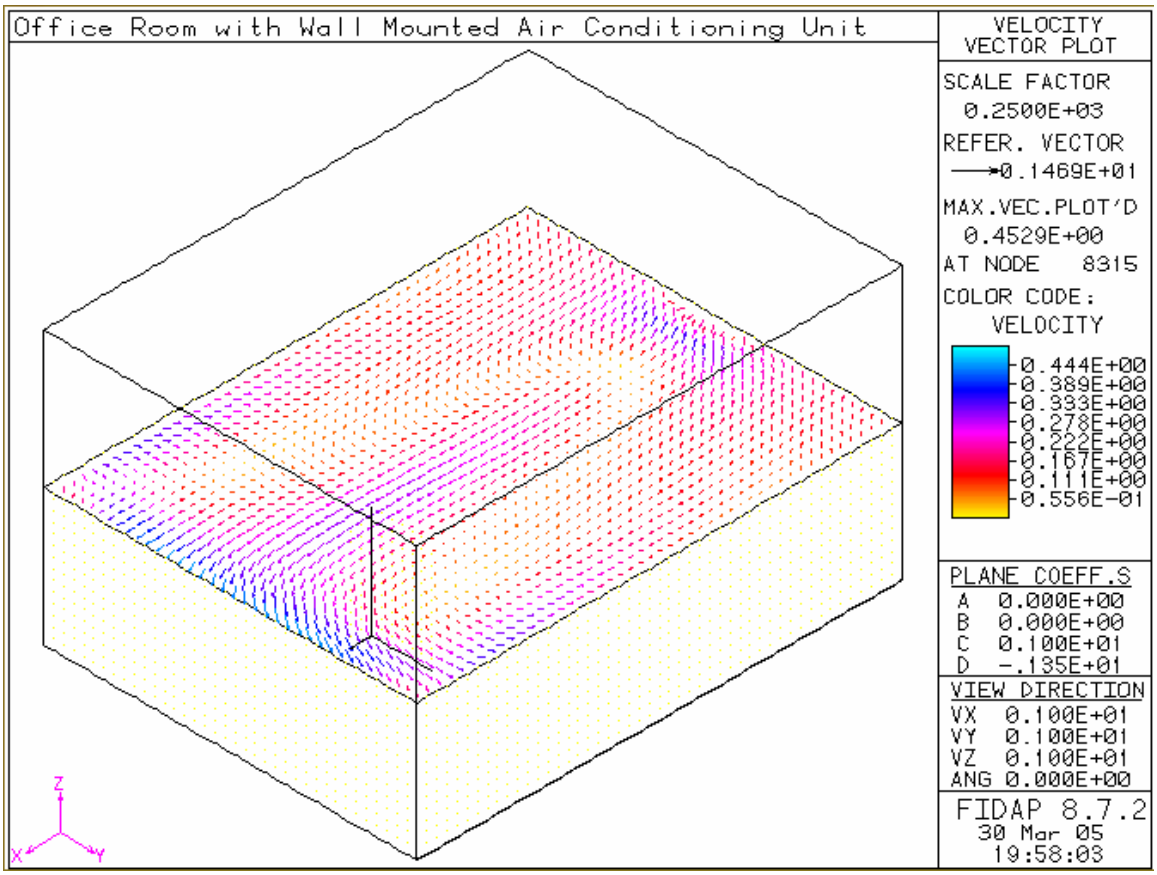

Figure 4-45 Velocity profile on plane 4, inlet angle of 20^{o}

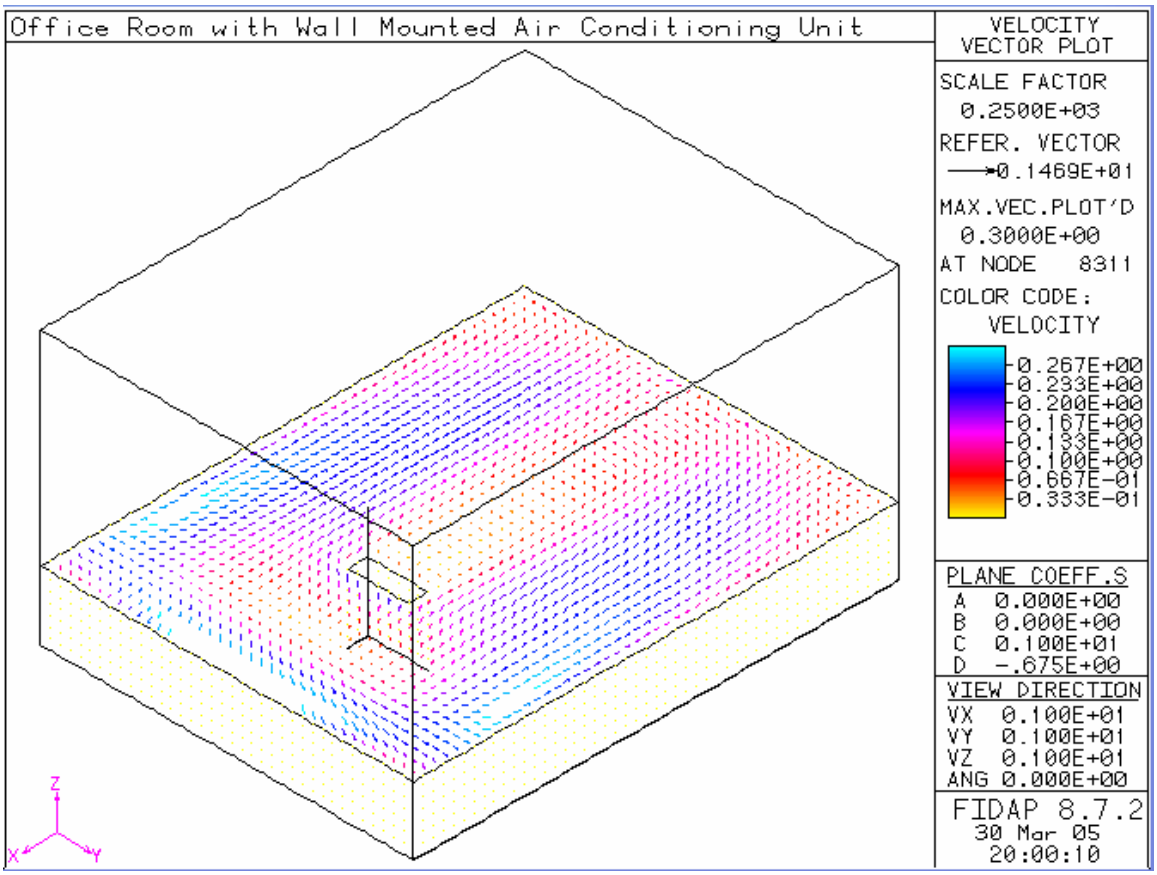

Figure 4-46 Velocity profile on plane 5, inlet angle of 20^{o}

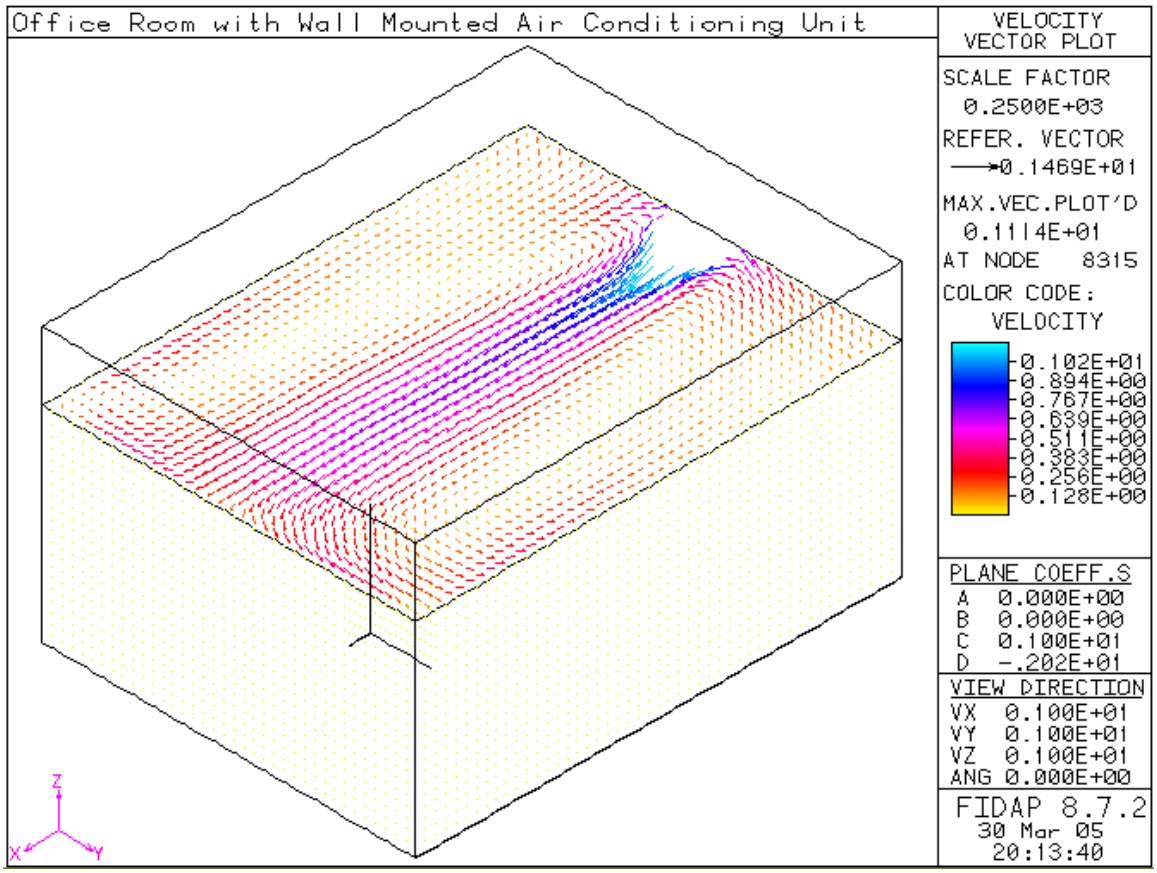

Figure 4-47 Velocity profile on plane 6, inlet angle of 20^{o}

As Table 4-9 shows the numerical value of the average relative humidity in the horizontal planes 4, 5, and 6 increases as height increases. Cool airflow velocity in the upper planes of the room is very high which explains the increase in average relative humidity in the high sections of the office room. The heat around the occupant is presumed transferred at a high constant rate that heats air surrounding it, raising its temperature thus decreasing the immediate relative humidity. Fig.4-48 and Fig.4-49 show planes that do no intersect with the occupant, yet as temperature in Fig.4-40 and the convective heat transfer ratio predict it, the relative humidity is low immediately above the person and as the air get closer to the light fixture.

Table 4-9 Relative humidity in the studied planes

Planes	Relative Humidity %
1	39.96
2	59.57
3	59.57
4	69.96
5	70.33
6	67.74

Notice from Table 4-9 that relative humidity is very low in plane 1 even with cold air flowing in it. This explained by the presence of the light and the occupant in plane 1.

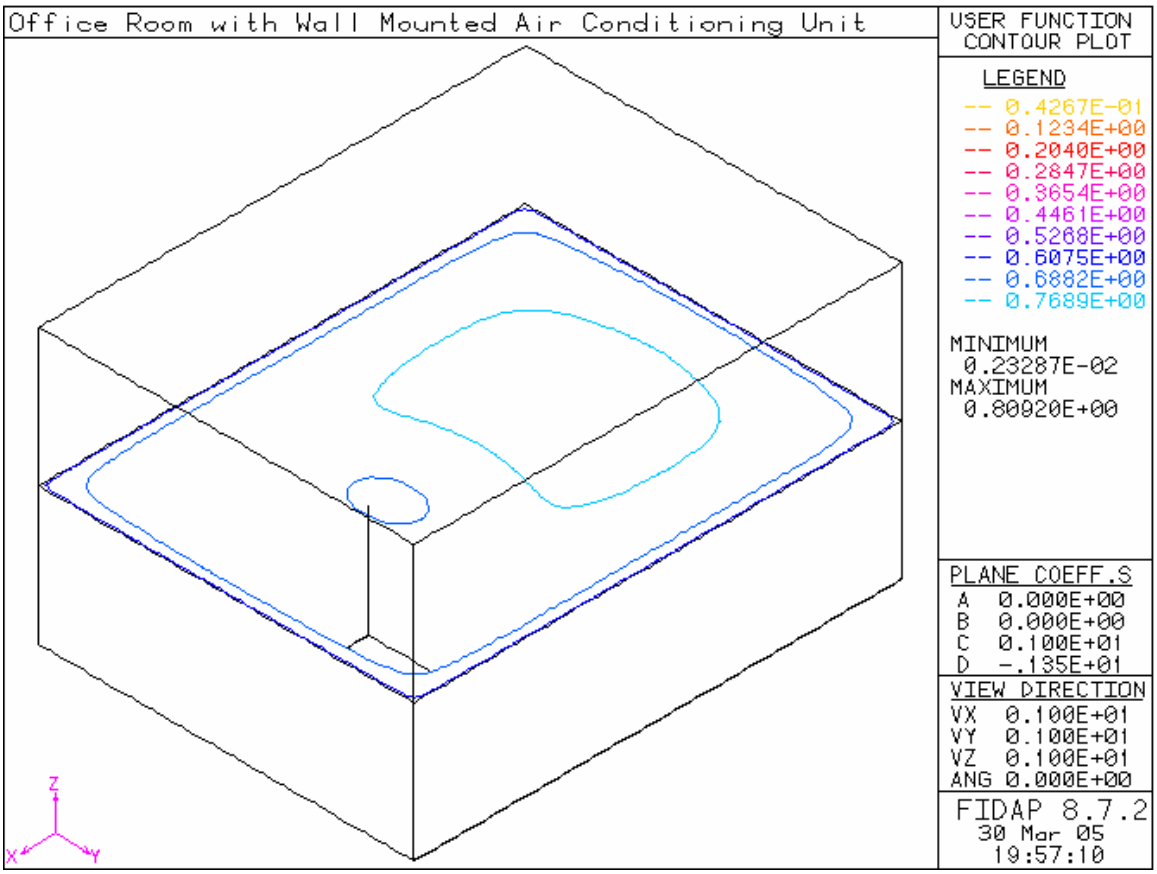

Figure 4-48 Relative Humidity on plane 4, inlet angle of 20^{o}

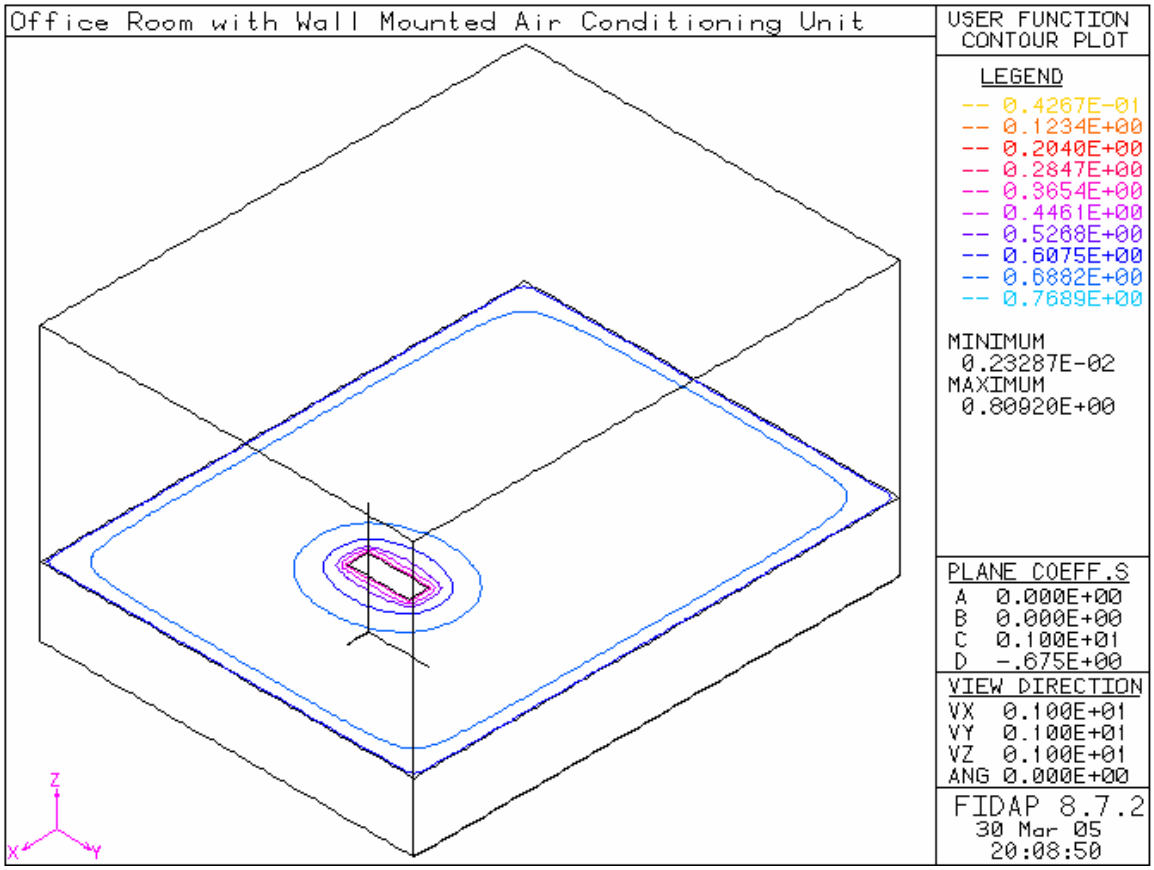

Figure 4-49 Relative Humidity on plane 5, inlet angle of 20^{o}

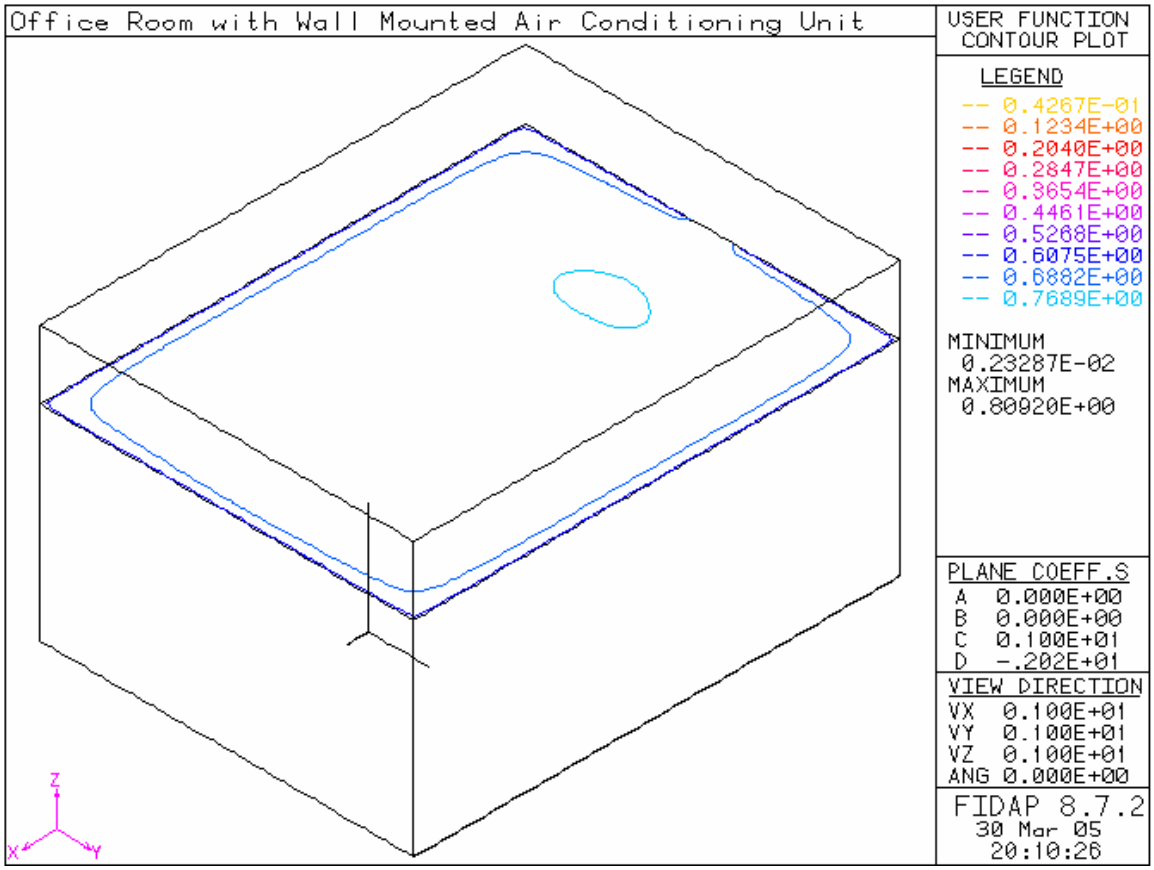

Figure 4-50 Relative Humidity on plane 6, inlet angle of 20^{o}

4.3.3 Simulation with 40^{o} inlet angle

Temperature distribution throughout the room is analyzed first in the three vertical planes shown in Fig.4-51, Fig.4-52, and Fig.4-53. In Fig.4-51 the temperature rises around the light fixture and the occupant, the heat transfer from the light is very significant because of the high local temperature. The same is true around the occupant where the surrounding air gets warmer as it get closer to the person. Fig.4-52 and Fig.4-53 are identical in describing the temperature profile as expected by the symmetry of the simulation and the position of the planes studied, the temperature magnitude is on the low

side since from both ends; the two studied planes do no intersect with the person and the light fixture.

In addition Table 4-10 shows a comparison between the 3-D model and the corresponding 2-D model shown in Chapter 3.

Table 4-10 Comparison of relative humidity and temperature in 40^{o} inlet angle 2-D and 3-D models

Simulated Models	Average Relative Humidity %	Average Temperature ^{0}C
Three Dimensional	52.15	25.32
Two Dimensional	56.98	23.43

Again the 3-D model show higher temperatures and low relative humidity in the office room. The amount of nodes averaged in the 3-D model exceeds the one in the 2-D model which explains the differences.

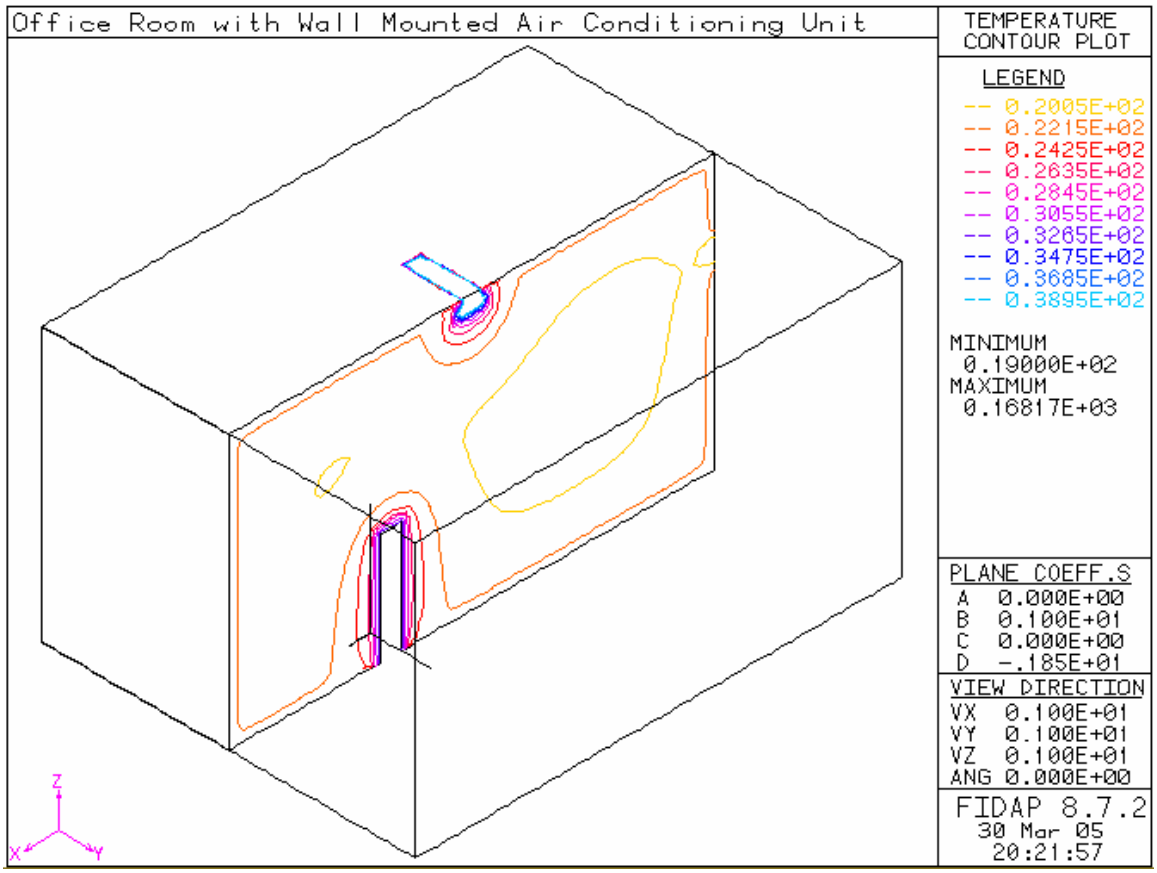

Figure 4-51 Temperature profile on plane 1, inlet angle of 40^{o}

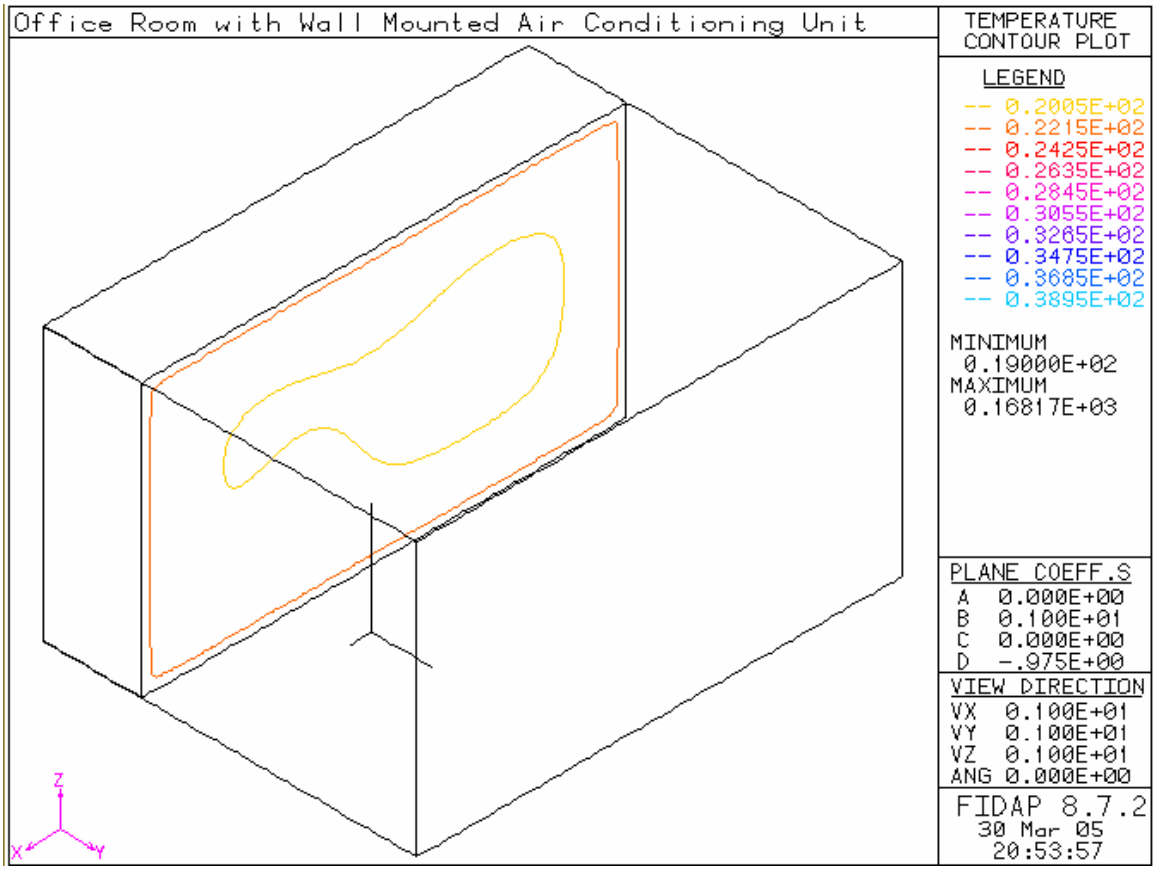

Figure 4-52 Temperature profile on plane 2, inlet angle of 40^{o}

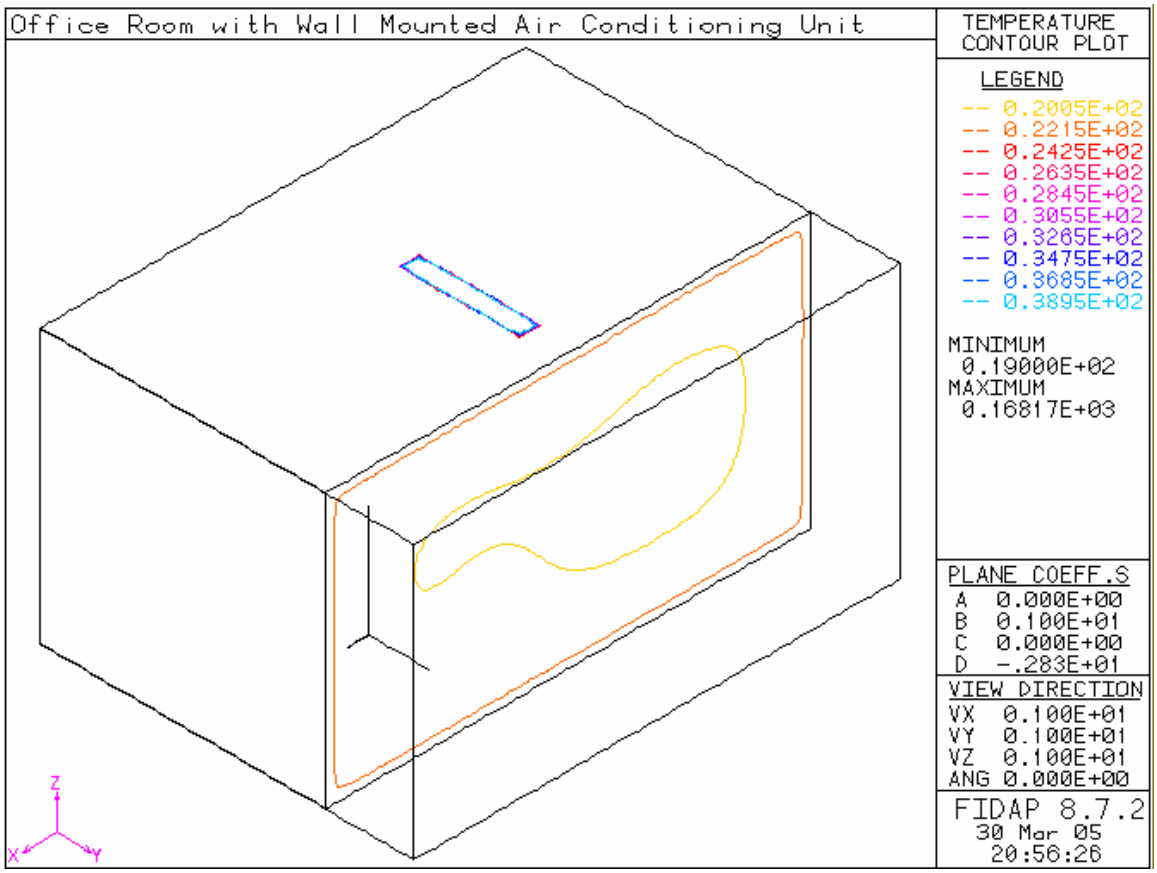

Figure 4-53 Temperature profile on plane 3, inlet angle of 40^{o}

Contaminant concentration is very noticeable in Fig.4-54 it showing how contaminant is cleared from the occupant in a downward fashion and pushed in the direction of the office floor. Table 4-11 shows that the contaminant is more present at the bottom planes of the office room; this is due low velocities of the returned air shown in Fig.4-57.

Table 4-11 Concentration of contaminant and CRE, for 40^{o} inlet angle

Studied planes	Contaminant concentration	CRE
1	0.00288	1.51E-5
2	7.19E-7	0.06091
3	7.19E-7	0.06091
4	0.000963	4.53E-5
5	0.000841	5.19E-5
6	0.001246	3.50E-5

As predicted by the inlet angle of 40^{o}, the contaminant is more present in this case than the two cases mentioned above. Especially on the bottom planes where the airflow velocity is low, the contaminant is more concentrated at these planes.

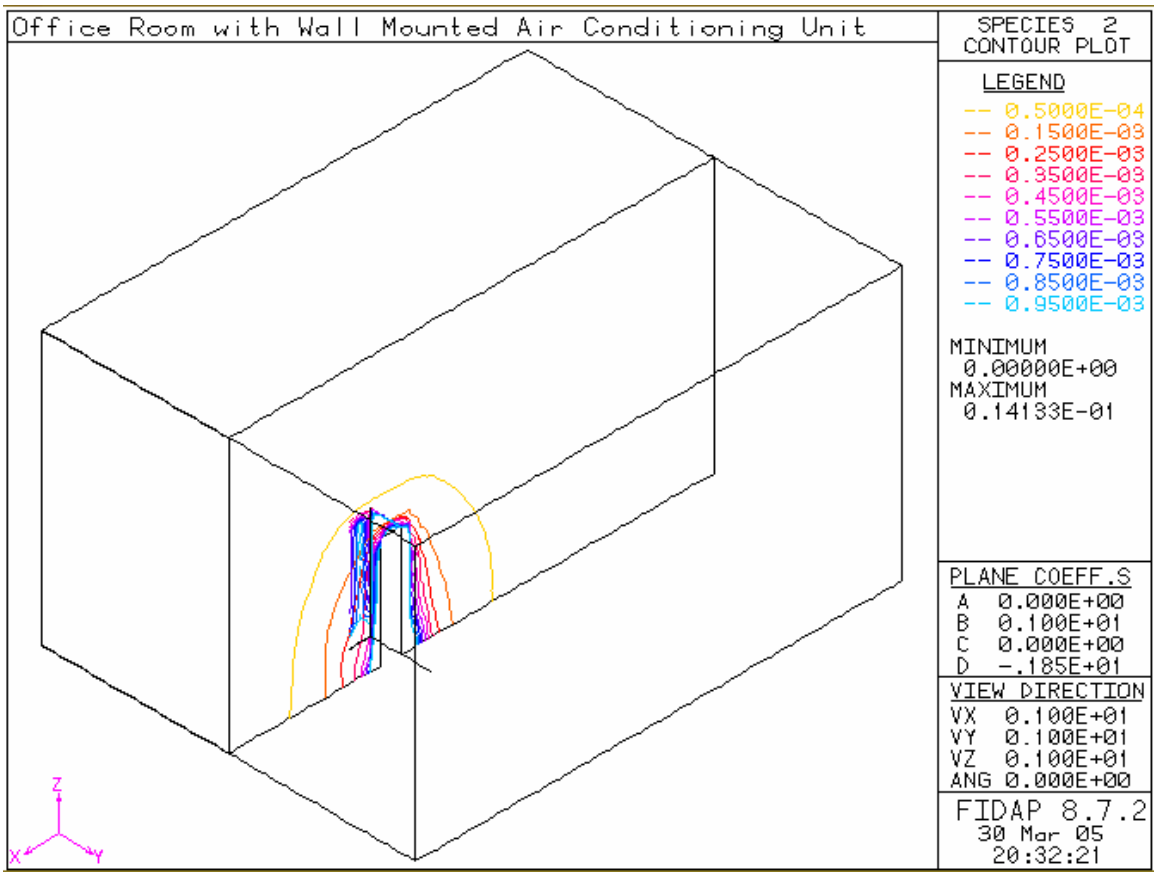

Figure 4-54 Contaminant profile on plane 1, inlet angle of 40^{o}

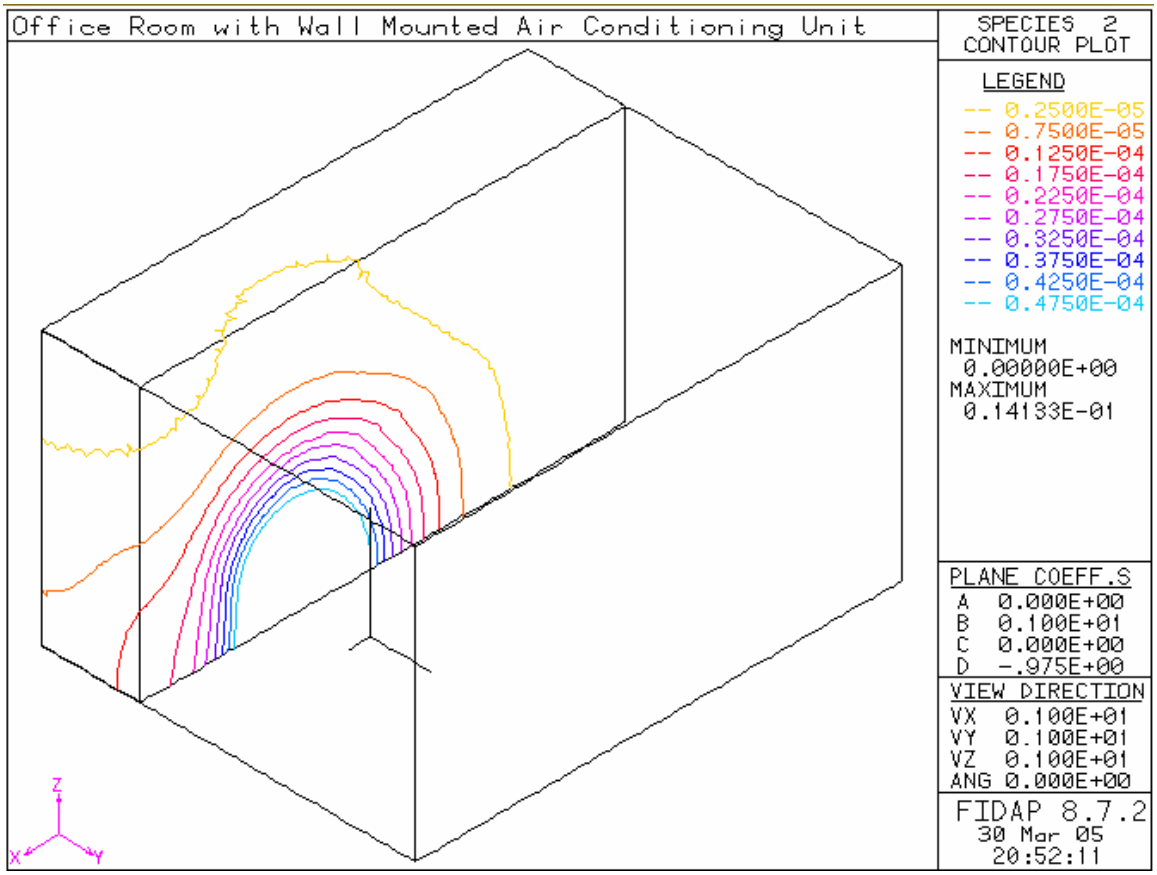

Figure 4-55 Contaminant profile on plane 2, inlet angle of 40^{o}

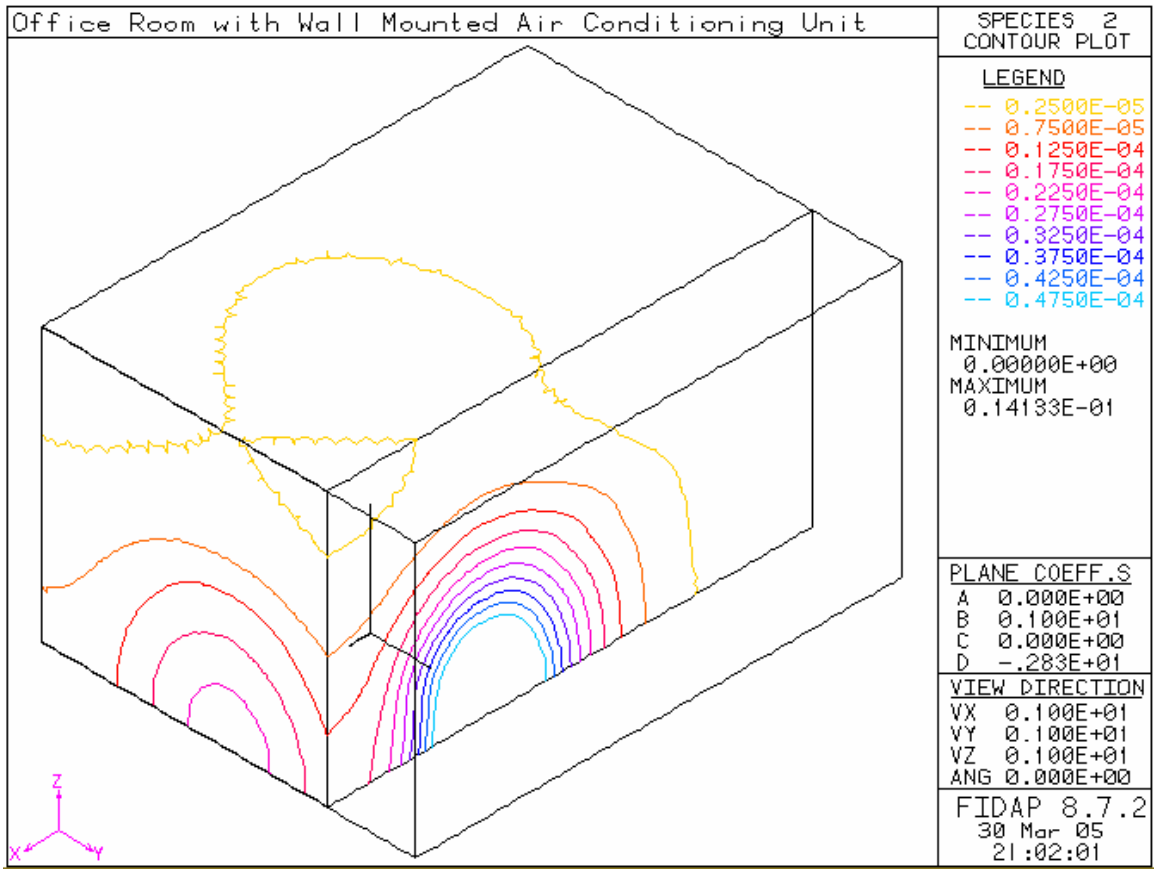

Figure 4-56 Contaminant profile on plane 3, inlet angle of 40^{o}

Figure 4-57, Figure 4-58, and Figure 4-59 show the velocity profile in the vertical planes, the flow enters the office room with a discharge angle of 40o then it is directed toward the ceiling as for previous cases. In the horizontal planes 4, 5, and 6 Fig.4-69, Fig.4-70, and Fig.4-71, airflow follow the same behavior only at lower velocities which explains the high concentration of contaminant in the bottom of the room

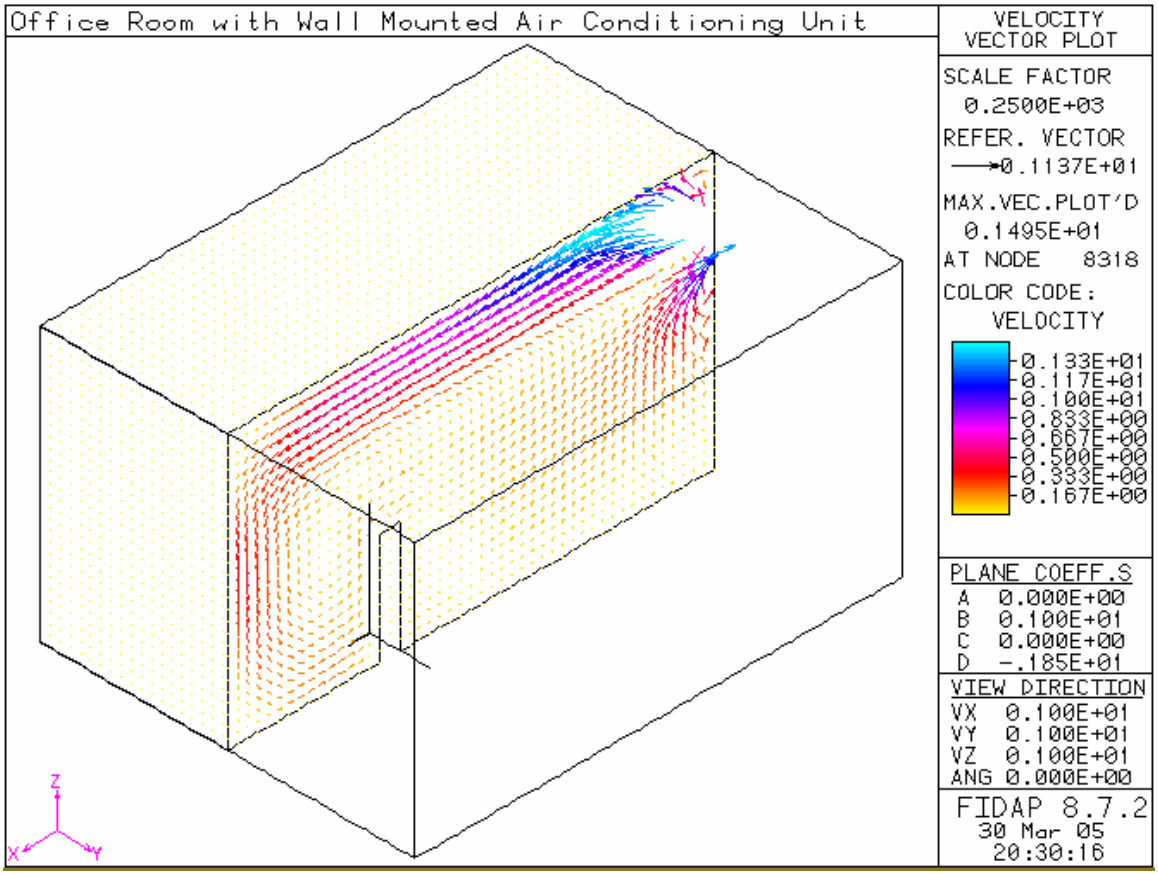

Figure 4-57 Velocity profile on plane 1, inlet angle of 40^{o}

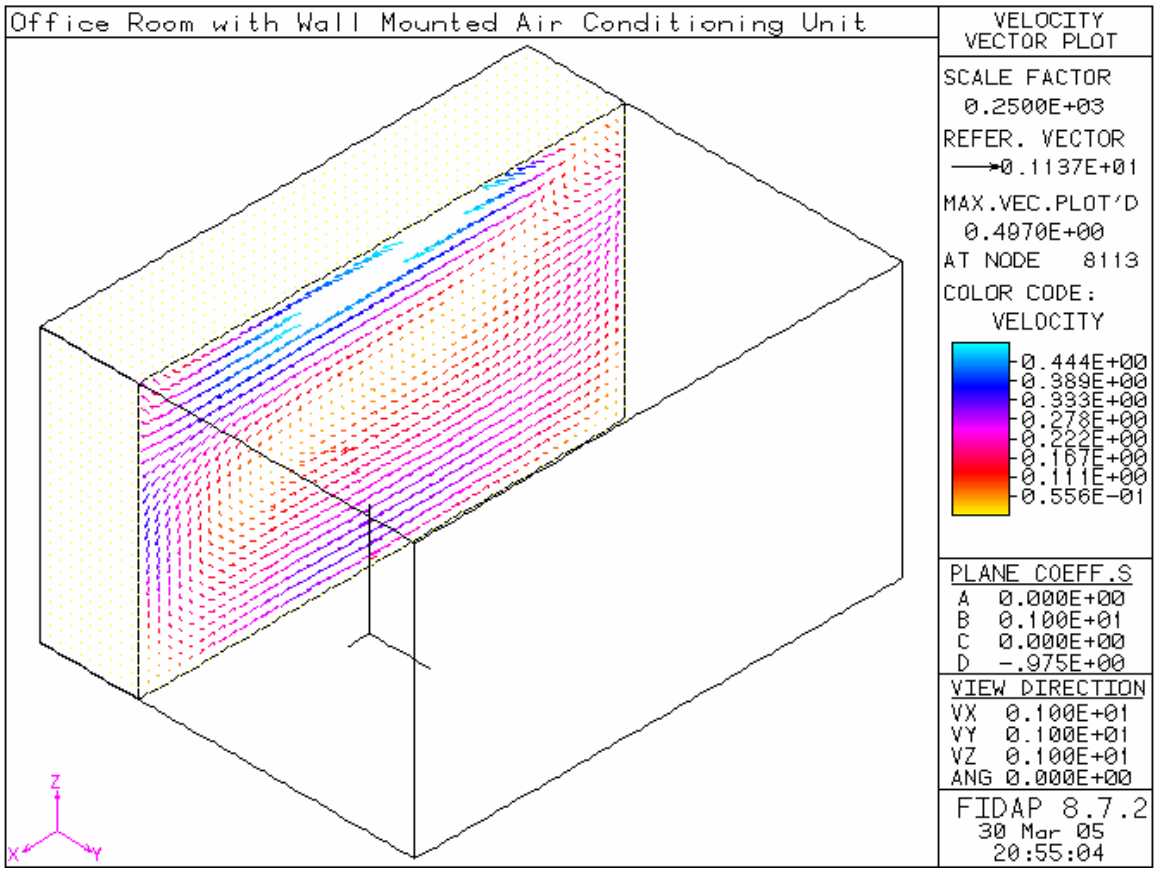

Figure 4-58 Velocity profile on plane 2, inlet angle of 40^{o}

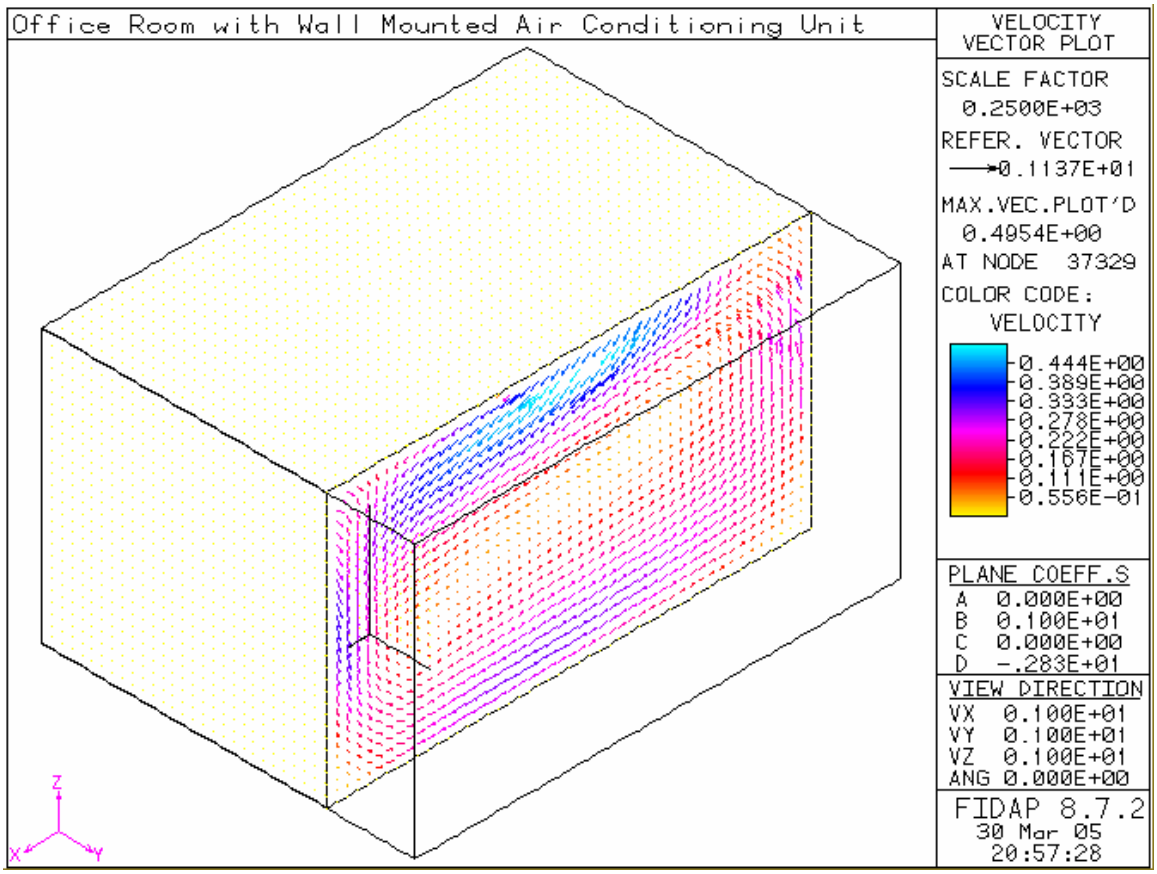

Figure 4-59 Velocity profile on plane 3, inlet angle of 40^{o}

Relative humidity is a very important factor of indoor human thermal comfort especially in office rooms cooled by wall-mounted units. Table 4-12 shows values of average relative humidity in the studied planes. Knowing the symmetry of the simulation and, in agreement with Fig.4-61 and Fig.4-62 the values of relative humidity are very acceptable. Notice that values of relative humidity in the vertical planes 3 and 4 in Table 4-12 are equals and the profiles shown in Fig.4-61 and Fig.4-62agree to the numerical values. Even though the numerical value of relative humidity in the center plane 2 is lower than the adjacent planes, Table 4-12. Fig.4-60 shows a high relative humidity around the light and the person with is explained by the heat transfer magnitude at these locations due to high temperatures. Fig.4-60 agrees with this profile. Further more due to

high temperature, the relative Humidity decreases considerably as the airflow get closer to the occupant.

Table 4-12 Relative humidity in the studied planes

Planes	Relative Humidity %
1	39.90
2	58.72
3	58.72
4	68.44
5	67.73
6	70.56

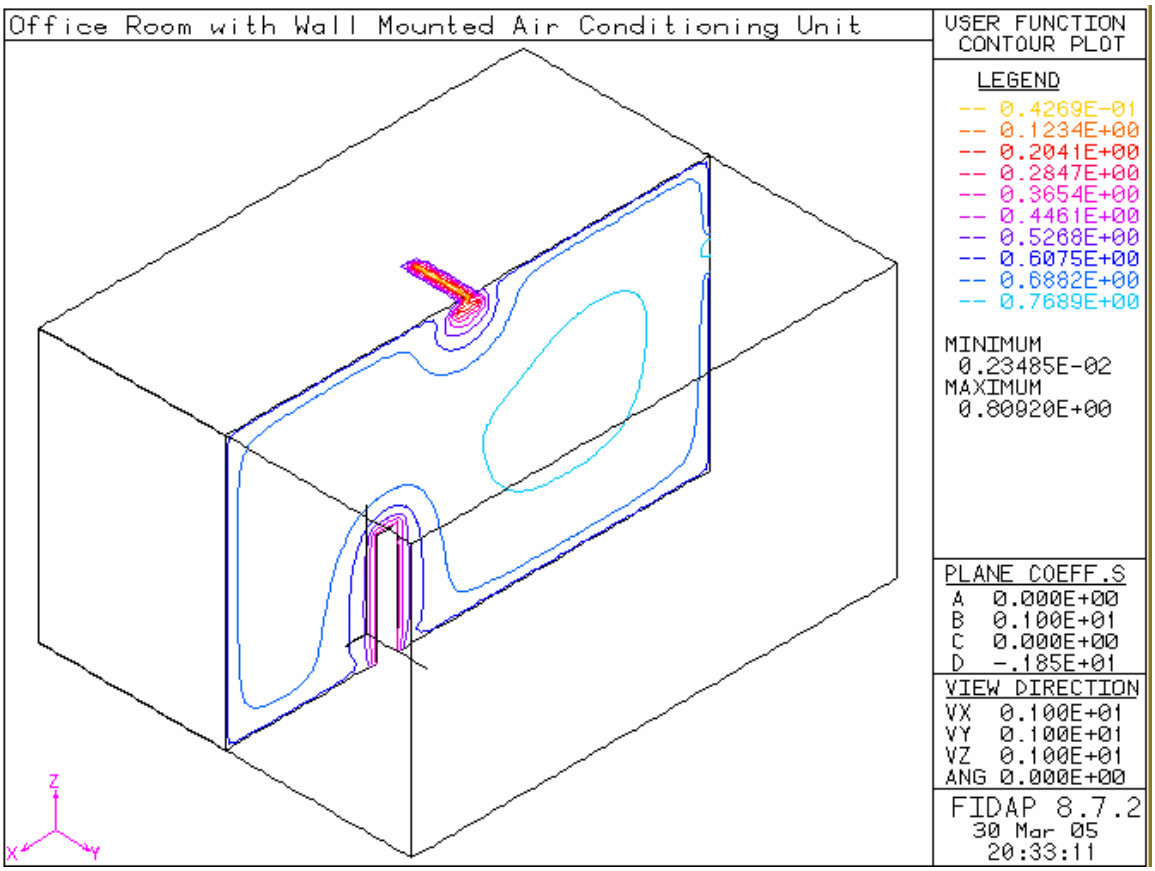

Figure 4-60 Relative Humidity on plane 1, inlet angle of 40^{o}

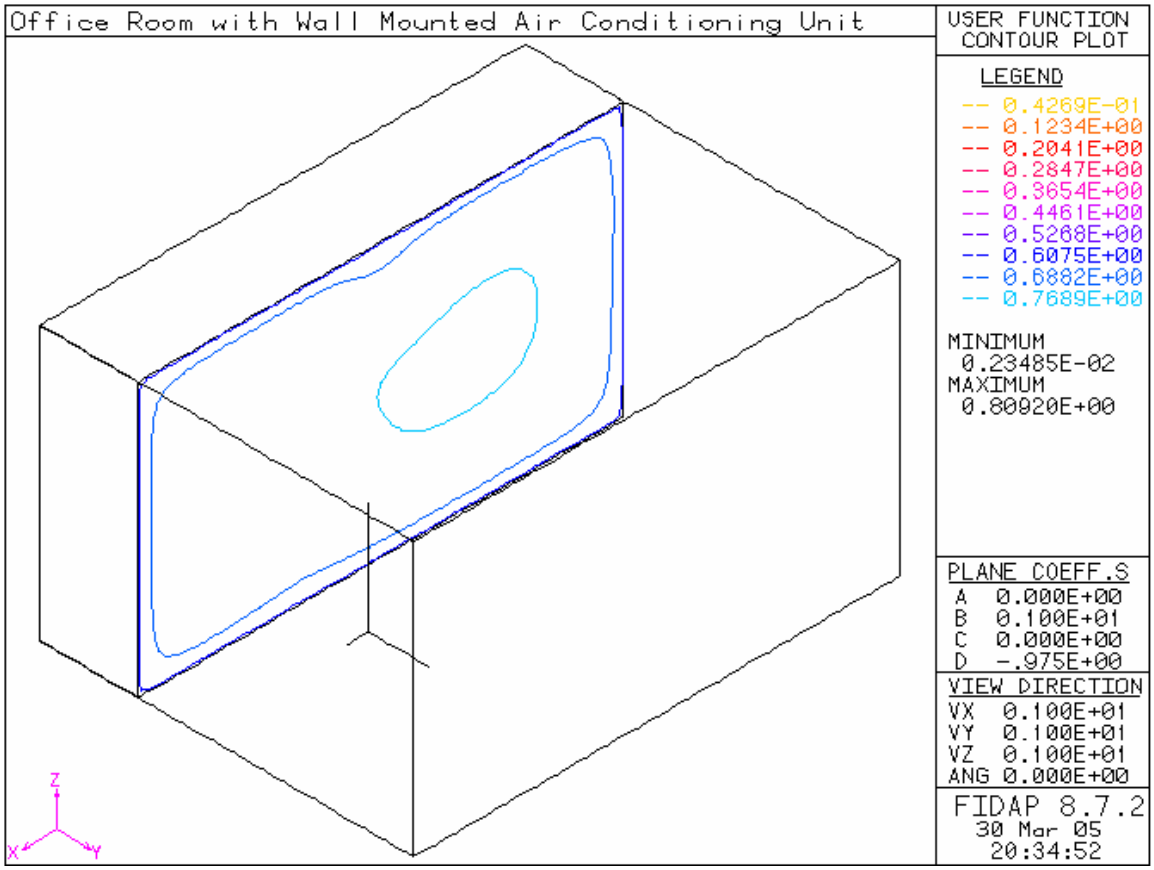

Figure 4-61 Relative Humidity on plane 2, inlet angle of 40^{o}

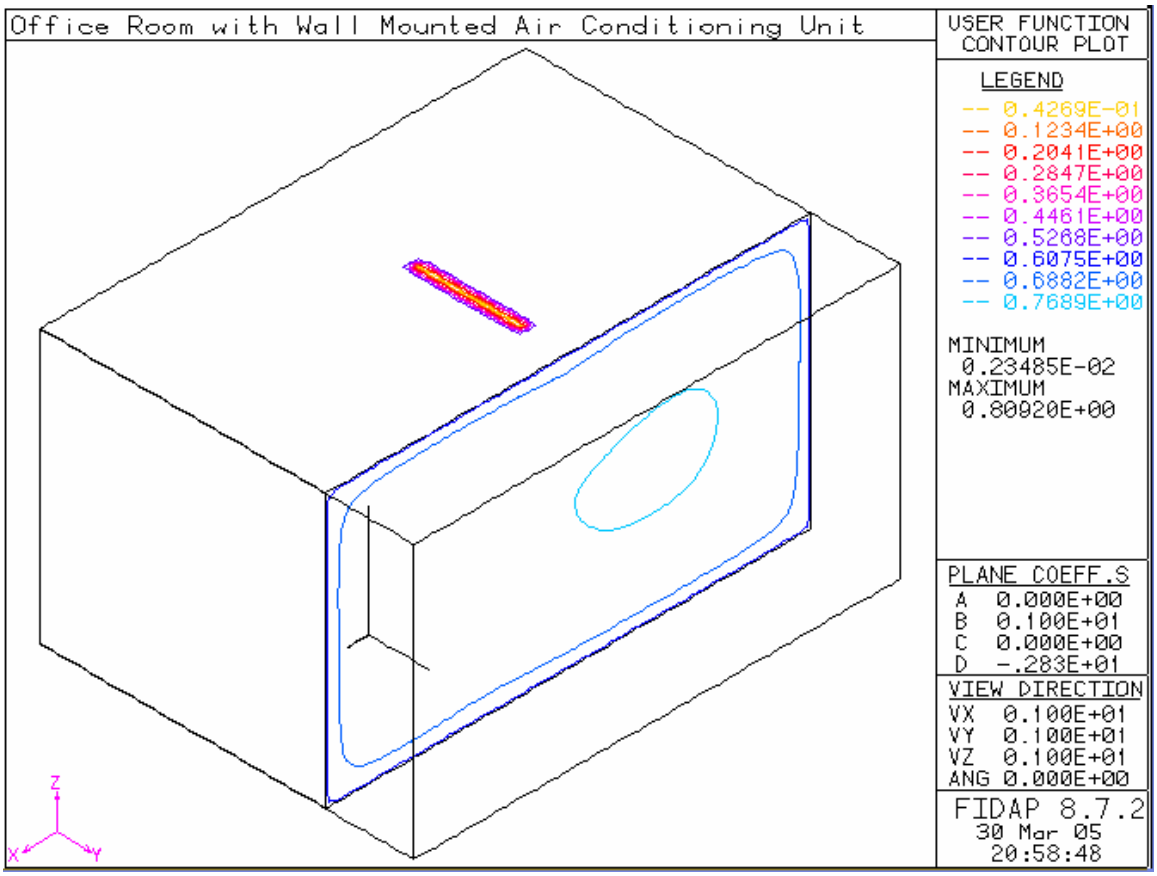

Figure 4-62 Relative Humidity on plane 3, inlet angle of 40^{o}

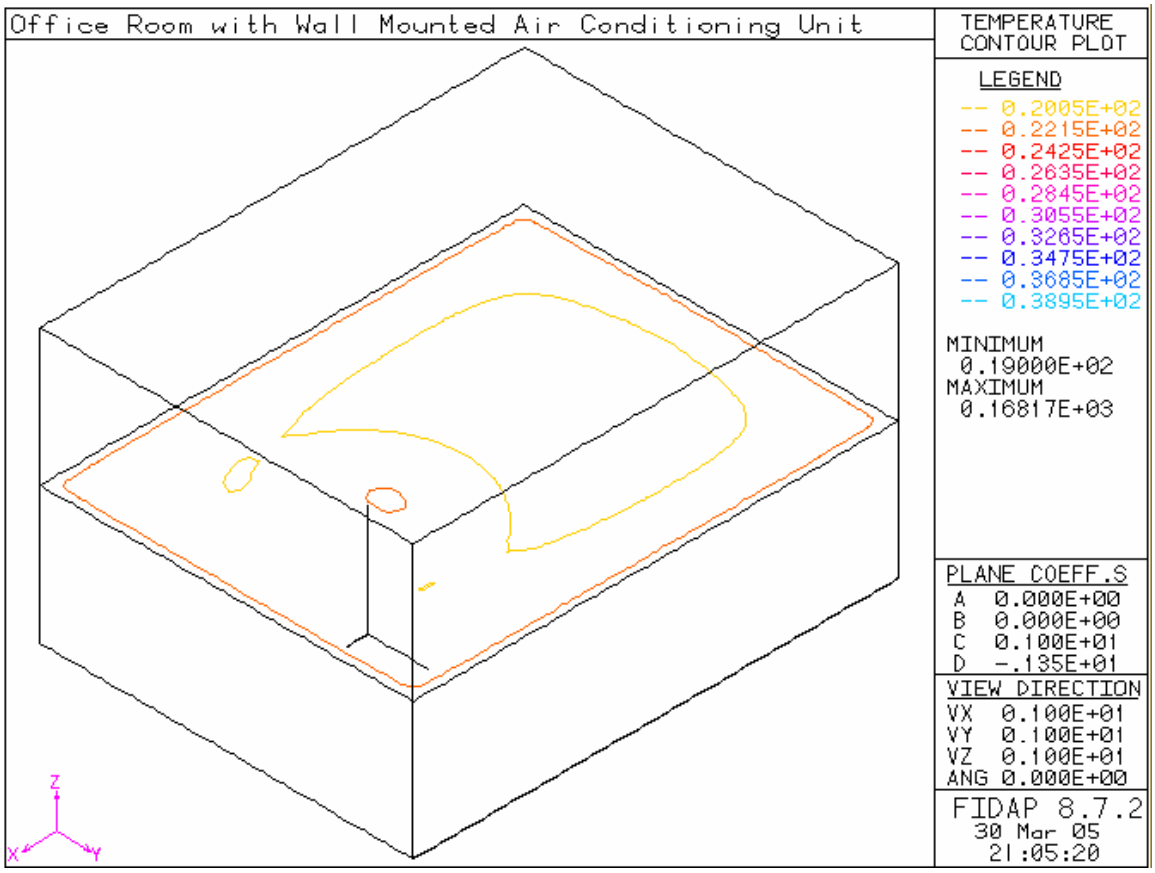

Figure 4-63 Temperature profile on plane 4, inlet angle of 40^{o}

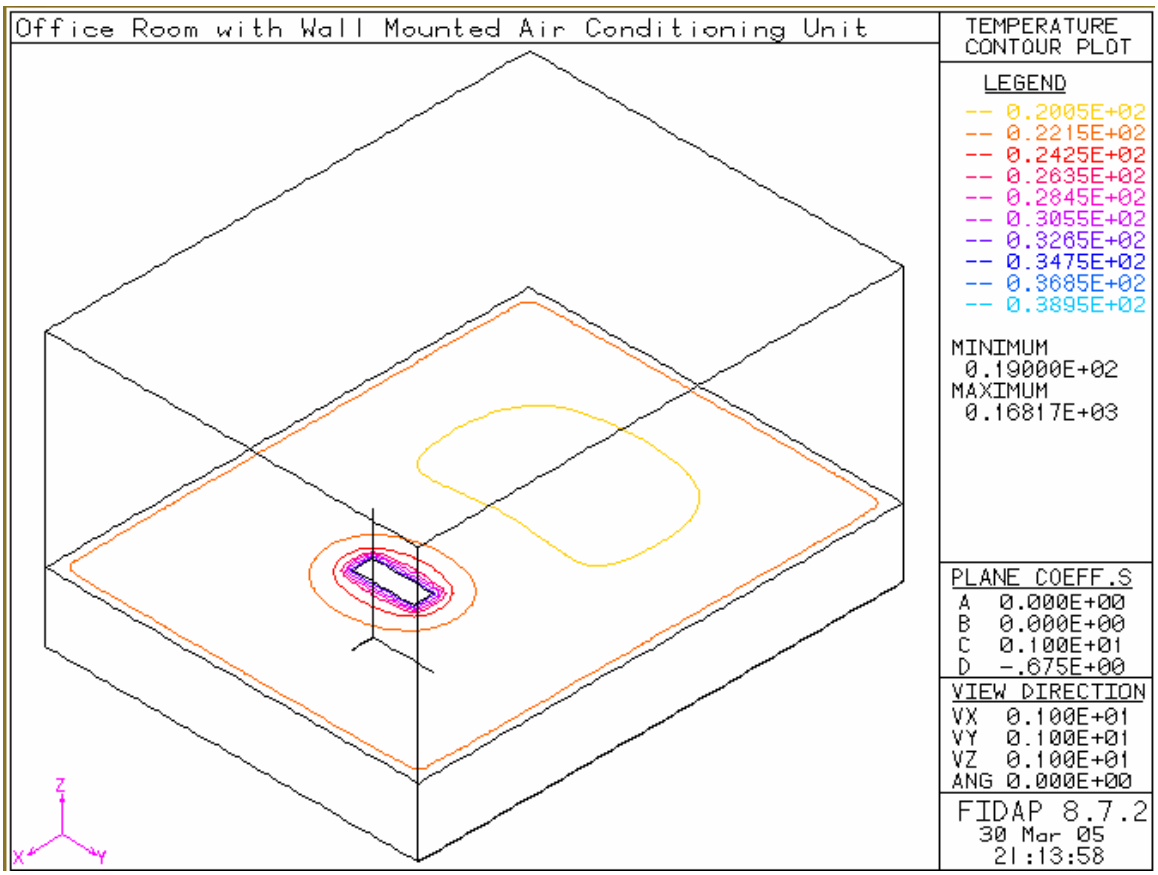

Figure 4-64 Temperature profile on plane 5, inlet angle of 40^{o}

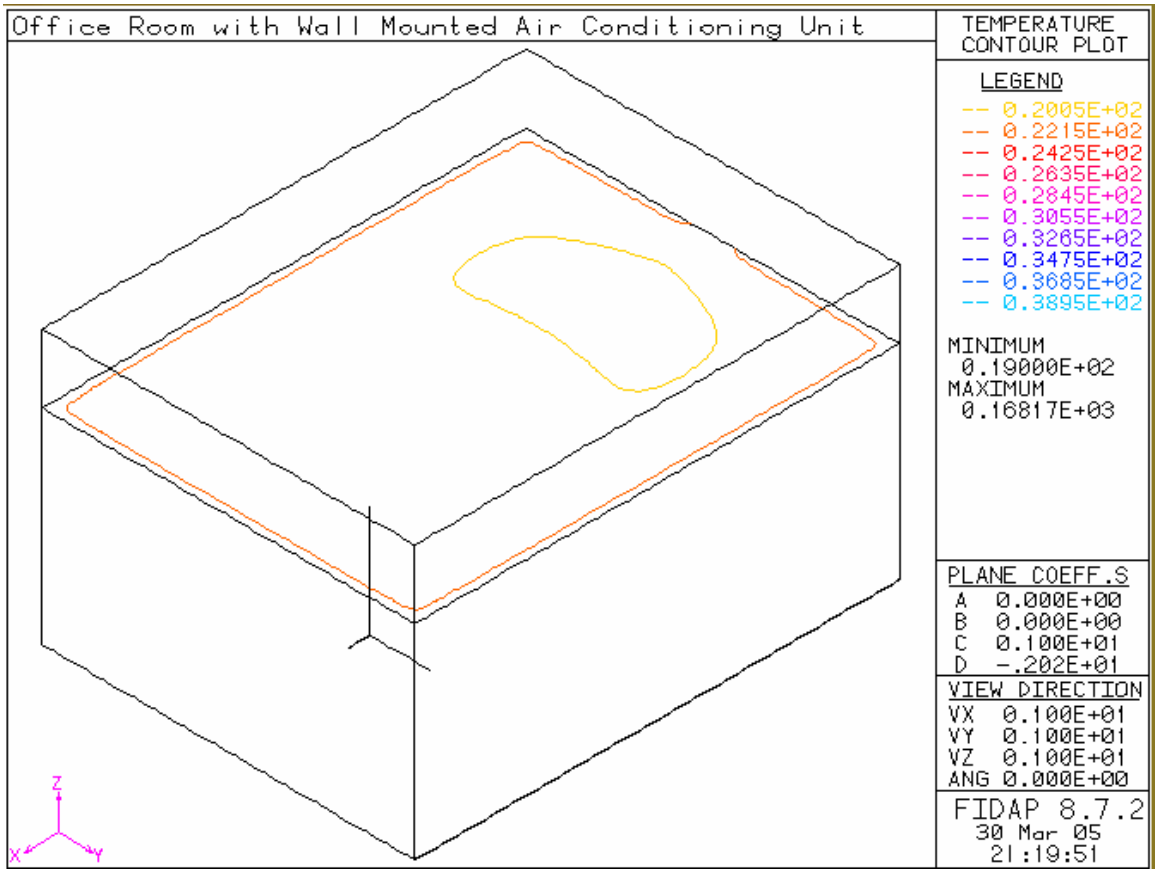

Figure 4-65 Temperature profile on plane 6, inlet angle of 40^{o}

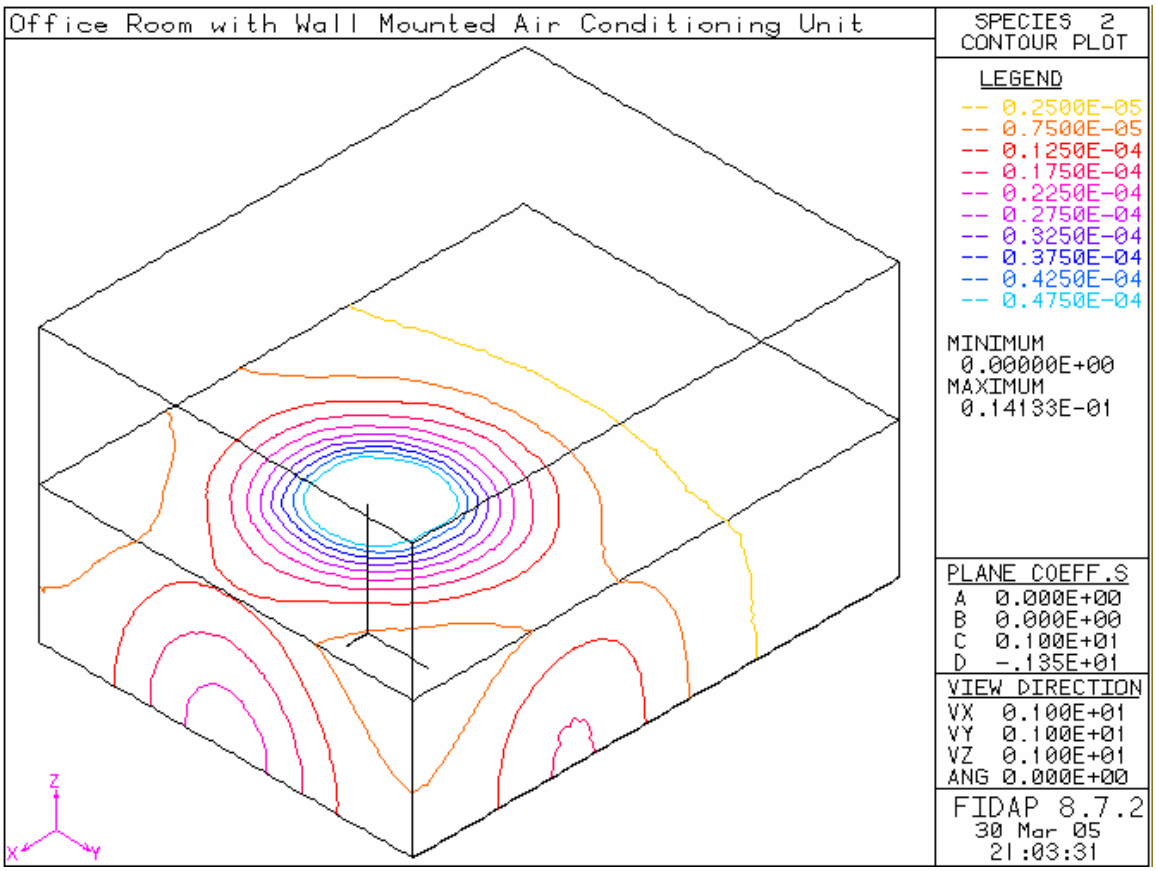

Figure 4-66 Contaminant profile on plane 4, inlet angle of 40^{o}

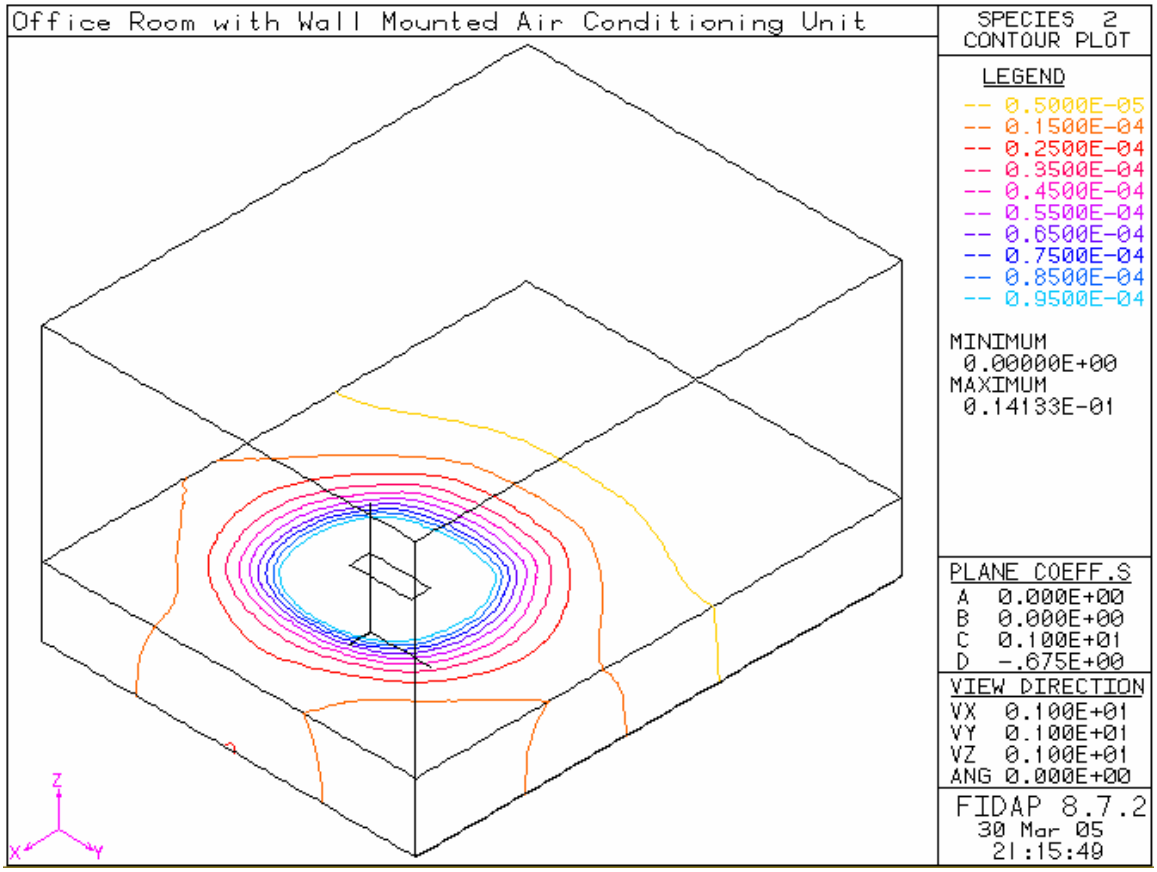

Figure 4-67 Contaminant profile on plane 5, inlet angle of 40^{o}

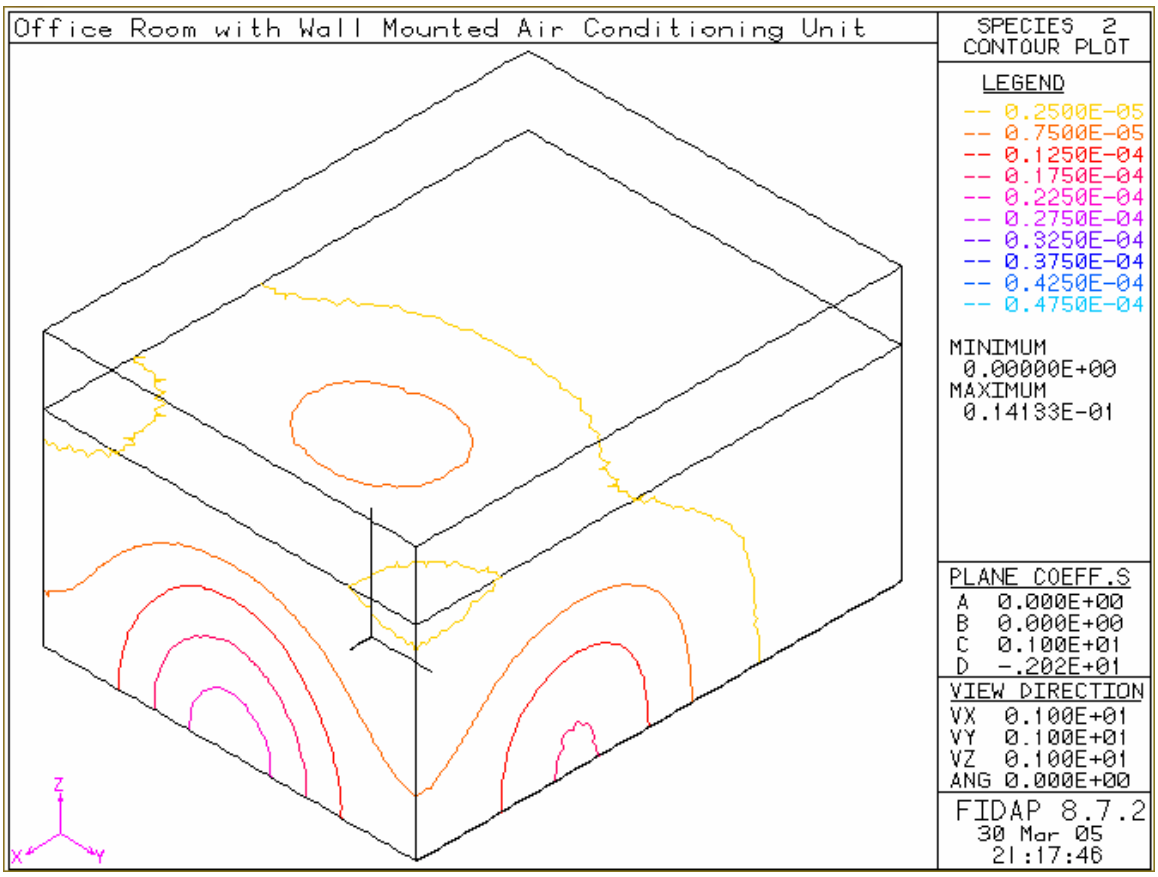

Figure 4-68 Contaminant profile on plane 6, inlet angle of 40^{o}

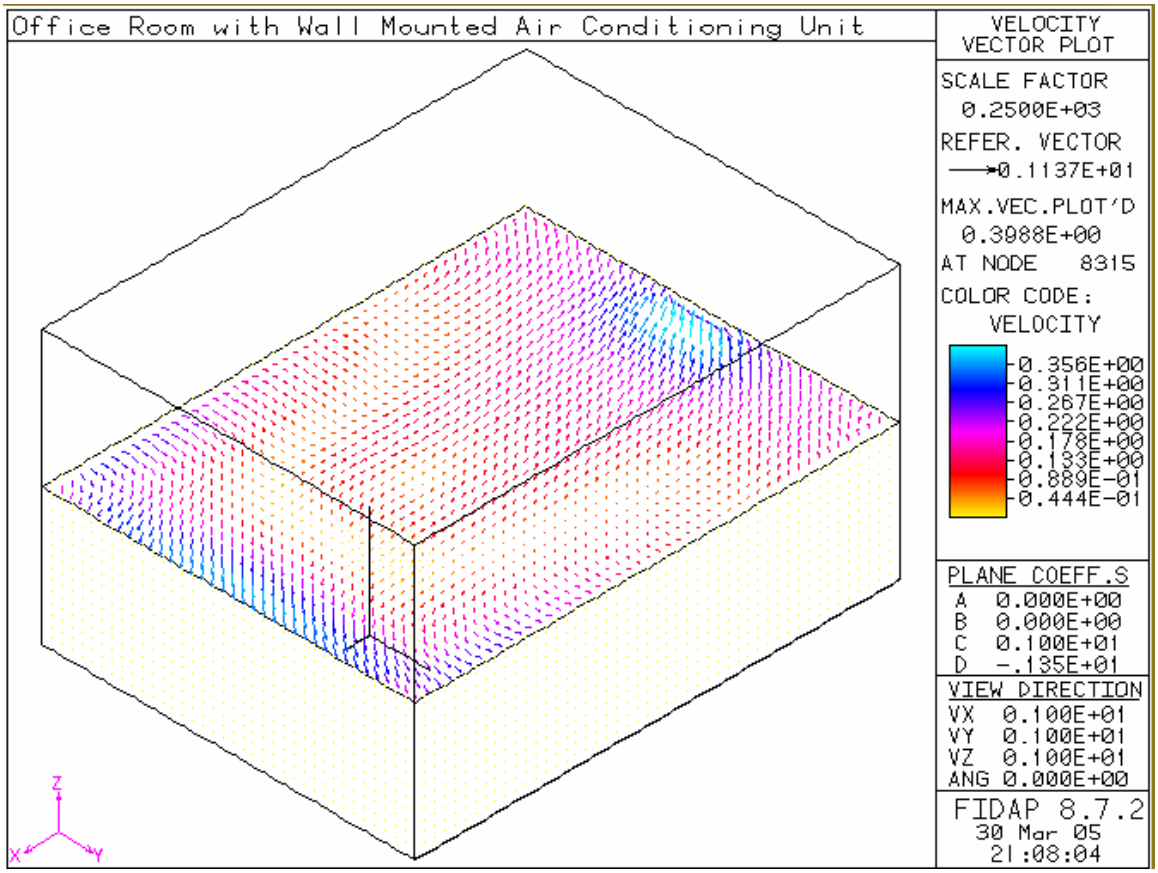

Figure 4-69 Velocity profile on plane 4, inlet angle of 40^{o}

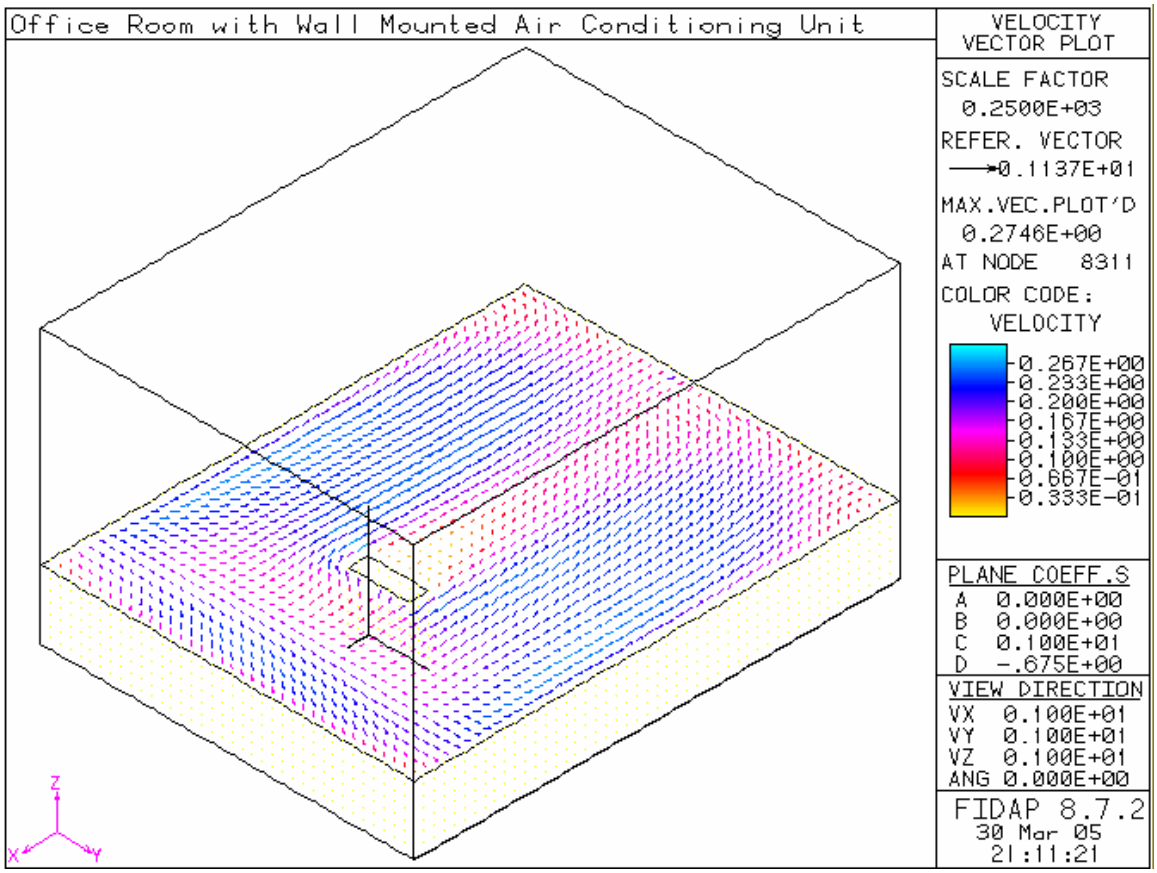

Figure 4-70 Velocity profile on plane 5, inlet angle of 40^{o}

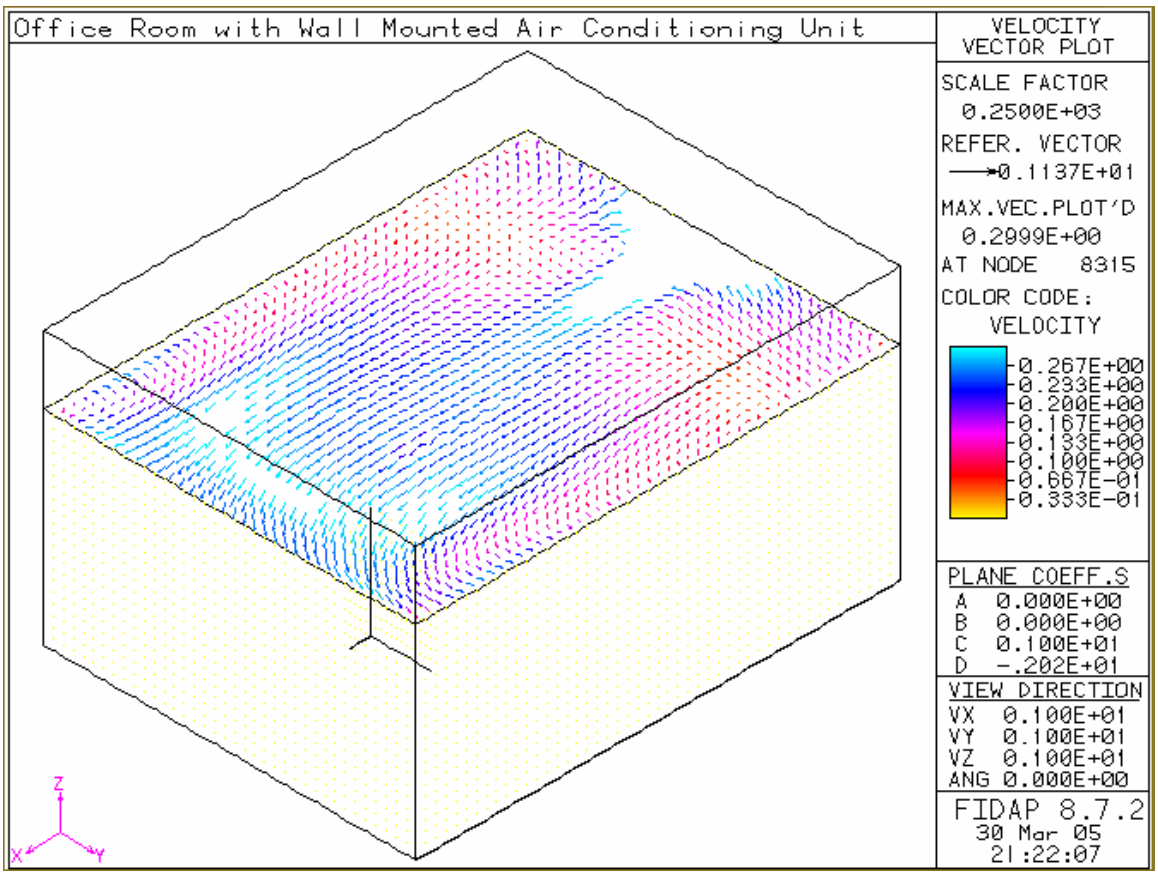

Figure 4-71 Velocity profile on plane 6, inlet angle of 40^{o}

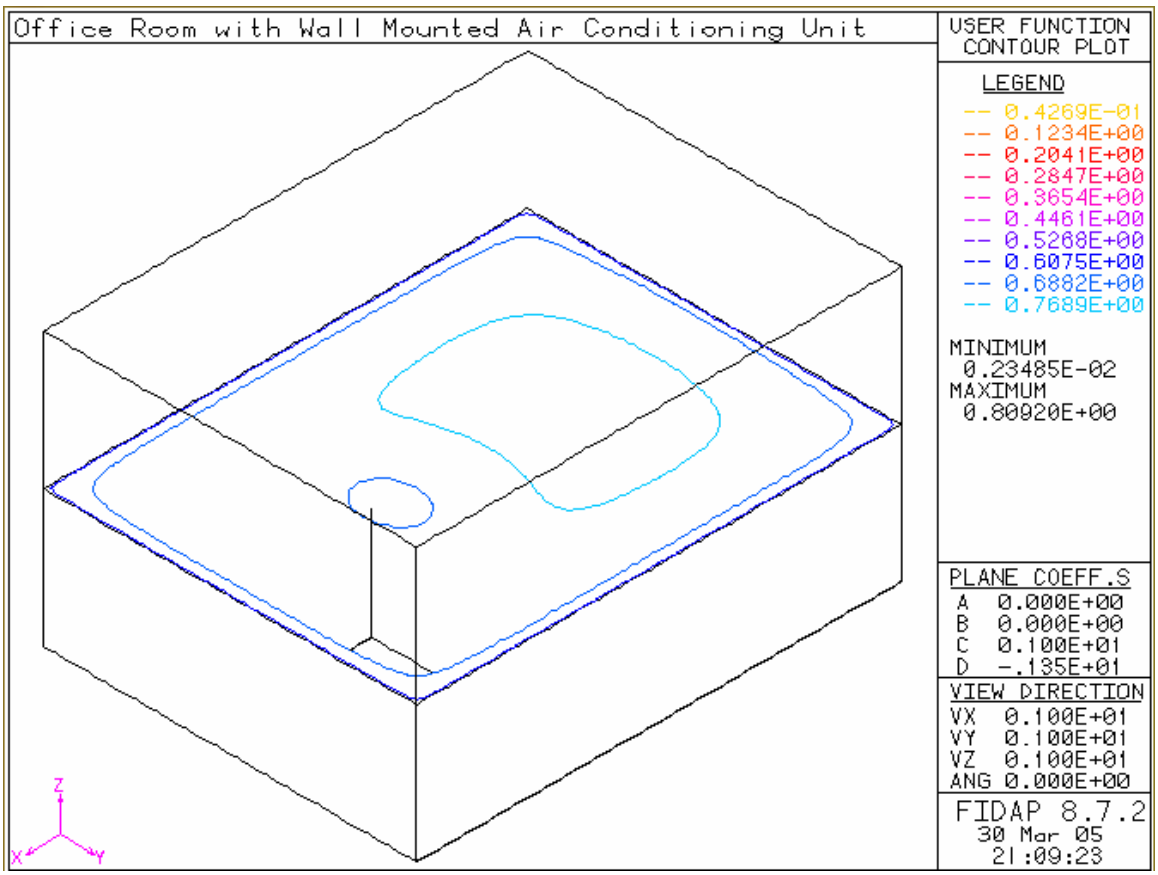

Figure 4-72 Relative Humidity on plane 4, inlet angle of 40^{o}

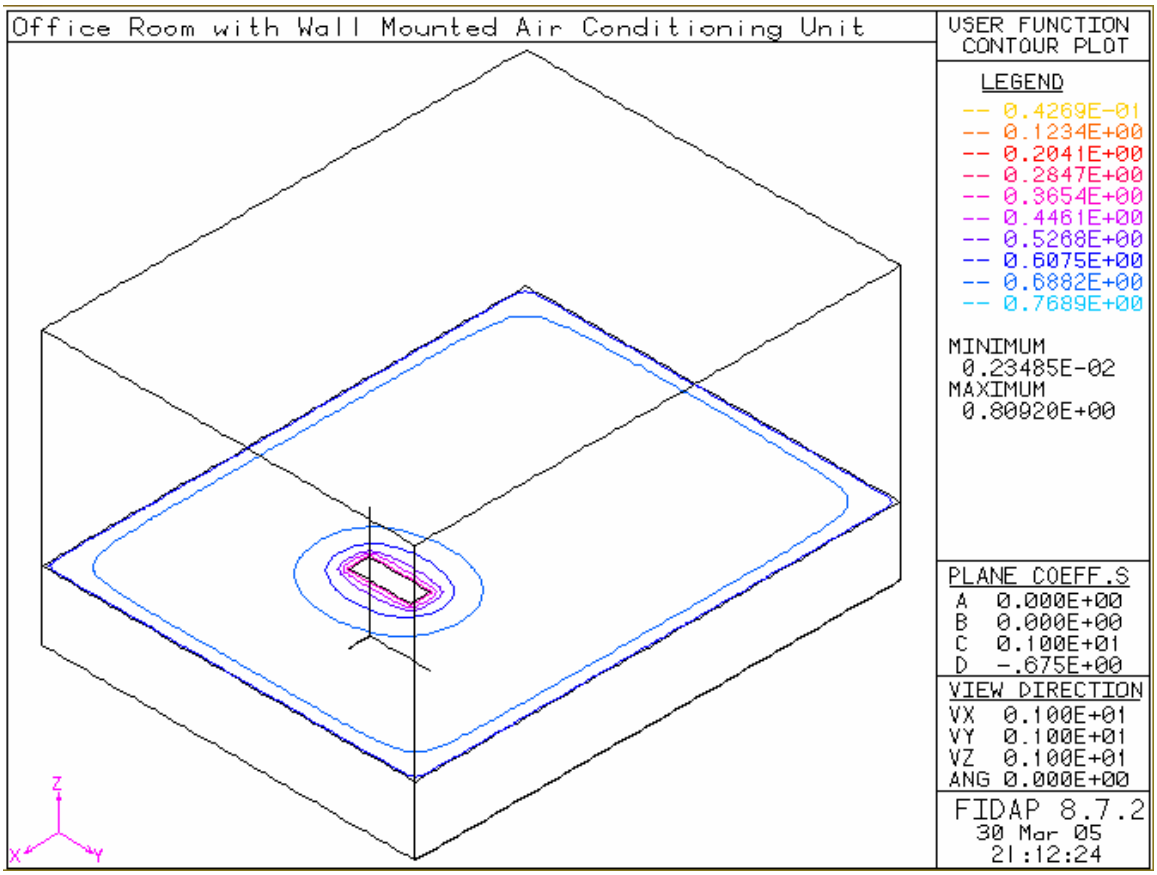

Figure 4-73 Relative Humidity on plane 5, inlet angle of 40^{o}

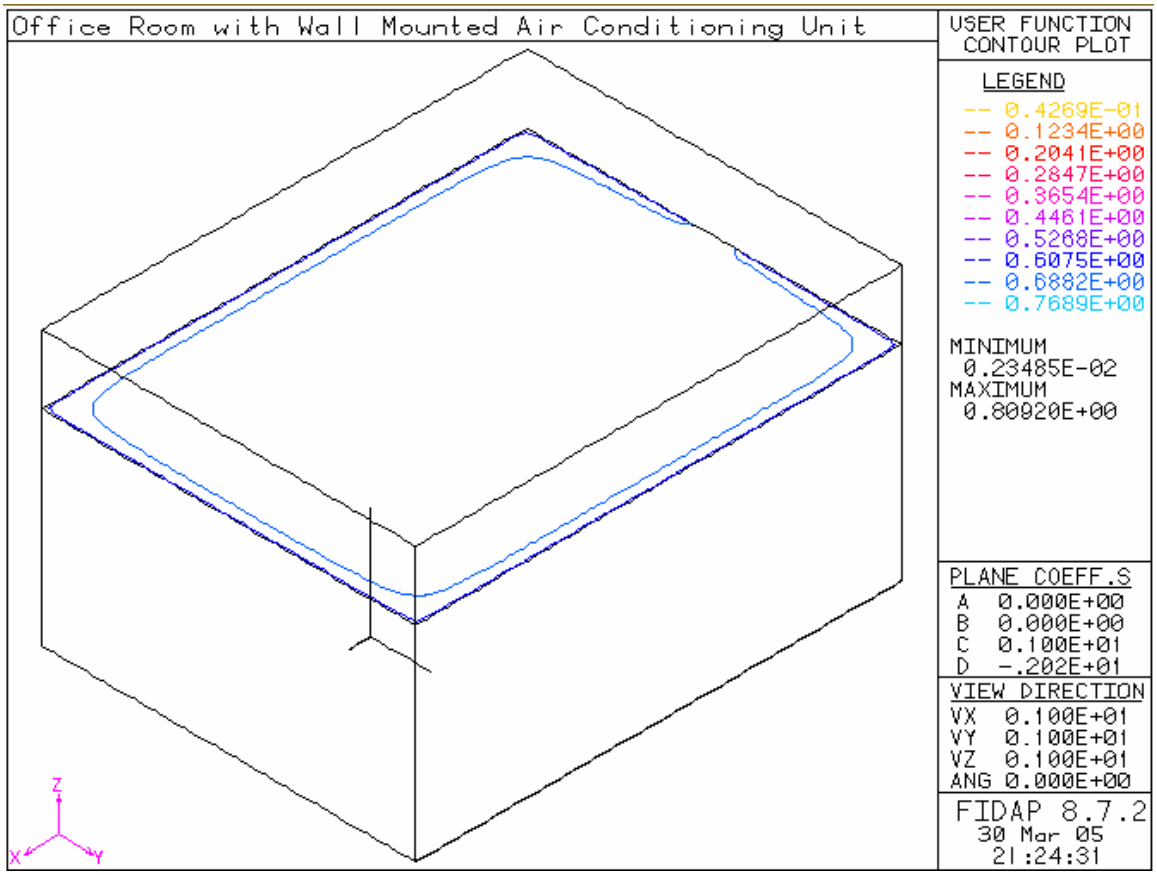

Figure 4-74 Relative Humidity on plane 6, inlet angle of 40^{o}

Chapter 5 - Conclusions and Recommendations

5.1 Two Dimensional Simulation of Office Room

Multiple cases could be taken and studied for HVAC office rooms with the use of CFD. The present simulations have demonstrated that the position of the wall-mounted air conditioner has a significant effect on the comfort level of the person occupying it.

In Chapter 3, it is clear that the base case (case 2, Table 3-2) is very comfortable for one person doing minimal work in an office using a window air conditioner. If PMV is considered, the base case and the 40 degree inlet angle case (case 3, Table 3-2) are comfortable regardless of the thermal sensation index because as it is shown above, inlet angle has very little effect on PMV index. Considering moving the unit either up or down has a significant effect on the occupant's comfort as shown above. As airflow velocity becomes greater around the occupant creating a very cold sensation, the level of discomfort increases (PPD). This is an indicator that height of the air conditioning unit has a great effect on the air velocity's direction and magnitude inside the office room, thus on the comfort of occupants. Moving the person closer to the air conditioning units (case 6, Table3- 2) increases his or her sensation of cold, which is a good indicator that preferable distance needed away from the is necessary to create good thermal comfort.

Contaminant Removal Effectiveness CRE is greatly affected by the speed of airflow as well as its temperature. As demonstrated, the greatest CRE occurs when velocities around the occupant, who is the main source of air contamination in this study. Case 1, Table 3-

2, displays the maximum CRE because airflow velocity is high as well as temperature. On the other hand cases 4 and 5 show great CRE however air temperature prevents an effective contaminant removal.

Energy savings in the 40^{o} angle case (case 3, Table 3-2) is the preferable since minimum energy is needed to create comfort, since the relative humidity (Table 3-7) is low in this case. Case 6, where the occupant is closer to the air conditioning unit, shows similar energy saving value; however thermal comfort is not ideal in this case.

5.2 Three Dimensional Simulation of Office Room

HVAC designs are increasingly improving due to a significant increase in CFD usage, FLUENT used in this study was a credible tool for the present simulations. The solution obtained concurred with the predicted results and previous simulations using FIDAP and other CFD softwares. Also, the present simulation agreed with experimental data collected for a similar layout with similar boundary conditions.

The location of a window type air-conditioner has great influence on the heat transfer and comfort level in office rooms. It is clear, after studying this office room, that airflow around the room has a very specific pattern, which clearly influences the heat, relative humidity, and CRE for occupants.

As demonstrated CRE is affected by airflow velocity and temperature, CRE is great when velocities are high which allow a great clean up of the surrounding air especially considering that CRE is a ratio involving the outlet contaminant concentrations.

Relative humidity is inversely proportional to the temperature, as discussed above in regions (cells) where temperature is high; the relative humidity is low e.g. surrounding the person and around the light fixture. Also, following the airflow trajectory through the room and since air is cooler than the entities around it, we can see that relative humidity is higher on the regions adjacent to the person and low on the section intersecting with the person which a source of heat to the surroundings.

Horizontally, relative humidity is high in the high sections of the office room, again this due to the high cool airflow velocities and low temperature throughout air trajectory.

5.3 Recommendations

There is always a combination of inlet angle, height of air-conditioning unit, and occupant position that are ideal for each application. Not only for office rooms but also in general use, it is shown now that a window air conditioner has a particular setting for each application.

This study can help the manufacturers or suppliers focus on potential consumer needs for a specific application, in order to achieve the ideal thermal comfort.

Also, if window air conditioners are used in the properly, fewer occupants would experience thermal discomfort and more demand will be noticed. For instance it is known that central units as stated above are more efficient and eventually more reliable, however central units cool whole buildings including spaces that do not to be cooled. If prior to an

application, a simulation of the design is performed including all the boundary conditions involved, a window unit could be a perfect fit for a small office room.

Two dimensional models are very affective when describing heat transfer and thermal comfort in HVAC applications. The results from the two dimensional model were very accurate and in accordance with three dimensional models and experimental data. It is however critical to make the proper assumptions in order to compensate for the differences. However, three dimensional modeling is more reliable because it is closer to actual studied problems and also demands less correctional assumptions.

Now CFD softwares are very reliable, cost of HVAC design will drop considerably if more CFD simulations are performed instead of physical collection of data that takes time, laboratory equipment, and money that could be invested elsewhere.

Other studies can be inspired by the present work, using CFD, preferably three dimensions modeling. Residential and commercial spaces can be analyzed and more data can be obtained for different conditions. More occupants can be added to the CFD models. Houses or working spaces can be studied, which will provide critical information about the proper location of wall-mounted air conditioners in order to create ideal thermal comfort.

References

[1] Principles of Heating Ventilating and Air Conditioning by Sauer H,J., Howell R.H. and Coad W.J. Edited by ASHRAE 2001.

[2] Energy-Efficient Air Conditioning US Department of Energy http://www.eere.energy.gov/consumerinfo/factsheets/aircond.html.

[3] Chow W.F., and Fung W.F., 1996, "*Numerical studies on indoor air flow in occupied zone of ventilated and air-conditioned space*," Building and Environment, 31, pp.319-344.

[4] Emmerich S.J., 1997, "*Use of computational fluid dynamics to analyze indoor air quality issues*," NISTIR 5997, Building and Fire Research Laboratory, National Institute of Standards of Technology, Gaithersburg, MD.

[5] Gadgil A.J., Finlayson E.U., Hong K.H., and Sextro R.G., 1999, " *Commercial CFD software capabilities for modeling a pulse release of pollutant in a large indoor space*," Proceeding of Indoor Air '99, Edingburg, 4, pp. 749.

[6] Hirnikel D.J., Lipowicz P.J., and Law R.W., 2002, "*Predicting contaminant removal effectiveness of three air distribution systems by CFD modeling*," ASHRAE Transactions, 108 (1), pp.350-359.

[7] Y.C. Shih, H, Chiang, and R.J Shyu., 2000, *The impact of the "Coanda Effect" On Indoor Air Motion Generated by a Window-Type Air-Conditioner*, Chutung, Hisinchu, Taiwan 310, R.O.C.

[8] H.C Hsu, H, Chiang, Y.C. Shih and R.J Shyu., 2000, *Implementation of displacement ventilation System by Using Wall-Mounted Air Conditioning,* Hisinchu, Taiwan, R.O.C.

[9] Son Hong Ho, 2004, *Numerical Simulation of Thermal Comfort and Contaminant Transport*, USF, Florida.

[10] Fountain, M., C. Huizenga, 1995, *A thermal sensation model for use by the engineering profession*. ASHRAE Project 781-PR Final report

[11] G. Yanzheng, B. W Jones, M.H Hosni, T.P Gielda, 2003, Literature Review of the Advances in Thermal Comfort Modeling, ASHRAE, Kansas City.

[12] ASHRAE, 1997, *ASHRAE Handbook of Fundamentals*, American Society of Heating, Refrigerating and Air Conditioning Engineers, Inc., Atlanta, Georgia.

[13] Fanger P.O., 1970, *Thermal Comfort analysis and applications in environmental engineering*, McGraw-Hill, New York.

[14] Rohles F.H.Jr. and Nevins R.G., 1971, *The Nature of Thermal Comfort for Sedentary Man, ASHREA Transactions*, 77 (1), pp.239-244.

[15] ANSI/ASHRAE Standard 55, 1992, Thermal Environment conditions for Human Occupancy. American Society of Heating, Refrigerating and Air Conditioning Engineers, Inc., Atlanta, Georgia.

[16] Gaspar. P. D., Barroca. R.F., Pitarma R.A., 2003," Performance Evaluation of CFD codes in Building Energy and Environmental Analysis", Eighth International IBPSA Conference, Eindhoven, Netherlands, August 11-14.

[17] Richtr .J.,Jicha .M., Katolicky .J., 2001, " Numerical Modeling of The Influence of Angle Adjustment of A/C Diffuser Vanes on Thermal Comfort in a Computer Room" Sventh International IBPSA Conference, Rio de Janeiro, Brazil, August 13-15.

Appendices

Appendix A: FIDAP Program for Two Dimensional Simulation for

Office Room

```
      TITLE (  )
      Wall mounted air conditioning unit (2D)
      / FI-GEN
      FI-GEN( ELEM = 1, POIN = 1, CURV = 1, SURF = 1, NODE = 0,
MEDG = 1, MLOO = 1,
      MFAC = 1, BEDG = 1, SPAV = 1, MSHE = 1, MSOL = 1, COOR = 1
)

      / ADD POINTS
      POINT( ADD, COOR, X = 0, Y = 0 )
      POINT( ADD, COOR, X = 0, Y = 10 )
      POINT( ADD, COOR, X = 0, Y = 120 )
      POINT( ADD, COOR, X = 0, Y = 162 )
      POINT( ADD, COOR, X = 0, Y = 192 )
      POINT( ADD, COOR, X = 0, Y = 206 )
      POINT( ADD, COOR, X = 0, Y = 270 )
      POINT( ADD, COOR, X = 480, Y = 0 )
      POINT( ADD, COOR, X = 480, Y = 10 )
      POINT( ADD, COOR, X = 480, Y = 120 )
      POINT( ADD, COOR, X = 480, Y = 162 )
      POINT( ADD, COOR, X = 480, Y = 192 )
      POINT( ADD, COOR, X = 480, Y = 206 )
      POINT( ADD, COOR, X = 480, Y = 270 )
      POINT( ADD, COOR, X = 240, Y = 0 )
      POINT( ADD, COOR, X = 260, Y = 0 )
      POINT( ADD, COOR, X = 320, Y = 0 )
      POINT( ADD, COOR, X = 340, Y = 0 )
      POINT( ADD, COOR, X = 240, Y = 270 )
      POINT( ADD, COOR, X = 260, Y = 270 )
      POINT( ADD, COOR, X = 320, Y = 270 )
      POINT( ADD, COOR, X = 340, Y = 270 )
      POINT( ADD, COOR, X = 320, Y = 120 )
      POINT( ADD, COOR, X = 340, Y = 120 )
      POINT( ADD, COOR, X = 320, Y = 10 )
      POINT( ADD, COOR, X = 340, Y = 10 )
      POINT( ADD, COOR, X = 320, Y = 162 )
      POINT( ADD, COOR, X = 320, Y = 192 )
      POINT( ADD, COOR, X = 320, Y = 206 )
      / ADD LINES
      POINT( SELE, ID )
          1,     7
      CURVE( ADD, LINE )
      POINT( SELE, ID )
          8,    14
      CURVE( ADD, LINE )
```

Appendix A (continued)

```
      POINT( SELE, ID )
          1
         15,    18
          8
```

```
CURVE( ADD, LINE )
POINT( SELE, ID )
    7


 19,    22
   14
CURVE( ADD, LINE )
POINT( SELE, ID )
   23
   24
   26
   25
   23
CURVE( ADD, LINE )
POINT( SELE, ID )
   23
   27
   28
   29
   21
CURVE( ADD, LINE )
POINT( SELE, ID )
   17
   25
CURVE( ADD, LINE )
POINT( SELE, ID )
   18
   26
CURVE( ADD, LINE )
POINT( SELE, ID )
   10
   24
CURVE( ADD, LINE )
/ ADD SURFACES
POINT( SELE, ID )
    7
   14
    1
    8
SURFACE( ADD, POIN, ROWW = 2 )
/ ADD MESH EDGES
CURVE( SELE, ID = 1 )
MEDGE( ADD, SUCC, INTE = 10, RATI = 0, 2RAT = 0, PCEN = 0 )
```

Appendix A (continued)

```
CURVE( SELE, ID = 2 )
MEDGE( ADD, SUCC, INTE = 17, RATI = 0, 2RAT = 0, PCEN = 0 )
CURVE( SELE, ID = 3 )
MEDGE( ADD, SUCC, INTE = 14, RATI = 0, 2RAT = 0, PCEN = 0 )
CURVE( SELE, ID = 4 )
MEDGE( ADD, SUCC, INTE = 13, RATI = 0, 2RAT = 0, PCEN = 0 )
CURVE( SELE, ID = 5 )
MEDGE( ADD, SUCC, INTE = 11, RATI = 0, 2RAT = 0, PCEN = 0 )
CURVE( SELE, ID = 6 )
MEDGE( ADD, SUCC, INTE = 16, RATI = 0, 2RAT = 0, PCEN = 0 )
CURVE( SELE, ID = 7 )
```

```
      MEDGE( ADD, SUCC, INTE = 10, RATI = 0, 2RAT = 0, PCEN = 0 )
      CURVE( SELE, ID = 8 )
      MEDGE( ADD, SUCC, INTE = 17, RATI = 0, 2RAT = 0, PCEN = 0 )
      CURVE( SELE, ID = 9 )


      MEDGE( ADD, SUCC, INTE = 14, RATI = 0, 2RAT = 0, PCEN = 0 )
      CURVE( SELE, ID = 10 )
      MEDGE( ADD, SUCC, INTE = 13, RATI = 0, 2RAT = 0, PCEN = 0 )
      CURVE( SELE, ID = 11 )
      MEDGE( ADD, SUCC, INTE = 11, RATI = 0, 2RAT = 0, PCEN = 0 )
      CURVE( SELE, ID = 12 )
      MEDGE( ADD, SUCC, INTE = 16, RATI = 0, 2RAT = 0, PCEN = 0 )
      CURVE( SELE, ID = 13 )
      MEDGE( ADD, FRST, INTE = 60, RATI = 0.2, 2RAT = 0.2, PCEN =
0 )
      CURVE( SELE, ID = 14 )
      MEDGE( ADD, SUCC, INTE = 14, RATI = 0, 2RAT = 0, PCEN = 0 )
      CURVE( SELE, ID = 15 )
      MEDGE( ADD, SUCC, INTE = 14, RATI = 0, 2RAT = 0, PCEN = 0 )
      CURVE( SELE, ID = 16 )
      MEDGE( ADD, SUCC, INTE = 12, RATI = 0, 2RAT = 0, PCEN = 0 )
      CURVE( SELE, ID = 17 )
      MEDGE( ADD, SUCC, INTE = 18, RATI = 0, 2RAT = 0, PCEN = 0 )
      CURVE( SELE, ID = 18 )
      MEDGE( ADD, FRST, INTE = 60, RATI = 0.2, 2RAT = 0.2, PCEN =
0 )
      CURVE( SELE, ID = 19 )
      MEDGE( ADD, SUCC, INTE = 14, RATI = 0, 2RAT = 0, PCEN = 0 )
      CURVE( SELE, ID = 20 )
      MEDGE( ADD, SUCC, INTE = 14, RATI = 0, 2RAT = 0, PCEN = 0 )
      CURVE( SELE, ID = 21 )
      MEDGE( ADD, SUCC, INTE = 12, RATI = 0, 2RAT = 0, PCEN = 0 )
      CURVE( SELE, ID = 22 )
      MEDGE( ADD, SUCC, INTE = 18, RATI = 0, 2RAT = 0, PCEN = 0 )
      CURVE( SELE, ID = 23 )
      MEDGE( ADD, SUCC, INTE = 12, RATI = 0, 2RAT = 0, PCEN = 0 )
```

Appendix A (continued)

```
      CURVE( SELE, ID = 24 )
      MEDGE( ADD, SUCC, INTE = 17, RATI = 0, 2RAT = 0, PCEN = 0 )
      CURVE( SELE, ID = 25 )
      MEDGE( ADD, SUCC, INTE = 12, RATI = 0, 2RAT = 0, PCEN = 0 )
      CURVE( SELE, ID = 26 )
      MEDGE( ADD, SUCC, INTE = 17, RATI = 0, 2RAT = 0, PCEN = 0 )
      CURVE( SELE, ID = 27 )
      MEDGE( ADD, SUCC, INTE = 14, RATI = 0, 2RAT = 0, PCEN = 0 )
      CURVE( SELE, ID = 28 )
      MEDGE( ADD, SUCC, INTE = 13, RATI = 0, 2RAT = 0, PCEN = 0 )
      CURVE( SELE, ID = 29 )
      MEDGE( ADD, SUCC, INTE = 11, RATI = 0, 2RAT = 0, PCEN = 0 )
      CURVE( SELE, ID = 30 )
      MEDGE( ADD, SUCC, INTE = 16, RATI = 0, 2RAT = 0, PCEN = 0 )
      CURVE( SELE, ID = 31 )
      MEDGE( ADD, SUCC, INTE = 10, RATI = 0, 2RAT = 0, PCEN = 0 )
      CURVE( SELE, ID = 32 )
      MEDGE( ADD, SUCC, INTE = 10, RATI = 0, 2RAT = 0, PCEN = 0 )
```

```
CURVE( SELE, ID = 33 )
MEDGE( ADD, SUCC, INTE = 18, RATI = 0, 2RAT = 0, PCEN = 0 )
/ ADD MESH LOOPS
CURVE( SELE, ID )
    1,     6
   18
   19

 20
   30
   29
   28
   27
   26
   31
   15
   14
   13
MLOOP( ADD, MAP, EDG1 = 6, EDG2 = 3, EDG3 = 6, EDG4 = 3 )
CURVE( SELE, ID )
   23
   33
    9
   10
   11
   12
   22
   21
   30
   29
```

Appendix A (continued)

```
   28
   27
MLOOP( ADD, MAP, EDG1 = 2, EDG2 = 4, EDG3 = 2, EDG4 = 4 )
CURVE( SELE, ID )
   32
   24
   33
    8
    7
   17
MLOOP( ADD, MAP, EDG1 = 2, EDG2 = 1, EDG3 = 2, EDG4 = 1 )
CURVE( SELE, ID )
   31
   25
   32
   16
MLOOP( ADD, MAP, EDG1 = 1, EDG2 = 1, EDG3 = 1, EDG4 = 1 )
/ ADD MESH FACES
SURFACE( SELE, ID = 1 )
MLOOP( SELE, ID = 1 )
MFACE( ADD )
SURFACE( SELE, ID = 1 )
MLOOP( SELE, ID = 2 )
MFACE( ADD )
SURFACE( SELE, ID = 1 )
```

```
      MLOOP( SELE, ID = 3 )
      MFACE( ADD )
      SURFACE( SELE, ID = 1 )
      MLOOP( SELE, ID = 4 )
      MFACE( ADD )
      / MESH MESH FACES
      MFACE( SELE, ID )
          1,     4

      MFACE( MESH, MAP, ENTI = "air" )
      MFACE( SELE, ALL )
      MFACE( MESH, MAP, ENTI = "air" )
      / MESH MAP
      ELEMENT( SETD, EDGE, NODE = 2 )
      MEDGE( SELE, ID = 5 )
      MEDGE( MESH, MAP, ENTI = "inlet" )
      MEDGE( SELE, ID = 4 )
      MEDGE( MESH, MAP, ENTI = "outlet" )
      MEDGE( SELE, ID = 19 )
      MEDGE( MESH, MAP, ENTI = "light" )
      MEDGE( SELE, ID )
         23,    26
      MEDGE( MESH, MAP, ENTI = "person" )
```

Appendix A (continued)

```
      MEDGE( SELE, ID )
          1,     3
          6,    18
         20,    22
      MEDGE( MESH, MAP, ENTI = "walls" )
      END(  )

      FIPREP(  )
      DENSITY( SET="air", CONS = 0.0012047 )


      VISCOSITY( SET="air", CONS = 0.0001817)
      / Using the two equations •• model)
      CONDUCTIVITY(SET="air",  CONS = 2563 )
      SPECIFICHEAT( SET="air", CONS = 10040000 )

      DIFFUSIVITY( SET ="water_vapor" , CONS = 0.2513)
      DIFFUSIVITY( SET ="contam_gas" , CONS = 0.2308)

      ENTITY(  FLUI,  NAME  =  "air",  PROPERTY="air",  SPECIES=1,
MDIFF="water_vapor",SPECIES=2, MDIFF="contam_gas" )
      ENTITY( PLOT, NAME = "inlet" )
      ENTITY( PLOT, NAME = "outlet")
      ENTITY( PLOT, NAME = "walls" )
      ENTITY( PLOT, NAME = "person" )
      ENTITY( PLOT, NAME = "light" )


      BCNODE( VELO, ENTI = "inlet", CONS, X = 303.1, Y = 175 )
      BCNODE( VELO, ENTI = "walls", ZERO )
      BCNODE( VELO, ENTI = "person", ZERO )
      BCNODE( VELO, ENTI = "light", ZERO )
```

```
      BCNODE( TEMP, ENTI = "inlet", CONS = 19 )
      BCNODE( TEMP, ENTI = "walls", CONS = 24 )
      BCNODE( TEMP, ENTI = "person", CONS = 34 )
      BCFLUX( HEAT, ENTI = "light", CONS = 5000 )


      BCNODE( SPEC=1, ENTI = "inlet", CONS = 0.010 )
      BCFLUX( SPEC=1, ENTI = "person", CONS = 6E-8 )

      BCNODE( SPEC=2, ENTI = "inlet", CONS = 0 )
      BCFLUX( SPEC=2, ENTI = "person", CONS = 1E-6 )

      CLIPPING( MINI )
      0,     0,     0,     0,    19,    0,  0,    0,     1e-20,
1e-20
      CLIPPING( MAXI )
```

Appendix A (continued)

```
      0,     0,     0,     0,    0,     0,  0,    0,    1,     1


      DATAPRINT( CONT )
      EXECUTION( NEWJ )
      OPTIONS( UPWI )
      PRINTOUT( NONE, BOUN )
      ICNODE( VELO, READ, ALL)
      PROBLEM( 2-D, NONL,TURB,ENER, SPEC = 1, SPEC = 2)

      END
```

Appendix B: FIDAP Program for Three Dimensional Simulation for

Office Room

```
      /
*****************************************************************
      / Disclaimer: This file was written by GAMBIT and contains
      / all the continuum and boundary entities and coordinate
systems
      / defined in GAMBIT. Additionally, some frequently used
FIPREP
      / commands are added. Modify/Add/Uncommment any necessary
commands.
      / Refer to FIPREP documentation for complete listing of
commands.
      /
*****************************************************************
      /
      /          CONVERSION OF NEUTRAL FILE TO FIDAP Database
      /
      FICONV( NEUTRAL )
      INPUT( FILE="3dr.FDNEUT" )
      OUTPUT( DELETE )
      END
      /
      TITLE
      Office Room with Wall Mounted Air Conditioning Unit
      /
      FIPREP
      /
      /          PROBLEM SETUP
      /
      EXECUTION( NEWJOB )
      PRINTOUT( NONE, BOUN )
      DATAPRINT( CONT )
      /
      /          CONTINUUM ENTITIES
      /
      ENTITY( FLUI, NAME = "fluid", PROPERTY="fluid", SPECIES=1,
MDIFF="water_vapor",SPECIES=2, MDIFF="contam_gas" )
      /
      /          BOUNDARY ENTITIES
      /
      ENTITY ( NAME = "walls", WALL )
      ENTITY ( NAME = "light", WALL )
      ENTITY ( NAME = "outlet", PLOT )
      ENTITY ( NAME = "inlet", PLOT )
      ENTITY ( NAME = "person", WALL )
      /
```

Appendix B (continued)

```
      /          LOCAL COORDINATE SYSTEMS DEFINED
      /
      /COORDINATE ( SYSTEM = 2, MATRIX,CARTESIAN )
```

```
      /0.000000  0.000000  0.000000  1.000000  0.000000  0.000000
0.000000 1.000000 0.000000 0.000000 0.000000 1.000000
      /
      /          SOLUTION PARAMETERS
      /
      SOLUTION( SEGREGATED = 100, VELCONV = .01 )
      /PRESSURE( MIXED = 1.E-8, DISCONTINUOUS )

      RELAX( HYBRID )
      OPTIONS( UPWINDING )

      /
      /          MATERIAL PROPERTIES
      /
      / Partial list of Material Properties data
      /
      DENSITY( SET = "fluid", CONSTANT = 1.2 )
      VISCOSITY( SET = "fluid", CONSTANT = 1.8e-5, MIXLENGTH )

      CONDUCTIVITY( SET = "fluid", CONSTANT = 2.5776E-2 )
      SPECIFICHEAT( SET = "fluid", CONSTANT = 1.0043 )

      DIFFUSIVITY( SET ="water_vapor" , CONS = 2.513E-5)
      DIFFUSIVITY( SET ="contam_gas" , CONS = 2.308E-5)
      /
      /          INITIAL AND BOUNDARY CONDITIONS
      /
      /
      BCNODE( VELO, CONSTANT = 0, ENTITY = "walls" )
      BCNODE( VELO , CONSTANT = 0, ENTITY = "light" )
      BCNODE( VELO, CONSTANT, X = 3.03, Y = 0, Z= 1.75, ENTITY =
"inlet" )
      BCNODE( VELO, CONSTANT = 0, ENTITY = "person" )
      BCNODE( TEMP, ENTI = "inlet", CONS = 19 )
      BCNODE( TEMP, ENTI = "walls", CONS = 24 )
      BCNODE( TEMP, ENTI = "person", CONS = 34 )
      BCFLUX( HEAT, ENTI = "light", CONS = 50 )


      BCNODE( SPEC=1, ENTI = "inlet", CONS = 0.011 )
      BCFLUX( SPEC=1, ENTI = "person", CONS = 5E-7 )

      BCNODE( SPEC=2, ENTI = "inlet", CONS = 0 )
      BCFLUX( SPEC=2, ENTI = "person", CONS = 1E-5 )
      CLIPPING( MINI )
```

Appendix B (continued)

```
      0,     0,     0,     0,    19,    0,   0,    0,     0.011,
1e-20
      CLIPPING( MAXI )
      0,     0,     0,     0,    0,     0,   0,    0,    1,     1

      ICNODE( VELO, READ, ALL)

      PROBLEM( 3-D, TURB,ENER, SPEC = 1, SPEC = 2)

      END
```